

แบบจำลองคณิตศาสตร์สำหรับเวลาการรักษาของการติดเชื้อก่อโรคในเลือดหลังได้รับยาปฏิชีวนะ



บทคัดย่อและแฟ้มข้อมูลฉบับเต็มของวิทยานิพนธ์ตั้งแต่ปีการศึกษา 2554 ที่ให้บริการในคลังปัญญาจุฬาฯ (CUIR)
เป็นแฟ้มข้อมูลของนิสิตเจ้าของวิทยานิพนธ์ ที่ส่งผ่านทางบัณฑิตวิทยาลัย

The abstract and full text of theses from the academic year 2011 in Chulalongkorn University Intellectual Repository (CUIR)
are the thesis authors' files submitted through the University Graduate School.

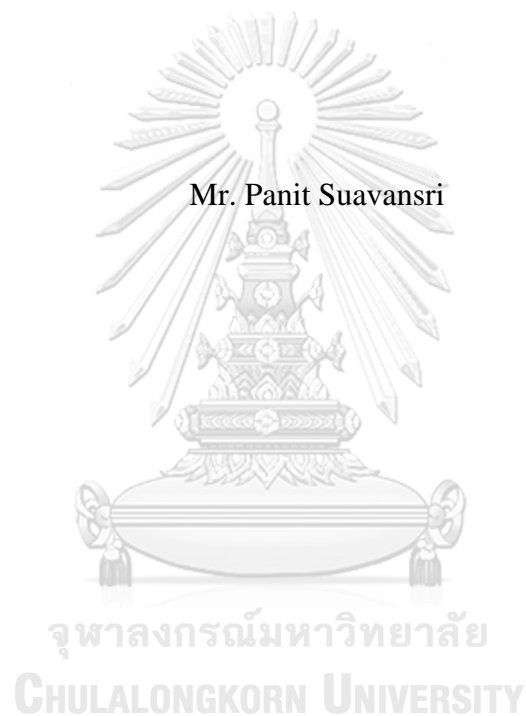
วิทยานิพนธ์นี้เป็นส่วนหนึ่งของการศึกษาตามหลักสูตรปริญญาวิทยาศาสตรดุษฎีบัณฑิต
สาขาวิชาคณิตศาสตร์ประยุกต์และวิทยาการคอมพิวเตอร์ ภาควิชาคณิตศาสตร์และวิทยาการคอมพิวเตอร์

คณะวิทยาศาสตร์ จุฬาลงกรณ์มหาวิทยาลัย

ปีการศึกษา 2560

ลิขสิทธิ์ของจุฬาลงกรณ์มหาวิทยาลัย

MATHEMATICAL MODELS FOR TREATMENT TIME OF PATHOGENIC
INFECTION IN BLOOD AFTER ANTIBIOTICS ADMINISTRATION



Mr. Panit Suavansri

A Dissertation Submitted in Partial Fulfillment of the Requirements
for the Degree of Doctor of Philosophy Program in Applied Mathematics and
Computational Science
Department of Mathematics and Computer Science
Faculty of Science
Chulalongkorn University
Academic Year 2017
Copyright of Chulalongkorn University

| | |
|----------------|---|
| Thesis Title | MATHEMATICAL MODELS FOR TREATMENT TIME OF PATHOGENIC INFECTION IN BLOOD AFTER ANTIBIOTICS ADMINISTRATION |
| By | Mr. Panit Suavansri |
| Field of Study | Applied Mathematics and Computational Science |
| Thesis Advisor | Associate Professor Nataphan Kitisin, Ph.D. |

Accepted by the Faculty of Science, Chulalongkorn University in Partial
Fulfillment of the Requirements for the Doctoral Degree

..... Dean of the Faculty of Science
(Associate Professor Polkit Sangvanich, Ph.D.)

THESIS COMMITTEE

..... Chairman
(Professor Paisan Nakmahachalasint, Ph.D.)

..... Thesis Advisor
(Associate Professor Nataphan Kitisin, Ph.D.)

..... Examiner
(Assistant Professor Khamron Mekchay, Ph.D.)

..... Examiner
(Assistant Professor Petarpa Boonserm, Ph.D.)

..... External Examiner
(Associate Professor Montri Maleewong, Ph.D.)

CHULALONGKORN UNIVERSITY

พนิต เตื่อวรรณศรี : แบบจำลองคณิตศาสตร์สำหรับเวลาการรักษาของการติดเชื้อก่อโรค
ในเลือดหลังได้รับยาปฏิชีวนะ (MATHEMATICAL MODELS FOR
TREATMENT TIME OF PATHOGENIC INFECTION IN BLOOD AFTER
ANTIBIOTICS ADMINISTRATION) อ.ที่ปริกษาวิทยานิพนธ์หลัก: รศ. ดร. ฉัฐ
พันธ์ กิตติสิน, 143 หน้า.

วิทยานิพนธ์เล่มนี้มีจุดประสงค์เพื่อทำนายระยะเวลาที่จำเป็นเพื่อล้างเชื้อโรคออกไปจาก
กระแสเลือดหลังได้รับยาปฏิชีวนะซึ่งจะมีผลต่อเวลาเพื่อหยุดการให้ยากับผู้ป่วยโดยการ
ใช้แบบจำลองคณิตศาสตร์ ในงานนี้ผู้เขียนจะหาระดับความหนาแน่นของเชื้อแบคทีเรียและมาลาเรีย
ในกระแสเลือด โดยเปรียบเทียบกับผลตรวจเลือดจากการส่งตัวอย่างเลือดของผู้ป่วยไปยัง
ห้องปฏิบัติการซึ่งใช้เวลาไม่ต่ำกว่า 2-3 วันจากการเพาะเชื้อและหาค่าความหนาแน่นของเชื้อโรค
เนื่องจากการทำนายระยะเวลาการรักษาดังกล่าว โดยใช้แบบจำลองทางคณิตศาสตร์จะแสดงผลลัพธ์
ได้ไม่กีวินาที ดังนั้นการหาผลลัพธ์เชิงตัวเลขสามารถทำได้อย่างรวดเร็วโดยใส่ข้อมูลบางอย่างและ
ใช้โปรแกรมทางคณิตศาสตร์ประมวลผลออกมา ขั้นตอนการวิจัยจะประกอบด้วยการสร้างอัตรา
การตายของเชื้อแบคทีเรียและมาลาเรียในรูปแบบจำลองคณิตศาสตร์ภายใต้สมมติฐานที่มีตัวแปร
ต้นเป็นค่าระดับความเข้มข้นของยาในเลือดและค่าพารามิเตอร์อื่นบนพื้นฐานความรู้ทางด้านทฤษฎี
ความน่าจะเป็น ความเร็วสัมพัทธ์ กลไกการจับกันระหว่างโมเลกุลของยากับเชื้อโรคโดยการพดพา
ของเลือด โครงสร้างโมเลกุลและคุณสมบัติของยาปฏิชีวนะรวมทั้งเชื้อแบคทีเรียและมาลาเรีย ตัว
แปรตามคือความหนาแน่นของเชื้อโรค ผลลัพธ์ที่ได้จากงานวิจัยนี้สอดคล้องกับข้อมูลจริงทาง
คลินิกจากการเปรียบเทียบกับกราฟของเชื้อโรคในผู้ป่วย

จุฬาลงกรณ์มหาวิทยาลัย
CHULALONGKORN UNIVERSITY

| | | |
|----------|-------------------------------|----------------------------|
| ภาควิชา | คณิตศาสตร์และวิทยาการ | ลายมือชื่อนิติ |
| | คอมพิวเตอร์ | ลายมือชื่อ อ.ที่ปริกษาหลัก |
| สาขาวิชา | คณิตศาสตร์ประยุกต์และวิทยาการ | |
| | คณนา | |

ปีการศึกษา 2560

5572826823 : MAJOR APPLIED MATHEMATICS AND COMPUTATIONAL SCIENCE

KEYWORDS: BACTERIA / MALARIA / DEATH RATE / PROBABILITY

PANIT SUAVANSRI: MATHEMATICAL MODELS FOR TREATMENT TIME OF PATHOGENIC INFECTION IN BLOOD AFTER ANTIBIOTICS ADMINISTRATION. ADVISOR: ASSOC. PROF. NATAPHAN KITISIN, Ph.D., 143 pp.

The objective in this thesis is to create a mathematical model to predict the period of time needed to clear out the pathogens from the bloodstream after the patient receives certain antibiotics. The result will lead to the time where the drug administration can be terminated. This research is to compute the densities of bacteria and malaria in bloodstream at any given time and to compare this level with the actual results of the patient's blood sampling, which was sent to the laboratory for investigation. The laboratory process of the blood sampling will usually take more than 2-3 days to culture and to calculate the density of pathogens. However, the prediction of treatment duration by using our mathematical model can get the results within few seconds. Therefore, the numerical results can be done faster by entering some certain parameters and running the mathematical program. The research method consists of the formulation of the death rates of bacteria and malaria in the mathematical forms under our assumptions. We assume that the independent variable is the plasma drug concentration and other parameters, based on the probabilistic theory, the relative velocity, the binding mechanism between drug molecules and pathogens by the blood convection, the structure and properties of antibiotics including bacteria and malaria. The dependent variable is the density of pathogens. The results from this research are consistent with the actual clinical data by comparing with the patient pathogen density graph.

Department: Mathematics and Student's Signature

Computer Science Advisor's Signature

Field of Study: Applied Mathematics
and Computational
Science

Academic Year: 2017

ACKNOWLEDGEMENTS

There are many people who have helped me along the way until I completed my doctoral dissertation.

First, I would like to express my special thanks to my advisor, Associate Professor Dr. Nataphan Kitisin, for his guidance. Moreover, he gave me a lot of suggestions and comments about my research until my articles were published.

Secondly, I would like to thank Professor Dr. Paisan Nakmahachalasint, Associate Professor Dr. Montri Maleewong, Assistant Professor Dr. Khamron Mekchay and Assistant Professor Dr. Petarpa Boonserm, for being my committees and their valuable comments about my thesis.

Moreover, I would like to thank Chulalongkorn University for the 60/40 Scholarship to support my study.

Furthermore, I would like to thank my family for their sacrifices and their encouragement.

Finally, I wish that my work would be beneficial to physicians, pharmacists, biologists and mathematicians, who may find it useful.

CONTENTS

| | Page |
|---|------|
| THAI ABSTRACT | iv |
| ENGLISH ABSTRACT..... | v |
| ACKNOWLEDGEMENTS | vi |
| CONTENTS..... | vii |
| CHAPTER 1 INTRODUCTION | 1 |
| 1.1 Literature Review and Background Information | 1 |
| 1.2 Background Information and Significance of the Research Problem | 2 |
| 1.2.1 Pathology of Bacteria and Malaria | 3 |
| 1.2.1.1 Bacteria..... | 3 |
| 1.2.1.1.1 Background..... | 3 |
| 1.2.1.1.2 Routes of infection and Signs and symptoms..... | 3 |
| 1.2.1.1.3 Pathogenesis | 3 |
| 1.2.1.1.4 Mathematical model | 4 |
| 1.2.1.2 Malaria..... | 5 |
| 1.2.1.2.1 Pathogenesis of Malaria Parasite | 5 |
| 1.2.1.2.1.1 <i>Plasmodium falciparum</i> | 5 |
| 1.2.1.2.1.2 Sequestration | 5 |
| 1.2.1.2.2 Mathematical models..... | 6 |
| 1.3 The Initial Point of All Three Articles..... | 8 |
| 1.4 The Method of Mathematical Modeling in Each Articles | 8 |
| 1.4.1 Assumptions and Hypotheses in this research | 9 |
| 1.4.2 Parameters of Bacteria, Malaria, and Human Profiles | 10 |
| 1.5 The Study of This Research in Each Articles | 11 |
| 1.6 Connection between Articles | 12 |
| 1.7 The differences between three articles..... | 15 |
| 1.8 Research Challenges | 18 |
| 1.9 The Objective of the Research..... | 19 |
| 1.10 The Scope of the Research..... | 19 |

| | Page |
|---|------|
| 1.11 Anticipated Benefit from the Research..... | 20 |
| CHAPTER 2 PREDICTING THE DURATION OF ANTIBACTERIAL TREATMENT WITH CELL WALL SYNTHESIS INHIBITORS BY USING MATHEMATICAL MODELS..... | 22 |
| CHAPTER 3 PREDICTING THE DURATION OF ANTIMALARIAL TREATMENT WITH HEME DEGRADATION INHIBITORS OF BLOOD SCHIZONTICIDES USING MATHEMATICAL MODELS..... | 50 |
| CHAPTER 4 PREDICTING THE DURATION OF CHLOROQUINE, MEFLOQUINE, HALOFANTRINE AND ARTESUNATE FOR BLOOD SCHIZONTICIDAL EFFECT USING MATHEMATICAL MODELS OF MALARIA WITH IMMUNE RESPONSE..... | 80 |
| CHAPTER 5 CONCLUSION AND DISCUSSION | 120 |
| 5.1 Main Concepts and Analysis of the Dissertation..... | 120 |
| 5.2 The Differences of Results between Bacteria and Malaria | 121 |
| 5.3 Numerical Results in Case of Malaria | 122 |
| 5.3.1 Monotherapy with or without Immune Response | 122 |
| 5.3.2 Differences between Monotherapy and Drug Resistance with Immune Response in both of them..... | 124 |
| 5.4 Connection of the Results from Researches between Three Articles..... | 126 |
| 5.5 Limitation of the Research..... | 128 |
| 5.6 Suggestion and Future Research..... | 129 |
| 5.7 Conclusion and Discussion..... | 131 |
| REFERENCES | 132 |
| APPENDIX..... | 133 |
| APPENDIX A..... | 133 |
| NUMERICAL METHOD | 133 |
| A.1 Background Information | 133 |
| A.2 Numerical Methods for Solving Initial Value Problems in the System of Differential Equations | 134 |
| A.2.1 The initial value problem..... | 134 |
| A.2.2 Euler method | 136 |

| | Page |
|---|------|
| A.2.3 Systems of equations | 137 |
| A.2.4 Runge-Kutta method | 138 |
| A.2.5 Determination of Treatment Duration | 141 |
| A.3 Conclusion | 142 |
| VITA | 143 |



จุฬาลงกรณ์มหาวิทยาลัย
CHULALONGKORN UNIVERSITY

CHAPTER 1

INTRODUCTION

First, the formulation of the death rate of pathogens in this dissertation is based on various scientific knowledges and hypotheses. The full details of the derivation are explained in Chapters 2 to 4. In this chapter, we will mention the connection between articles, background and significance of the research problem, research challenges, the objective of research, the scope of the research, and anticipated benefit from the research.

1.1 Literature Review and Background Information

Before formulating the death rate of both bacteria and malaria, the pathogenesis in both of them must exist the parameters, and availability of bacterial and malarial profiles are needed in order to translate them into the mathematical formulas. For instance, biologists can measure some parameters such as the doubling time or half-life of pathogens. Afterward, we will use mathematical framework to translate these parameters into the system of differential equations or other forms, such as incorporating the indirect proportion of both doubling time and half-life of pathogens into the natural growth and death rate of pathogens, respectively.

Some ideas of the mathematical model of pathogens needs to be considered. For instance, the term βxm in the model of malarial parasite is based chemistry principles of the rate of mass action, where x and m are the density of normal RBCs and merozoites, respectively. Since the rate of mass action depends on the density of both x and m , this term conforms the real-world situation. Observe that the binding

mechanism between x and m differs from the binding mechanism between drug molecules and iRBCs because of the blood convection.

1.2 Background Information and Significance of the Research Problem

The infectious diseases are one of the main causes of the patient's death. Various pathogens that can infect human hosts are bacteria, virus, parasites, fungi, etc. Moreover, the ability to control the density of pathogens in patient's blood during infection is necessary in order to prevent the patients from further complications such as the spreading of pathogens into brain, heart, lungs or liver.

At present, the World Health Organization (WHO) has put much affords to reduce the spreading of pathogens around in the world. Furthermore, WHO also promote the prevention of non-infectious diseases such as malnutrition, aging problem, cancer, etc [1].

Only few studies have used the human physiology and the mechanism of drug action to construct the mathematical models of the death rate of pathogens [2, 3]. Some research used the rate of mass action to formulate the death rate of pathogens [2]. Therefore, this research will try to adapt the physiology of human, the pathophysiology of pathogens and the mechanism of drug action in pharmacology to construct such the mathematical model of the death rate of bacteria and malaria.

1.2.1 Pathology of Bacteria and Malaria

This section will review the pathology of bacteria and malaria in order to understand their pathogenesis before translating into the mathematical models.

1.2.1.1 Bacteria

1.2.1.1.1 Background

Bacteria are separated into two main types. The first type is the nonpathogenic bacteria or normal flora, which do not cause the infectious disease in human. The other type is pathogenic bacteria, which we use in this work [4].

1.2.1.1.2 Routes of infection and Signs and symptoms

There are many ways for the bacteria to infection human (see Table 1).

Table 1. Table 1 illustrates the examples of bacteria and their characteristics.

| Bacteria | Route of infection | Signs and symptoms |
|-----------------------------------|------------------------|--------------------|
| <i>Clostridium perfringens</i> | Wound | Gas gangrene |
| <i>Mycobacterium tuberculosis</i> | Respiratory tract | Cough |
| <i>Vibrio cholerae</i> | Gastrointestinal tract | Diarrhea |

1.2.1.1.3 Pathogenesis

First, bacteria from various routes get into the mucous membranes of each system as in Table 1. Then, they attach to human cells, duplicate themselves, and spread into the target organs to hibernate or attack. For example, *Neisseria meningitidis*, which

appears in this research, invades the membranes that cover the brain and spinal cord, called meninges, after they duplicate and spread in human host [4].

Therefore, bacteria that are chosen in this research must reside in human bloodstream, called bacteremia. Other bacteria that infect only local target organ such as bacterial gastritis is excluded from our work.

1.2.1.1.4 Mathematical model

The simple birth-death model of bacteria from [2] is used in this research. It can be described by the following equation

$$\frac{dP}{dt} = (g - \mu)P,$$

where P is the population of bacteria at time t , g and μ are the natural growth and death rate of bacteria, respectively. We use this bacterial model in [2] since there are enough parameters and data available for this model. Other models, such as Malthusian model, there is not enough real data available to generate or simulate the numerical results. Thus, after coupling this model of bacteria with the death rate of bacteria due to drug, we obtain the following model,

$$\frac{dP}{dt} = (g - \mu)P - \varphi(k),$$

where $\varphi(k)$ is the death rate of bacteria due to plasma drug concentration k (see Chapter 2 in details).

1.2.1.2 Malaria

Similarly, we choose malarial parasites as a key pathogen since they reside in bloodstream, which satisfy our assumption.

1.2.1.2.1 Pathogenesis of Malaria Parasite

When a female *Anopheles* mosquito bites a human, sporozoites in this mosquito are released from the mosquito's saliva gland via saliva, and enter the human body. Afterward, they will travel to the human's liver via the blood circulation. Then, sporozoites will infect liver cells and duplicate themselves and become schizonts within liver cells. When schizonts mature, called merozoites, the liver cells eruption will occur. Afterward, merozoites will be released from liver cells into the bloodstream. Finally, merozoites will reinfect normal RBCs and repeat the previous process over again [3, 5].

1.2.1.2.1.1 *Plasmodium falciparum*

The pathogenesis of *P. falciparum* is quite different from other malarial parasites. In particular, there is a process, called sequestration in *P. falciparum*, which we need to take account for when the mathematical model is created [6].

1.2.1.2.1.2 Sequestration

In case of *P. falciparum*, there are two types of iRBCs: circulating and sequestered iRBCs. First, after the normal RBCs are infected by merozoites, they

become circulating iRBCs. The pathophysiology of circulating iRBCs are similar to the case of *P. non-falciparum*, as they both move in the bloodstream by the convection. When circulating iRBCs mature, they become the sequestered iRBCs. Afterward, the sequestered iRBCs will attach to the luminal wall of capillaries and venules in all specific vital organs, which are brain, left and right lungs, liver, left and right kidneys, and heart [7, 8]. This process is called sequestration. Consequently, the death rate of malarial parasite in this stage can be determined only from the velocity of drug molecules and from some specific vital organs.

1.2.1.2.2 Mathematical models

In order to verify the numerical results to the actual results, the parameters in the mathematical models of malarial parasites must be available for us in order to compute the death rate of pathogens. Therefore, in case of *P. non-falciparum*, this work uses the mathematical models of within-host malarial parasite in [2] to generate the results. In particular, we use the following model:

$$dx / dt = \Lambda - \mu_x x - \beta xm,$$

$$dy / dt = \beta xm - \mu_y y - \left(\frac{y}{x + y} \right) \varphi(k),$$

$$dm / dt = gy - \mu_m m - \beta xm.$$

This model is similar to the case of bacteria, which is the simplest model of pathogen. Although this simple model has not taken into account of other influential factors, this is the starting point to verify that the death rate of malarial parasite in this research is compatible with the system of differential equations of malarial parasite. Therefore, if the numerical results in this case are compatible with the actual results, then the death rate of malarial parasite can be incorporated with more complex

situations such as the malarial infection with immune response, which will appear in the third.

In the case of *P. non-falciparum* with immune response, we use the mathematical models in [2, 3] for the case of *Plasmodium non-falciparum* with immune response, which are

$$\begin{aligned}\frac{dx}{dt} &= \Lambda - \mu_x x - \beta xm, \\ \frac{dy}{dt} &= \beta xm - \mu_y y - \frac{p_1 y E}{1 + \theta_1 y}, \\ \frac{dm}{dt} &= r y - \mu_m m - \frac{p_2 m E}{1 + \theta_2 m}, \\ \frac{dE}{dt} &= -\mu_E E + \frac{k_1 y E}{1 + \theta_1 y} + \frac{k_2 m E}{1 + \theta_2 m}.\end{aligned}$$

To ensure that the death rate of malarial parasites can be applied with the patients with complications, we modify the mathematical models of *Plasmodium falciparum* in [6] and the mathematical model of malarial parasite with immune response in [3]. In particular, we obtain the following model,

$$\begin{aligned}\frac{dx}{dt} &= \Lambda - \mu_x x - \beta xm, \\ \frac{dy_c}{dt} &= \beta xm - (\gamma_c + \mu_c) y_c - \frac{p_1 y_c E}{1 + \theta_1 y_c}, \\ \frac{dy_s}{dt} &= \gamma_c y_c - (\gamma_s + \mu_s) y_s - \frac{p_1 y_s E}{1 + \theta_1 y_s}, \\ \frac{dm}{dt} &= r \gamma_s y_s - \mu_m m - \frac{p_2 m E}{1 + \theta_2 m}, \\ \frac{dE}{dt} &= -\mu_E E + \frac{k_1 (y_c + y_s) E}{1 + \theta_1 (y_c + y_s)} + \frac{k_2 m E}{1 + \theta_2 m}.\end{aligned}$$

Note that our model contains the effect of the immune response. Afterward, the numerical results are generated. We found that the pattern and treatment durations in these results still conform to the actual results. Furthermore, since *P. falciparum* is

deadlier than *P. non-falciparum*, the treatment durations in case of *P. falciparum* are longer than in case of *P. non-falciparum*. Thus, the death rate of malarial parasites with immune response are still compatible even with the patients with complications.

1.3 The Initial Point of All Three Articles

The main initial points of all three articles are originated from the effect to predict the treatment duration by using the mathematical models of the death rate of pathogens. Afterward, we generate the numerical results to compare with the actual data from the real patients. We published our results in three articles, which are the cases of bacteria, *Plasmodium non-falciparum* and malaria (including *Plasmodium falciparum*) with immune response, respectively. Furthermore, this study can predict the drug dosage for bacterial and malarial treatment within the desired treatment duration as well.

1.4 The Method of Mathematical Modeling in Each Articles

The differences between the first, second, and third are the complexity in their system of differential equations of the mathematical models. Note that the case of bacteria in the first research is the simplest model of the death rate of pathogens. The next model, which is the model of the death rate of malarial parasite, excluding *P. falciparum*, is more complex due to the effect of immunity.

However, the death rate of the malaria for the last model is the most complex due to the pathology of the *P. falciparum*. In particular, the pathogenesis of *P. falciparum*, considered within the third article, is different from *P. malariae*, *P. vivax*,

P. ovale and *P. knowlesi*. This difference is that *P. falciparum* has the process, called sequestration. When normal RBCs are infected with *P. falciparum*, they become circulating iRBCs, which have the same characteristic as iRBCs from *P. malariae*, *P. vivax*, *P. ovale* and *P. knowlesi*. Afterward, the circulating iRBCs mature and the process of sequestration by turning themselves into the second phase of iRBCs, called sequestered iRBCs. These sequestered iRBCs do not travel along the bloodstream but they will attach to the intraluminal wall of capillaries and venules in all specific vital organs, which are brain, heart, left and right lungs, left and right kidneys, and liver [7, 8]. Hence, the death rate in case of *P. falciparum* needs to be modified to take into account of its pathogenesis. For example, since sequestered iRBCs do not move along blood current, we have $v_s^{(iRBC)} = 0$, where $v_s^{(iRBC)}$ is the velocity of sequestered iRBCs. Thus, $v^{(relative)} = v_s^{(drug)} = G^{(drug)} v_s^{(blood)}$, where $G^{(drug)}$ is the local lag coefficient of drug molecules, and $v^{(relative)}$, $v_s^{(drug)}$, and $v_s^{(blood)}$ are the relative velocity, the velocity of drug molecules in case of sequestration, and the velocity of bloodstream within capillaries or venules in case of sequestration [5]. Finally, although the mathematical models of malarial parasite with immune response in the third research is the most complex in this research, the numerical results show that the treatment durations is still compatible with the real clinical data.

1.4.1 Assumptions and Hypotheses in this research

Since the formulation of the death rate of pathogens is in the mathematical form, there are several mathematical assumptions that we need to make as the follows.

1. The shape of both drug molecules and bacteria are prolate spheroid.
2. The shape of infected red blood cells (iRBCs) are spherical.
3. Each type of drug molecules are equal in size and properties.
4. Each type of bacteria are equal in size and properties.
5. The velocities of drug molecules, bacteria and iRBCs occur from the convection of bloodstream which are based on theoretical physics. Thus, to apply the death rate with other pathogens, they must reside in the bloodstream.
6. All probability factors: position, binding, capture, orientation, and population, are independent.
7. All patients in this research receive antibiotics by dripping via intravenous route in order to maintain the constant level of plasma drug concentration. The reason is that the level of plasma drug concentration needs to be kept between the therapeutic level and the toxic level to complete drug action. Thus, by assumption, the input and output rate of drug are equal.

1.4.2 Parameters of Bacteria, Malaria, and Human Profiles

Before we can generate the numerical results, the parameters of bacteria, malaria, and human profiles must be available. Some of those parameters are range bound and do not have exact value. We also need to make proper changes of their units. Thus, all parameters, which are used in this work, need to be recalibrated otherwise the numerical results will not be correct. We list all the parameters in case of bacteria and malaria in Table of each articles (in Chapter 2, 3 and 4).

1.5 The Study of This Research in Each Articles

In first article, we study the treatment durations in case of bacteria since this case is the simplest dynamical system of all pathogens. Our model only consists of only the simple natural growth and death rate of bacteria. After generating the numerical results by using the death rate of bacteria, the results conform to the real situation, i.e. the treatment durations for both of them are quite the same.

However, to ensure that the death rate of pathogens in this research can be applied with other types of pathogens, we choose *P. non-falciparum* to be the second case to verify that the treatment durations of *P. non-falciparum* are also compatible with the real data. Therefore, in the second article, we focus on the treatment duration in case of *P. non-falciparum*. After generating the numerical results, the results are compatible with the real case of *P. non-falciparum*, i.e. the treatment durations, determined from these results, are 1-2 weeks, which are close to the real data.

Furthermore, to show that the death rate of malaria in this research can apply to more complex mathematical models of malaria such as the patients with malarial infection and immune response. Hence, we choose this case for our study and publish our results in the third article. In particular, in the third article, we study the treatment durations in case of patient with malarial infection and immune response. After generating the numerical results, the treatment durations are still 1-2 weeks. Hence, these results also conform to the actual results.

However, we note that the treatment durations from both the second and third articles are quite similar. This result contradicts to the real situation that the immune response should help patients reduce the parasite density and therefore shorten the

treatment duration. Thus, we have to modify the initial immune effectors. As a result, we find that the treatment durations are shortened, which are more compatible with the real situation. Note that the numerical results and illustrations are described in the section of the discussion of Chapter 5 in details.

1.6 Connection between Articles

The main objective in this dissertation is to predict the treatment duration of the patient with bacterial infection and malarial infection. The dissertation contains three articles which are already published as follows:

- 1) “Predicting the duration of antibacterial treatment with cell wall synthesis inhibitors using mathematical models” detailed in Chapter 2
- 2) “Predicting the duration of antimalarial treatment with heme degradation inhibitors of blood schizonticides using mathematical models” detailed in Chapter 3
- 3) “Predicting the Duration of Chloroquine, Mefloquine, Halofantrine and Artesunate for Blood Schizonticidal Effect using Mathematical Models of Malaria with Immune Response” detailed in Chapter 4

All the above articles are to meet the dissertation requirement for the doctoral degree in the Applied Mathematics and Computational Science.

In Chapter 2, we present the first article that contains the formulation of the death rate of bacteria. This mathematical model represented the most primitive form of pathogens. The reason that we use bacteria as one of the first examples of pathogens is that the pathogenesis of bacteria is not very complex. Furthermore, the mathematical

model of bacteria consists only the natural growth and natural death rates, which can be described with only one differential equation [2]. Afterward, the numerical results will be generated. For the case of bacteria, the results show that all durations of treatment are 2-7 days, which are compatible to the actual treatment duration from the real clinical data. Nevertheless, to show that the formulation of the death rate can be effective under some other assumptions, we apply this mathematical model of death rate to other pathogens. Thus, the next pathogen, used for our study, is the malaria parasite. The second article is presented in the next Chapter.

In Chapter 3, we present the second article that contains the formulation of the death rate of malaria parasite in all *Plasmodium species* except *Plasmodium falciparum*. Note that the pathogenesis of *Plasmodium falciparum* is exactly different from other *Plasmodium species* (the case of *Plasmodium falciparum* will be presented in Chapter 4). The case of malaria parasite is more complex than the case of bacteria since it involves many differential equations comparing to just a single differential one for the case of bacteria [2]. In general, the pathogenesis of within-host malaria parasite consists of three main types of populations as follows: 1) normal or healthy red blood cells (RBCs), 2) infected or parasitized red blood cells (iRBCs), and 3) extracellular parasites or merozoites. Hence, mathematically, it requires the system of three differential equations to model the malaria parasite population. Furthermore, since the pathogenesis of malaria parasite and the mechanism of antimalarial drugs are different from the case of bacteria, therefore the formation of the death rate of malaria parasite must also be different as well. However, the pathology of *Plasmodium falciparum* is even more complex than *P. malariae*, *P. vivax*, *P. ovale* and *P. knowlesi*. In this dissertation, we will also cover this case and compare the

results from *Plasmodium falciparum* with *P. malariae*, *P. vivax*, *P. ovale* and *P. knowlesi*.

For the case of *Plasmodium falciparum*, the pathogenesis of *Plasmodium falciparum* is more complicated than *P. malariae*, *P. vivax*, *P. ovale* and *P. knowlesi* since there are four main types of populations as follows: 1) normal or healthy red blood cells (RBCs), 2) circulating infected or parasitized red blood cells (circulating iRBCs), 3) sequestered infected or parasitized red blood cells (sequestered iRBCs), and 4) extracellular parasites or merozoites. Remark that there are two types of iRBCs, which are the circulating and the sequestered iRBCs. As soon as the RBCs are infected by merozoites, they are transformed into the first phase of iRBCs, called the circulating iRBCs [6]. Consequently, the pathogenesis of the circulating iRBCs and the sequestered iRBCs needs to be taken into account in the mathematical models before we can generate the numerical results. For instance, we have to compute the relative velocity between the drug molecules and the iRBCs in case of the circulating iRBCs but not in case of the sequestered iRBCs. Furthermore, since sequestered iRBCs occur only in the certain vital organs: brain, heart, lungs, kidneys and liver, the calculation in case will exclude the sequestered iRBCs from other organs by using the ratio of all specific vital organs weight against to weigh of the whole body. After translating this pathogenesis of malaria parasite into the mathematical models completely, we then can compare the results between both cases of *Plasmodium falciparum* to *P. malariae*, *P. vivax*, *P. ovale* and *P. knowlesi*. Finally, we were able to publish our study of the case of *Plasmodium falciparum* with immune response, which is the third article in this dissertation. In summary, chapter 4 will consist of the cases of all *Plasmodium species* with immune response and investigate how immune response can affect the mathematical models of

within-host malaria parasites with antimalarial drugs. To achieve this goal, we have to add one more differential equation to incorporate the immune effectors, which will represent such immune response.

Finally, in Chapter 5, we will present the “Conclusion and Discussion” of our three articles. The discussion will focus on the analysis of all aspects of the research such as the connection of each articles and comparison of the results.

1.7 The differences between three articles

The main objective of all three articles is to predict the treatment duration of patients with bacterial and malarial infection by using the mathematical model. This work contains three articles with different mathematical models to determine the death rates of three pathogens, which are bacteria, *P. non-falciparum*, and malaria with immune response. The differences between three articles can be seen in Table 1.

Table 1. The conclusion of the differences between three mathematical models of bacteria, *P. non-falciparum* and malaria with immune response.

| Case | Bacteria | <i>P. non-falciparum</i> | Malaria with Immune |
|----------------------------|--|---|---|
| 1. Probability | | | |
| 1.1 Binding | $\frac{1}{2} \left(\frac{r^{(receptor)} N^{(receptor)}}{\pi r^{-(bacteria)} + r^{(receptor)} N^{(receptor)}} \right)$ | | $\frac{V^{(parasite)}}{V^{(iRBC)}}$ |
| 1.2 Population | Not use | $\frac{y}{x+y}$ | $\frac{y}{x+y+E}$ $\frac{y_c}{x+y_c+y_s+E}$ $\frac{y_s}{x+y_c+y_s+E}$ |
| 2. Relative velocity | Use | | Use only circulating iRBCs, not sequestered iRBCs |
| 3. Death rate | | | |
| 3.1 Time | independent | depended on x, y, y_c, y_s and E | |
| 4. Numerical results | | | |
| 4.1. Pattern of decreasing | Exponentially decreasing | log-linearly decreasing | |
| 4.2 Exact solution | Available | Unavailable | |
| 4.3 Treatment duration | Course of antibiotics administration (1-2 weeks) | | |
| 5. Immune effect | No | Improve (shorten the treatment duration if there are enough the immune effectors) | |

The main differences between the cases of bacteria and malaria can also be described as follows:

1. The binding probability factor: The binding mechanism in the bacterial case happens between the binding site of drug molecules and the disk of receptors on the surface of bacteria. On the other hand, we use the formula in [9] to compute the binding probability factor for the case of malaria. The probability factor involves the fraction of volumes between two volumes of the intracellular parasite and the iRBC. This fraction of volume bases on [10].
2. The population probability factor is used only in case of malaria since the binding of the drug molecule can happen to the normal RBCs as well. Thus, the population probability factor in case of malaria needs to be considered while the case of bacteria does not.
3. The death rate of malarial parasites also depends on time since it is related to the variables of dynamical population in the population probability factor, which also depends on time. In contrast, there is no the population probability factor in the case of bacteria and therefore the death rate does not depend on time.
4. The cases of bacteria and *P. non-falciparum* use the relative velocity principle since drug molecules and the pathogens move along together in bloodstream. In contrast, the sequestered iRBCs in case of *P. falciparum* attached to the intraluminal wall of capillaries and venules in all specific vital organs, and therefore we do not have to take the relative velocity into account.
5. The graph from numerical simulation shows the dramatically decrease in bacterial density since there is no effect of population probability factor to the death rate. In contrast, the pattern of numerical simulations in case of malaria shows the log-linear decreasing in density because of the effect of the

population probability factor for adjusting its death rate. When the malaria parasite density is very small, its death rate goes to zero, which conforms the real-world situation.

6. The system of differential equations in case of bacteria can be solved for the exact solution since it is not too complex. On the other hand, the system of differential equation in case of malaria consists of many nonlinear differential equations such as βxm and the population probability factor. Therefore, the exact solution from these nonlinear differential equations are almost impossible to obtain. However, we can use the numerical method in order to find the treatment duration.
7. Although the death rates of bacteria and malaria have different characteristic, the treatment durations of both cases of bacteria and malaria are roughly the same, which are 1-2 weeks and conform the actual data.

Furthermore, when there are enough the immune effectors, this immune response can have some effects on the death rate of the malarial parasites as shown in Figure 1 and 2 in Chapter 5.

1.8 Research Challenges

First, the pathophysiology of pathogens must be discovered using scientific method. Second, the mechanism of drug action with pathogens must be translated into mathematical forms. Finally, the most difficult challenges in this study are to create the formulas using physics and mathematics, and take into account of all the measured parameters involving the drug and pathogen.

1.9 The Objective of the Research

The aim of this study is to predict the treatment duration of patient with bacterial infection or malarial infection. Furthermore, our study can also predict the drug dosage, which will be used to treat the patient within the specific time frame. In conclusion, the work of this study contains the followings:

- 1) To formulate the death rate of pathogen in the form of mathematical models, based on physics, chemistry, microbiology, human physiology and pharmacology.
- 2) To generate and analyze the numerical results in order to find the relation between the density of pathogens in patient's blood and treatment duration.

1.10 The Scope of the Research

Before constructing the mathematical models of the death rate of pathogens, we need to know the nature of pathogens in human host and the drug action. First, the main action between a drug molecule and a pathogen is the binding mechanism between them. Hence, the actions of binding between both of them are described as follows:

- 1) The movements of a drug molecule and a pathogen are caused by the blood convection. Remark that the velocity of a drug molecule needs to be faster than a pathogen so that the binding or capture between both of them can occur.
- 2) Only the effective drug molecule, determined by the total probability, can kill a pathogen.

There are two types of the relative velocity between a drug molecule and a pathogen that we will consider. First, the case where both drug molecule and pathogen

are moving. The other one is that the drug molecules are moving while a pathogen stays put in the blood vessel (see the case of *Plasmodium falciparum*). Remark that the relative velocity between a drug molecule and a pathogen is constant and can be obtained from the calculation using theoretical physics.

The binding action between a drug molecule and a pathogen is based on physics and molecular chemistry. We base our model on the following five probabilities: 1) position probability factor, 2) binding probability factor, 3) capture probability factor, 4) orientation probability factor, and 5) population probability factor.

The mechanism of the drug action is based on the binding between the binding site of substrates (drug molecules) and the active site of enzymes such as PBPs in the case of bacteria or ferric ions in the case of malaria.

The pathogenesis of bacteria and malaria are assumed to be the only pathogenesis of the pathogens within human blood circulation.

1.11 Anticipated Benefit from the Research

We will use the mathematical modeling of the death rate of pathogens to predict the treatment duration or clear out time for the pathogens. Typical laboratory investigation for evaluating the density of pathogens will take quite more time. Furthermore, it costs more money as well.

Moreover, our models of the death rate of pathogens can be adapted to other pathogens within host blood. The model can be used further by modifying the profiles

of certain pathogens, i.e. their biological parameters such as the length and width of shape of pathogens, their natural growth and death rate, etc.



CHAPTER 2
PREDICTING THE DURATION OF ANTIBACTERIAL TREATMENT WITH
CELL WALL SYNTHESIS INHIBITORS BY USING MATHEMATICAL
MODELS

Panit Suavansri

Department of Mathematics and Computer Science, Faculty of Science,
Chulalongkorn University, Phayathai Road, Patumwan, Bangkok, 10330, Thailand)

*** Corresponding author, Email address: panitsuavansri@gmail.com**

This article appears in Thai Journal of Pharmaceutical Sciences (TJPS),
Volume 40, Number 3 (2016) p139-148.

Submitted 21 July 2016

Revised 1 September 2016

Accepted 12 September 2016

Published 26 September 2016

Abstract

Objective: This paper proposed a new mathematical model of within-host population dynamics of bacteria after cell wall synthesis inhibitors administration for practically predicting treatment duration and drug dosage. The aim of this paper is to predict the duration of antibacterial treatment with cell wall synthesis inhibitors using mathematical models. **Materials and Methods:** Our model deployed various concepts from different fields of probability, biology, physics, chemistry, pharmacology (pharmacokinetics and pharmacodynamics), and medical sciences. The following assumptions and hypotheses were established: (i) Binding or collision rate between drug molecule and bacteria depends on the relative velocity between drug molecule and bacteria, (ii) ability or probability of binding or capturing between drug molecule and bacteria can be evaluated using four probability factors, based on the principal of physics and chemistry, (iii) the number of bacteria dying from antibiotics is equal to the number of drug molecules binding bacteria. Thus, the bacterial death rate is equal to rate of drug molecules binding and killing bacteria (amount of drug molecules per second), and (iv) plasma drug concentration is constant and time-independent. In this paper, *Neisseria meningitidis* and *Pseudomonas aeruginosa* are selected to demonstrate the numerical results. **Conclusion:** In this result, duration of treatment are 2-7 days, which is nearly the same as course of antibacterial therapy.

Keywords: Mortality rate, Bacteria, Probability

1. Introduction

There have been several researches concerning the growth and mortality rate of bacteria to estimate the recuperation period of a patient in the forms of mathematical models. Those researches generally consist of pharmacodynamics (PD) and pharmacokinetics with drug absorption, drug distribution, metabolism, and drug elimination [1]. However, the factors regarding the vasculature, shapes of bacteria and drug molecule, velocity of blood flow, as well as the probability of binding between drug molecules and bacteria were not comprehensively encompassed.

In this study, the above factors are simultaneously considered to model the temporal interaction between the drug molecules and the bacteria. The drug molecules move toward the bacteria with a relative velocity defined in terms of the diameter of vasculature and blood stream acting as a transporter. Based on the theoretical relative velocities in physics, the velocity of drug molecules in blood flow is assumed to be higher than the velocity of bacterial agents resulting from the convection of blood flow. To effectively kill a bacterium, some drug molecules must be bound with the surface of bacterium. However, it is impossible to control the movement of drug molecules in the blood stream. A practical solution is to have much amount of drug molecules than the number of bacteria so that the probability of binding some drug molecules with the surface of bacterium can be increased. This solution confirms with the actual treatment. Therefore, in this study, it is assumed that the amount of drug molecules is much more than the number of bacteria and only some portions of drug molecules can bind with bacteria.

To consider the mechanism of drugs in molecular level, after cell wall synthesis inhibitors attach Penicillin-binding proteins (PBPs), which are bacterial enzymes for cell wall synthesis and located on bacterial cell wall, N-acetylmuramic acid (NAG) and N-acetylglucosamine (NAM) cannot enter to an active site on PBPs to be substrates for synthesis of peptidoglycan, which are components of cell wall (see details in Section 2). Although both Gram-positive and Gram-negative bacteria consist of cell wall with different amount of peptidoglycan, our model can also apply with both of them by the same mechanism. Hence, antibiotics with other mechanisms (not cell wall synthesis inhibition), such as DNA or RNA synthesis inhibitors, using Brownian movement for attaching intracellular enzymes, not convection by blood flow, are neglected in this paper. Second, since theoretical background in this paper uses the convective rate by blood flow, this model can apply with only systemic infection (bacteremia or septicemia). Since the most common Gram-positive bacteria, such as methicillin-resistant *Staphylococcus aureus* causing cellulitis or *Streptococcus pneumoniae* causing pneumonia, are local or organ infection, i.e., skin and lung infection, respectively, our model cannot apply with them. Therefore, in this study, *Neisseria meningitidis* in the case of nonresistance and *Pseudomonas aeruginosa*, representing extended spectrum beta-lactamase bacteria in case of resistance, are chosen for simulating numerical results since both of them are systemic infection (bacteremia or septicemia).

With the loss of generality, we assume that the structure of drug molecule and bacteria are sphere and prolate spheroid, respectively, as shown in Figure 1. The size of each drug molecule is smaller than the size of each bacterium, implying that drug molecule can follow bacteria to attach and kill them. First, since the shape and size of

each drug molecule as well as bacteria are not exactly the same, the concept of Stokes radius derived from Varani [2] was adopted to define the average radius of prolate spheroid-shaped of the drug molecule and bacteria. The principal is $V^{(sphere)} = V^{(prolate)}$, then $r^{(stoke)} = \left(r_w^{(particle)^2} r_l^{(particle)} \right)^{1/3}$, where $r_w^{(particle)}$ and $r_l^{(particle)}$ be the half width and half length of a particle having prolate shape. Thus, we have two average radii of drug molecule and bacteria, denoted as

$$\bar{r}^{(drug)} = \left(r_w^{(drug)^2} r_l^{(drug)} \right)^{1/3} \text{ and } \bar{r}^{(bacteria)} = \left(r_w^{(bacteria)^2} r_l^{(bacteria)} \right)^{1/3}, \text{ respectively.}$$

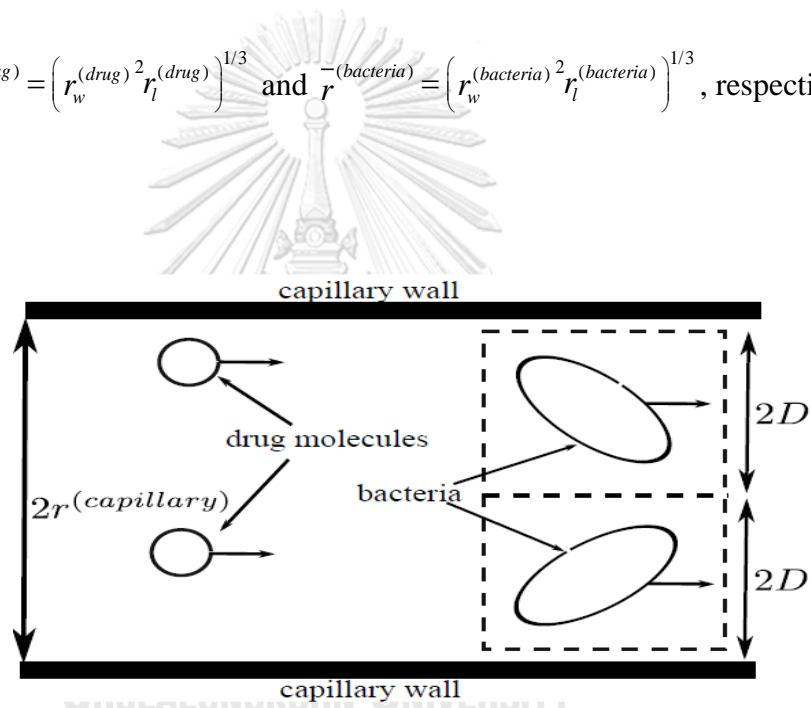


Figure 1. The scenario and assumptions of shape and size of drug molecule and bacteria made in our study. The drug molecules can chase the bacteria to bind and kill them in a lumen of capillary. $r^{(capillary)}$ is a radius of capillary and D is the width of cubic volume such that one bacterium can be found.

2. Material and Methods

2.1 Difference of Velocities of Drug Molecule and Bacteria

To derive the time of chasing bacteria by a drug molecule, the relative velocities of bacteria and drug molecule must be defined first. Since the velocities of the drug molecule and bacteria may be affected by their shapes and sizes, the transportation velocity of a rod-shaped particle in a cylindrical pore with the effect of convective hindrance introduced by Agasanapura *et al.* [3] were adapted to show the velocity difference. This difference is captured by a term called local lag coefficient and it is defined as the ratio of steady state of particle velocity and the fluid velocity in the absence of the particle in a cylindrical tube.

However, directly measuring the velocity of a drug molecule or bacteria is not simple. To ease this burden, the particle velocity can be transformed and written in terms of relative particle ratio defined as the ratio of known particle radius and tube radius instead. The word particle in this Section may refer to a drug molecule or bacteria depending on the context of discussion. By using the notations from the previous section, the relative particle ratio for drug molecule $\lambda^{(drug)}$ and for bacteria $\lambda^{(bacteria)}$ are defined as

$$\lambda^{(drug)} = \frac{r^{-(drug)}}{r^{(capillary)}} = \frac{\sqrt[3]{\left(r_w^{(drug)}\right)^2 r_l^{(drug)}}}{r^{(capillary)}} \approx 0.000156, \quad (1)$$

and

$$\lambda^{(bacteria)} = \frac{r^{-(bacteria)}}{r^{(capillary)}} = \frac{\sqrt[3]{\left(r_w^{(bacteria)}\right)^2 r_l^{(bacteria)}}}{r^{(capillary)}} \approx 0.21. \quad (2)$$

From the relative particle ratios in Equations 1 and 2, it can be seen that the relative drug ratio is much smaller than that of bacteria ($\lambda^{(bacteria)} > \lambda^{(drug)}$). Since $G^{(drug)} > G^{(bacteria)}$ and $v^{(particle)} = G^{(particle)}v^{(blood)}$, this implies that the flow velocity of drug molecule $v^{(drug)}$ is obviously much higher than that of bacteria $v^{(bacteria)}$ [3]. Thus, chasing and binding done by a drug molecule against bacteria is possible.

2.2 Position Probability Factor

The collision of drug molecules and bacteria can be modeled by modifying the probabilistic model of ship grounding which focused on traveling through a waterway in a straight forward line [4]. In our work, this probability is defined as the ratio of the projection area of bacterium to the contact area. Figure 1 shows different scenarios of how bacteria and drug molecules contact each other from various angles. However, the other human vessels, except capillaries, are not considered for evaluation since the local lag coefficient of drug molecule $G^{(drug)}$ is equal to local lag coefficient of bacteria $G^{(bacteria)}$. This means that drug molecule cannot chase bacteria because both have the same flow speed as discussed in Section 2.1. Thus, our position probability factor is

$$p^{(position)} = \frac{\left(r^{(drug)} + r_w^{(bacteria)} \right) \left(r^{(drug)} + \bar{d} \right)}{\left[r^{(capillary)} \right]^2}. \quad (3)$$

2.3 Binding Probability Factor

Once a drug molecule collides with bacteria, the drug molecule must bind with a disk of receptor, i.e., an active site of PBPs, to inhibit the signal transduction pathways

for cell wall synthesis by competing with NAG and NAM, as substrates, used for cell wall synthesis. In this study, binding probability from Berg and Purcell's study [5] must be modified because drug molecules can bind only the half of size of bacteria. Since the current of drug molecules is unidirectional, they can bind only bacterial receptors at one side of bacteria. Then, binding probability in this study is as follows:

$$p^{(binding)} = \frac{1}{2} \left(\frac{r^{(receptor)} N^{(receptor)}}{\left(\pi \bar{r}^{(bacteria)} + r^{(receptor)} N^{(receptor)} \right)} \right). \quad (4)$$

Where $N^{(receptor)}$ is the number of receptors on the cell surface and $r^{(receptor)}$ is the radius of disk of receptor of bacteria.

2.4 Capture Probability Factor

During colliding between drug molecule and bacteria, the drug molecule can deviate or be deviated by some factors. Thus, Berg and Purcell's study [5] defined the probability of ligands capturing the receptor on cell surface. In this paper, since drug molecules can deviate from the straight direction toward the position of bacterial target, capture probability must be calculated from the length between bacteria and drug molecules that drug molecules can follow bacteria to bind is $l^{(capillary)}$, where $l^{(capillary)}$ is the length of capillary and $\bar{r}^{(bacteria)}$ is the average radius of prolate spheroidal bacteria. Thus, our capture probability factor is as follows:

$$p^{(capture)} = \frac{\bar{r}^{(bacteria)}}{\bar{r}^{(bacteria)} + l^{(capillary)}}. \quad (5)$$

2.5 Orientation Probability Factor

In the aspect of chemical reaction, the reaction of particles will occur when particles collide with their accurate orientations in space. This implies that accurate orientations can increase the probability of collision and rate of reaction. Taroni *et al.* [6] defined the probability of attaching between a binding site of substrate and an active site of enzyme is the ratio of the surface area of amino acid binding to the molecule to the total surface area. In this paper, since drug molecule must bind a disk of receptor or an active site of PBPs with its binding site, i.e. beta-lactam ring of the drug molecule, orientation probability must be evaluated. Hence, our orientation probability factor is the ratio of binding area of drug molecule to the total surface area of drug molecule, i.e.,

$$p^{(orientation)} = \left(\frac{\pi z^2}{4} \right) / \left(2\pi \left(r_w^{(drug)} \right)^2 \left(1 + \frac{r_l^{(drug)}}{e r_w^{(drug)}} \sin^{-1} e \right) \right). \quad (6)$$

Where z is the diameter of binding site of drug molecule (beta-lactam ring) and

$$e = \sqrt{1 - \left(r_w^{(drug)} / r_l^{(drug)} \right)^2}.$$

2.6 Total Probability

The total probability of drug molecule to interact with bacteria is computed from the probabilities of all factors which are position probability, binding probability, capture probability, and orientation probability.

$$p^{(total)} = p^{(position)} \times p^{(binding)} \times p^{(capture)} \times p^{(orientation)}. \quad (7)$$

Each probability in equation (7) can be computed from equations 3-6, respectively.

2.7 Duration of Treatment by Dynamic Drug Model

From Section 2.1, the relative velocity with respect to those of drug molecule and bacteria is defined as

$$v^{(relative)} = v^{(drug)} - v^{(bacteria)} = (G^{(drug)} - G^{(bacteria)})v^{(capillary)}. \quad (8)$$

Where $G^{(drug)}$ and $G^{(bacteria)}$ are the local lag coefficients of drug molecules and bacteria with $G^{(drug)} > G^{(bacteria)}$, respectively. Once the relative velocity of drug molecules and bacteria is known, the number of drug molecules within a capillary tube at any unit time must be estimated before the computation of mortality rate of bacteria. The cross-sectional area of capillary $\pi(r^{(capillary)})^2$ is multiplied to the relative velocity to get the flow rate of drug molecules by blood volume. The blood volume can be transformed into the mass of drugs by multiplying the blood volume by the function of plasma drug concentration $C(t)$ at time t . The obtained result can be interpreted as the flow rate of drug mass. To link drug mass with the number of drug molecules, the drug mass is divided by the molecular mass of drug molecule M and multiplied by Avogadro's number A . Therefore, the number of drug molecules $N^{(drug)}$ at a given flow rate is equal to:

$$N^{(drug)} = \frac{\pi r^{(capillary)2} C(t) A (G^{(drug)} - G^{(bacteria)}) v^{(capillary)}}{M}. \quad (9)$$

To estimate the flow rate of drug molecules in host blood physiology, the capillary transit time τ and the circulatory time γ [7,8] when drug molecules chase a

bacterium in capillary must be involved. Then, ratio of time that drug molecules travel only in capillaries is τ/γ . Furthermore, only drug molecules in free form (not bounded with plasma protein) actually binding with the bacteria are taken into account. Thus, free drug fraction, denoted by α and defined as the ratio of free (unbound) drug molecules to all drug molecules, is also considered. Other parameters to be considered are the number of capillaries in human body defined as $N^{(capillary)}$ and the number of drug molecules that can kill only one bacterium defined as $N^{(kill)}$. The number of bacteria killed by drug molecules per second (called bacterial death rate $\varphi(t)$) can be computed by the following equation.

$$\varphi(t) = \frac{\pi\alpha N^{(capillary)} \tau r^{(capillary)^2} C(t) A p^{(total)} (G^{(drug)} - G^{(bacteria)}) v^{(capillary)}}{N^{(kill)} \gamma M}. \quad (10)$$

Thus, the bacterial population at time t , denoted as $P(t)$, can be evaluated from its dynamical system in the form of the first order linear differential equation with the birth-death rate of bacteria itself (denoted as g and μ), and the bacterial death rate due to drug previously computed as $\varphi(t)$ in the following equations.

$$\frac{d}{dt} P(t) = (g - \mu) P(t) - \varphi(t). \quad (11)$$

First, to solve Equation (11) for evaluating duration of treatment, assume that the plasma drug concentration $C(t)$ can become a constant k . Then, the bacterial death rate becomes a function of the constant k instead of time t and $\varphi(k)$ is used instead of $\varphi(t)$. Finally, after solving equation (11), the bacterial population $P(t)$ from equation (11) can be written as follows.

$$P(t) = \exp((g - \mu)t) \left(P(0) - \frac{\varphi(k)}{g - \mu} \right) + \frac{\varphi(k)}{g - \mu}. \quad (12)$$

2.8 Combination Therapy and Effect of Drug Resistance

Antagonist effect can also be found. We will use this principle of proportion [9] to apply with our bacterial death rate by multiplying $\left(\frac{\kappa^{(agonist)}}{\kappa^{(agonist)} + \kappa^{(antagonist)}}\right)$, where $\kappa^{(agonist)}$ and $\kappa^{(antagonist)}$ are two plasma concentrations of agonist and antagonist drugs, respectively. Thus, the bacterial death rate in this case is $\left(\frac{\kappa^{(agonist)}}{\kappa^{(agonist)} + \kappa^{(antagonist)}}\right)\varphi\left(\kappa^{(agonist)}\right)$.

Drug resistance of bacteria can be evaluated by defining the potency of the drug resistance as η ($0 < \eta < 1$), then $(1 - \eta)\kappa^{(agonist)}$ is the effective plasma drug concentration for killing bacteria without considering drug resistance. In this study, the potency of the drug resistance in our numerical example is $\eta = \frac{N^{(\beta)}}{N^{(\beta)} + N^{(PBP)}}$, where $N^{(PBP)}$ and $N^{(\beta)}$ is the number of two enzymes: PBPs and beta-lactamase, respectively. Note that beta-lactamase is a bacterial enzyme destroying beta-lactams, which is one of the mechanisms of drug resistance of bacteria.

Dual effect contains different drug action such as beta-lactams with beta-lactamase inhibitor for treating in the case of drug resistance. In the case of dual drug action, our numerical example uses clavulanic acid as a dual drug for inhibiting beta-lactamase (beta-lactamase inhibitor). Thus, the effective plasma ceftriaxone concentration, that can kill bacteria, is $\left(\frac{N^{(PBP)}}{(1 - \sigma)N^{(\beta)} + N^{(PBP)}}\right)k$, where $\sigma \equiv \frac{k^*/M^*}{(k/M) + (k^*/M^*)}$ is the potency of dual drug action, k and k^* are plasma drug and dual drug concentration, M and M^* are molecular weight of drug and dual drug, respectively.

Since our numerical example uses clavulanic acid as dual drug inhibiting beta-lactamase in bacteria [10]. Thus, we construct this probability, named dual action

probability and defined as $p^{(dual)}$. By using the fact that the active site of beta-lactam inhibiting enzyme (beta-lactamase) can choose ceftriaxone (beta-lactams) or clavulanic acid (beta-lactam analogs) by proportion of both molecules, then we have

$$p^{(dual)} = \frac{N}{N + N^*} = \frac{\frac{kVA}{M}}{\frac{kVA}{M} + \frac{k^*VA}{M^*}} = \frac{(k / M)}{(k / M) + (k^* / M^*)}. \quad (13)$$

Where A is the Avogadro's number, k and k^* are plasma drug and dual drug concentration, respectively, V is patient's whole blood volume, N and N^* are the number of drug molecules and dual drug molecules in patient's blood, respectively.

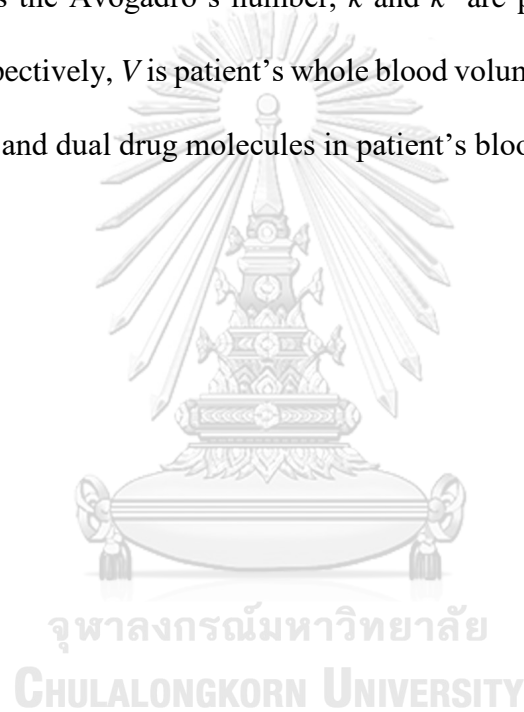


Table 1. The parameters used in our numerical example of patient with *N. meningitidis* infection

| Parameters | Value | Description | Source |
|--------------------|-----------------------|---|--------|
| $G^{(drug)}$ | 1 | Lag coefficient of drug molecule | [3] |
| $G^{(bacteria)}$ | 0.99 | Lag coefficient of bacteria ^a | [3] |
| $r_l^{(drug)}$ | 0.8142 | Half-length of drug molecule (nm) ^b | c |
| $r_w^{(drug)}$ | 0.3552 | Half-width of drug molecule (nm) ^b | c |
| z | 0.2105 | Diameter of binding site of drug molecule (nm) ^b | c,d |
| $r_l^{(bacteria)}$ | 1 | Half-length of bacteria (μm) ^a | [12] |
| $r_w^{(bacteria)}$ | 0.5 | Half-width of bacteria (μm) ^a | [12] |
| $r^{(receptor)}$ | 0.1052 | Radius of receptor (nm) ^a | [12] |
| $N^{(receptor)}$ | 3,100 | Number of receptors of bacteria ^a | [5] |
| g | 0.48 | Growth rate of bacteria (/day) | [10] |
| μ | 0.33 | Death rate of bacteria (/day) | [8] |
| γ | 60 | Blood circulatory time (s) | [8] |
| $r^{(capillary)}$ | 0.003 | Radius of capillary (mm) | [7] |
| τ | 1 | Transit time of capillary (s) | [7] |
| $l^{(capillary)}$ | 0.2 | Length of capillary (mm) | [13] |
| $v^{(capillary)}$ | 0.3 | Blood velocity in capillary (mm/s) | [7] |
| $N^{(capillary)}$ | 10^9 | Number of capillaries | [14] |
| V | 5 | Whole blood volume (l) | [15] |
| K | 18.18 | Average plasma ceftriazone concentration ($\mu\text{g/ml}$) | [16] |
| α | 0.05 | Free drug fraction | [16] |
| A | 6.02×10^{23} | Avogadro's number | [17] |
| M | 661.59 | Molecular weight of ceftriazone | [16] |
| k^* | 2.55 | Average plasma clavulanic acid concentration ($\mu\text{g/ml}$) | [18] |
| M^* | 199.16 | Molecular weight of clavulanic acid | [19] |

N. meningitides: *Neisseria meningitides*. ^aUsing *Neisseria meningitidis* for our numerical example, ^bUsing ceftriazone for our numerical example, ^cMeasured by using Accelrys Discovery Studio 3.5 client (DS visualizer) program, ^dCalculated by using a program

3. Results and Discussion

In this study, our first scenario or assumption is that there are patients' infected *N. meningitidis* with their different bacterial loads. These patients are treated by ceftriaxone, derivatives of 3rd generation cephalosporin. All parameters used in our simulation are summarized in Table 1. The plasma concentration of ceftriaxone is calculated by using time-weighted average plasma drug concentration with 0.5 g IV* (first row) of Table 2 in [11]. The results of monotherapy and combination therapy were reported in the following Sections.

Table 2. The parameters for evaluating the local lag coefficient

| Description | r_l (μm) | r_w (μm) | \bar{r} (μm) | ε | λ | G | g (/day) | μ (/day) | N/A | N/A | References |
|----------------------------------|----------------------------|----------------------------|--------------------------------|---------------|-----------------------------------|-------|---------------|-----------------|------------------------------------|------------------------------------|------------|
| Bacteria | | | | | | | | | | | |
| <i>P. aeruginosa</i> | 1 | 0.275 | 0.57 | 3.64 | 0.019 | 0.995 | 0.48 | 0.33 | N/A | N/A | [12,10] |
| Antibiotics | r_l (μm) | r_w (μm) | \bar{r} (μm) | ε | λ ($\times 10^{-5}$) | G | M | α | K ($\mu\text{g}/\text{ml}$) | k ($\mu\text{g}/\text{ml}$) | References |
| Penicillins | | | | | | | | | | | |
| Amoxicillin | 0.7768 | 0.3396 | 0.4474 | 2.2876 | 1.49 | 1 | 365.4042 | 0.85 | 5.6 | 0.21 | [19,21] |
| Ampicillin | 0.7265 | 0.4517 | 0.5292 | 1.6084 | 1.76 | 1 | 349.4048 | 0.8 | 4.8 | 0.18 | [19,21] |
| Cephalosporins | | | | | | | | | | | |
| 1st generation | | | | | | | | | | | |
| Cephalexin | 0.702 | 0.3237 | 0.4190 | 2.1687 | 1.40 | 1 | 347.3889 | 0.895 | 16 | 0.598 | [19-22] |
| Cefazolin | 0.8931 | 0.304 | 0.4353 | 2.9377 | 1.45 | 1 | 454.5072 | 0.26 | 188 | 7.031 | [19-22] |
| 2nd generation | | | | | | | | | | | |
| Cefuroxime | 0.8949 | 0.4559 | 0.5709 | 1.9626 | 1.90 | 1 | 424.3852 | 0.7 | 51 | 1.907 | [20-22] |
| Cefoxitin | 0.9067 | 0.3372 | 0.4689 | 2.6893 | 1.56 | 1 | 427.4521 | 0.27 | 110 | 4.114 | [20-22] |
| 3rd generation | | | | | | | | | | | |
| Cefotaxime | 0.8388 | 0.4600 | 0.5620 | 1.8235 | 1.87 | 1 | 455.4655 | 0.64 | 46 | 1.720 | [20-22] |
| Ceftazidime | 0.8299 | 0.6039 | 0.6715 | 1.3742 | 2.24 | 1 | 546.5761 | 0.9 | 69 | 2.580 | [20-22] |
| 4th generation | | | | | | | | | | | |
| Cefepime | 0.9549 | 0.4605 | 0.5872 | 2.0738 | 1.96 | 1 | 480.5611 | 0.8 | 70 | 2.618 | [19-21,23] |
| Phagocytes | r_l (μm) | r_w (μm) | \bar{r} (μm) | ε | λ | G | N/A | N/A | N/A | N/A | References |
| Neutrophil | | 8 | 8.618 | 1.25 | 0.2873 | 0.95 | N/A | N/A | N/A | N/A | [24] |
| Macrophage | 10 | 5 | 7.937 | 4 | 0.2646 | 0.94 | N/A | N/A | N/A | N/A | [24] |

P. aeruginosa: Pseudomonas aeruginosa

3.1 Results of Monotherapy, Combination Therapy and Drug Resistance

Figure 2(a) illustrates the logarithmic plots of different bacterial loads with the fixed plasma drug concentration. It is noticeable that the maximal of the initial bacterial loads of this figure does not decline, but still increases continuously. This means that the given plasma drug concentration cannot diminish or eliminate this initial bacterial density. On the contrary, the other bacterial loads below 1×10^7 copies/ml blood can be cleared within 1-7 days. After the patients have received antibacterial drugs, bacterial load in each patient gradually declines except for the one that still increases since this plasma drug concentration level is not enough to wipe out all bacteria from the patient's blood.

Figure 2(b) demonstrates the normal plots of various bacterial loads. Those initial bacterial loads below 1.5×10^7 copies/ml blood go down and become zero within 2-7 days. At the initial bacterial load, 1.5×10^7 copies/ml blood, there is no way for this bacterial load to become zero or be completely eliminated.

In Figure 2(c), the logarithmic plots of different plasma drug concentrations with a fixed initial bacterial load, 10^7 copies/ml blood are considered. It can be observed from these four plots that the time for treatment is about 2-11 days to clear bacteremia while the average plasma drug concentration, $10 \mu\text{g/ml}$, cannot reduce the bacterial density.

3.2 Peak and Mean Plasma Drug Concentration

All antibiotics, such as penicillins and cephalosporins, are complex to compare with each numerical result due to their drug dosage and plasma drug concentration. However, the peak plasma drug concentration can be available. Our model is based on the proportion of mean and peak plasma drug concentration of ceftriaxone. The profile of ceftriaxone concentration is given in Table 2 [22]. This section introduces peak plasma drug concentration of penicillins and cephalosporins to use them with other bacteria, *P. aeruginosa* for generating numerical results. Furthermore, these following variables are used for generating results: r_l and r_w are half of length and width, respectively. $\bar{r} = \sqrt[3]{(r_w)^2 r_l}$ is the geometric mean. $\varepsilon = r_l / r_w$ and $\lambda = \bar{r} / r^{(capillary)}$ are the particle aspect ratio and the relative particle radius, respectively, and used for finding the local lag coefficient. $G = v^{(particle)} / v^{(fluid)}$ is the local lag coefficient. $v^{(fluid)}$ and $v^{(particle)}$ are two velocities of fluid and particle, respectively, moving by convection of fluid. K and $k = K \left(\frac{k^{(ceftriazone)}}{K^{(ceftriazone)}} \right)$ are peak and mean plasma drug concentration, where $K^{(ceftriazone)} = 123 \mu\text{g/ml}$ and $k^{(ceftriazone)} = 4.6 \mu\text{g/ml}$ are peak and mean plasma ceftriaxone concentration, used for calculating k . M and α are the molecular weight and free fraction of drug molecules. N/A is non-applicable. Length and width of drug molecules are measured by using Accelrys Discovery Studio 3.5 client (DS Visualizer) program.

3.3 Results of Penicillin Group and Generations of Cephalosporin with *P.*

Aeruginosa

Other cell wall inhibitors, besides ceftriaxone, such as amoxicillin or ampicillin in penicillin group and 1st to 4th generation of cephalosporin are considered with the growth and death rate of *P. aeruginosa*, denoted by g and μ in Table 2, which are, respectively. Figure 3a-1 and 4a-1, and 5a-c show the numerical results of both penicillins and cephalosporins with *P. aeruginosa*.

Figure 5d-h shows five the fitting curves for the analysis of penicillin group and 1st to 4th generation of cephalosporin. First, in Figure 5(d), the orientation probability factor from penicillin group to 4th generation goes down, implying that the chance or probability of beta-lactamase for destroying beta-lactams in the mechanism of bacterial resistance decreases. This can be explained by increasing the steric effect of R-group or functional group of beta-lactams and then orientation probability factor decreases. Thus, this result confirms that the development of beta-lactams can prevent from bacterial resistance. Secondly, in Figure 5(e), the efficacy of dual action is higher by upgrading from penicillin group and 1st to 4th generation of cephalosporin. The reason is that beta-lactamase in bacteria cannot split many classes of beta-lactams with two previous reasons and then beta-lactamase will bind clavulanic acid instead of high beta-lactams. Finally, beta-lactamase is inactivated by clavulanic acid as beta-lactamase inhibitor. This result also confirms that high developmental beta-lactamase inhibitors can prevent from bacterial resistance. Other three Figures 5f-h show that the high beta-lactams can increase bacterial death rate with/without resistance and with dual action. In conclusion, bacterial death rate in our model, consisting of the orientation probability

factor, and dual action factor in this section, satisfies the low to high potency of penicillin and cephalosporin.



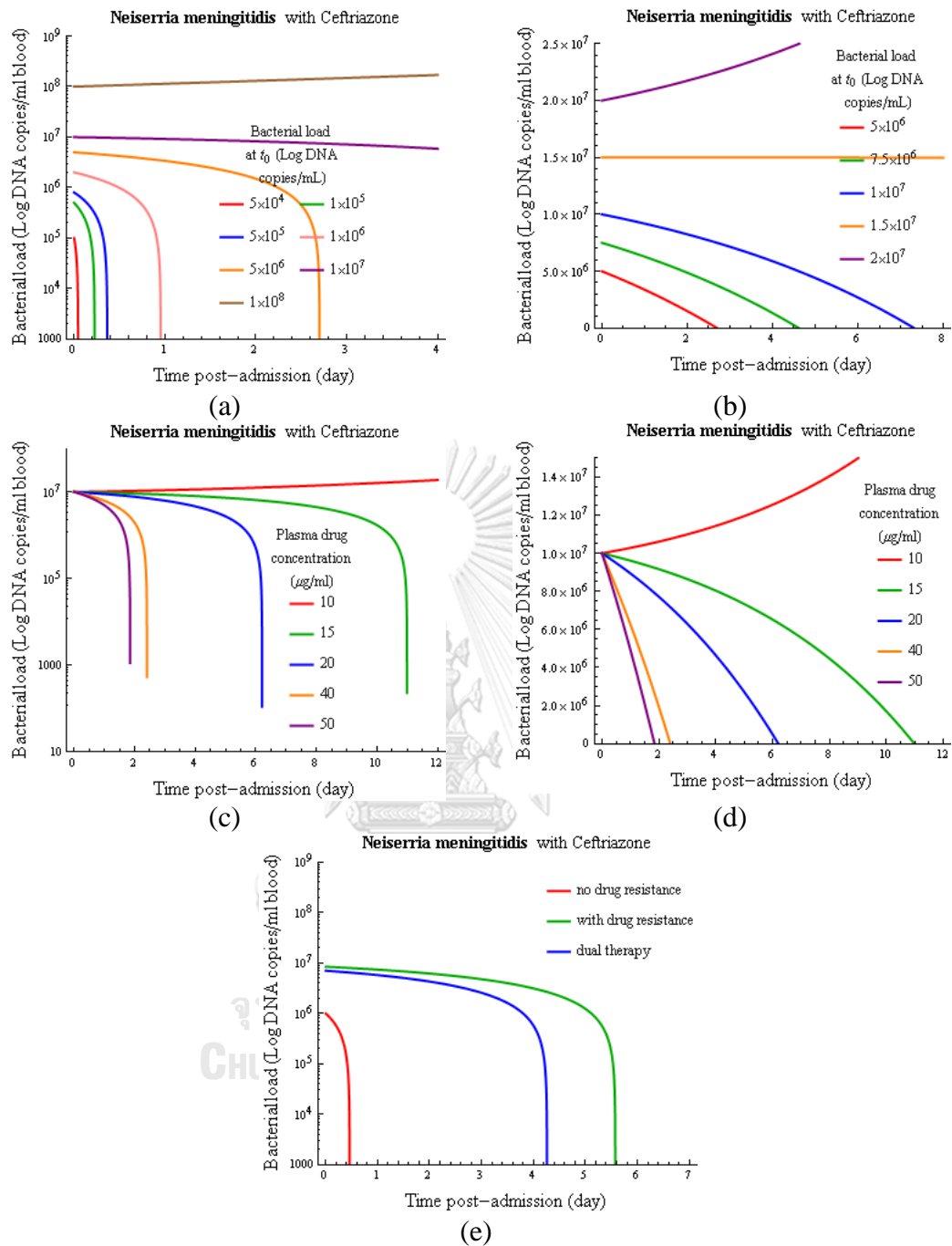


Figure 2. Our estimation results with different values of bacterial load, plasma drug concentration, number of post-admission days. (a) The logarithmic plots between time post-admission (day) and different initial bacterial loads with fixed plasma drug concentration. (b) The normal plots between time post-admission (day) and different

initial bacterial loads with fixed plasma drug concentration. (c) The logarithmic plots between time post-admission (day) and the same initial bacterial load with different plasma drug concentrations. (d) The normal plots between time post-admission (day) and the same initial bacterial load with different plasma drug concentrations. (e) Our results of no drug resistance, drug resistance, and dual therapy.



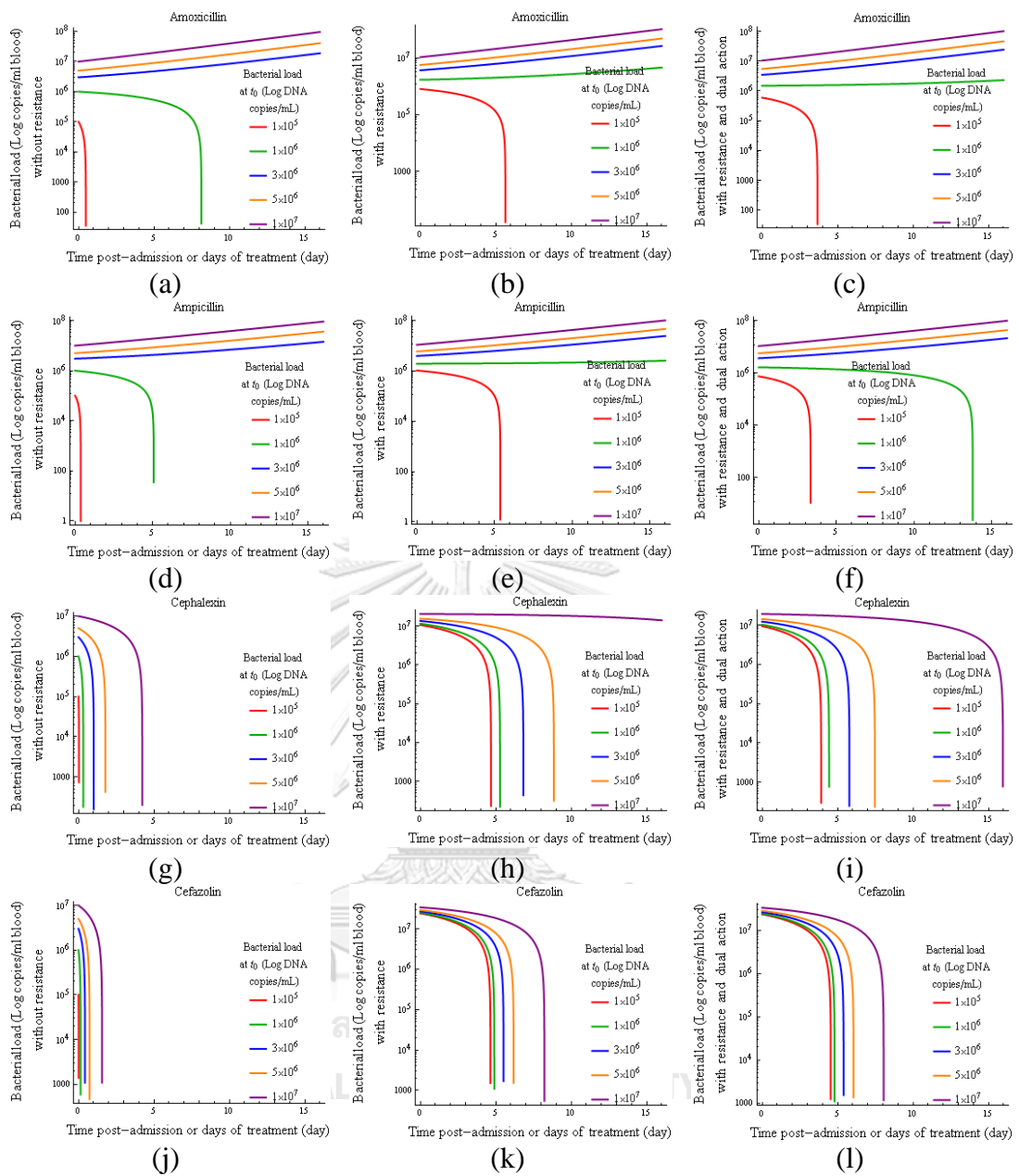


Figure 3. (a-l) show the numerical results between bacterial load of *Pseudomonas aeruginosa* and time after antibiotics administration. Amoxicillin in (a-c) and ampicillin in (d-f) of penicillin group, cephalexin in (g-i) and cefazolin in (j-l), representing 1st generation of cephalosporins were used for these simulations with/without resistance and with dual action of clavulanate as beta-lactamase inhibitors.

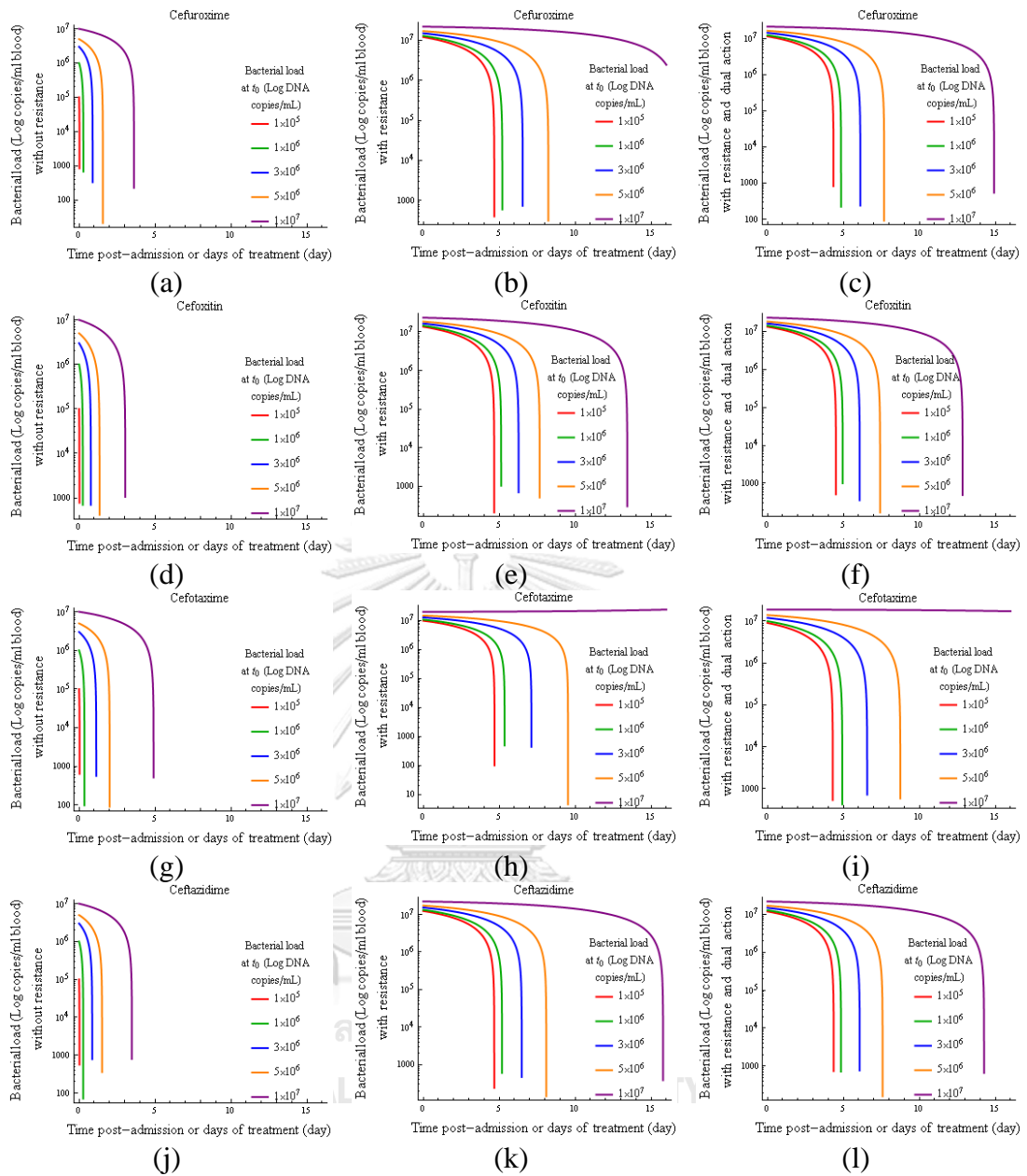


Figure 4. (a-l) shows the numerical results between bacterial load of *Pseudomonas aeruginosa* and time after antibiotics administration. Cefuroxime in (a-c) and cefoxitin in (d-f), representing 2nd generation of cephalosporins, cefotaxime in (g-i) and ceftazidime in (j-l), representing 3rd generation of cephalosporins are used for these simulations with/without resistance and with dual action of clavulanate as beta-lactamase inhibitors.

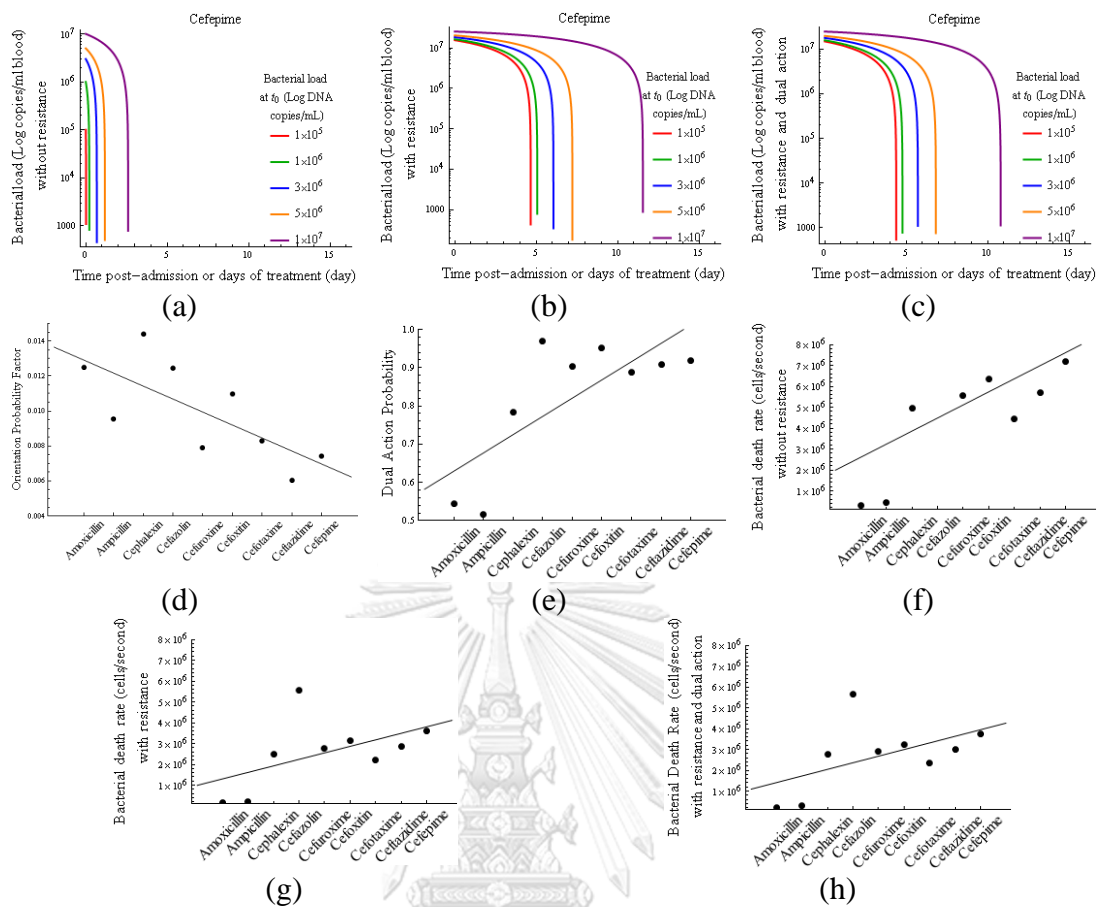


Figure 5. (a-c) The numerical results between bacterial load of *Pseudomonas aeruginosa* and Time after antibiotics administration. Cefepime in (a-c), representing 4th generation of cephalosporins, used for these simulations with/without resistance and with dual action of clavulanate as beta-lactamase inhibitors. (d-h) show the curve fitting of orientation probability factor, dual action probability and bacterial death rate with/ without resistance and dual action.

4. Conclusion

In this study, a set of mathematical models of bacteria in patient's blood after antibiotic treatment were focused by using PD, physics and chemistry. The proposed models can capture the recuperation behavior and time of patients treated with antibiotics for clearing bacteria in patient's blood. The probability of drug molecule binding bacteria was determined by assuming drug molecules to be spherical and bacteria to be prolate spheroid. All bacteria have different orientations. Furthermore, the mortality rate of bacteria in blood circulation due to drug, the relationship between the population of bacteria with respect to time, and the duration of treatment were modeled. Finally, we hope that our models will be an alternative choice for evaluating the duration of treatment of patient with bacterial infection in blood.

Acknowledgements



The authors would like to thank Professor Dr. Supa Hannongbua and Assistant Professor Dr. Patchreenart Sarpapakorn for helping about the measurement of drug molecules which have greatly increased the credit of our paper. We also thank Dr. Panadda Dechadilok for suggesting the theory of convective rate. This research was supported by scholarship 60/40 of Chulalongkorn University.

References

1. Austin DJ, White NJ, Anderson RM. The dynamics of drug action on the within-host population growth of infectious agents: Melding pharmacokinetics with pathogen population dynamics. *J Theor Biol* 1998;194:313-39.
2. Varani G. Diffusion and Molecular Shape and Size, Department of Chemistry; 2013. p. 4-5.
3. Agasanapura BN, Baltus RE, Chellam S. Effect of Convective Hindrance on Microfiltration of Rod Shaped Particles, *AIChE Journal*, Proceedings of Conference for Annual Meeting. 2011. p. 5-29.
4. Mazaheri A. A review of the literature, probabilistic modeling of ship grounding, Helsinki University of Technology. Faculty of Engineering and Architecture, Department of Applied Mechanics, 2009. p. 26-34.
5. Berg HC, Purcell EM. Physics of chemoreception. *Biophys J* 1977;20:193-219.
6. Taroni C, Jones S, Thornton JM. Analysis and prediction of carbohydrate binding sites. *Protein Eng* 2000;13:89-98.
7. Khurana I. Textbook of Medical Physiology; Dynamics of Circulation: Pressure and Flow of Blood and Lymph. New York: Elsevier; 2006. p. 327.
8. Dilsizian V, Pohost GM, Cardiac CT. PET and MR, Multislice Cardiac Tomography: Myocardial Function, Perfusion, and Viability. Chichester: Blackwell Publishing Ltd.; 2010. p. 260.
9. Friedman A, Lungu EM. Can malaria parasite pathogenesis be prevented by treatment with tumor necrosis factor-alpha? *Math Biosci Eng* 2013;10:609-24.

10. Middelboe M. Bacterial growth rate and marine virus-host dynamics. *Microb Ecol* 2000;40:114-24.
11. Drugs.com, Ceftriaxone - FDA Prescribing Information, Side Effects and Uses. Available from: <http://www.drugs.com/pro/ceftriaxone.html>. [Last cited on 2014 Nov 14].
12. Kowalski WJ, Bahnfleth WP, Whittam TS. Filtration of airborne microorganisms: Modeling and prediction. *ASHRAE Trans* 1999;105:5-6.
13. Krstic RV. Human Microscopic Anatomy: An Atlas for Students of Medicine and Biology. Germany: Springer-Verlag, Berlin Heidelberg; 1997. p. 54-5.
14. Pollak AN. Emergency care and transportation of the sick and injured. *The Human Body*. 10th ed. Ch. 4. USA: Jones and Bartlett publishers; 2005. p. 108-9.
15. Pocock G, Richards CD, Richards DA. Human physiology. *The Properties of Blood*. 4th ed. Ch.18. USA: C&C Offset Printing Co. Ltd.; 2013. p. 312-3.
16. Joynt GM, Lipman J, Gomersall CD, Young RJ, Wong EL, Gin T. The pharmacokinetics of once-daily dosing of ceftriaxone in critically ill patients. *J Antimicrob Chemother* 2001;47:421-9.
17. Staver JR, Lumpe AT. A content analysis of the presentation of the mole concept in chemistry textbooks. *J Res Sci Teaching* 1993;30:321-37.
18. Vree TB, Dammers E, Exler PS. Identical pattern of highly variable absorption of clavulanic acid from four different oral formulations of co-amoxiclav in healthy subjects. *J Antimicrob Chemother* 2003;51:373-8.
19. PubChem Open Chemistry Database, U.S. National Library of Medicine, National Center for Biotechnology Information. Available from:

<https://www.pubchem.ncbi.nlm.nih.gov/compound/5280980#section=Top>.

[Last accessed on 2016 Feb 02].

20. Hackett SJ, Guiver M, Marsh J, Sills JA, Thomson AP, Kaczmarek EB, *et al.* Meningococcal bacterial DNA load at presentation correlates with disease severity. *Arch Dis Child* 2002;86:44-6.
21. Masoud MS, Ali AE, Nasr NM. Chemistry, classification, pharmacokinetics, clinical uses and analysis of beta lactam antibiotics: A review. *J Chem Pharm Res* 2014;6:28-58.
22. Starlin R, Lin TL, Goodenberger DM. “Antimicrobial Agents”, The Washington Manual Infectious Diseases Subspecialty Consult, Department of Medicine. Ch. 27. Washington University School of Medicine; 2005. p. 248-57.
23. Wiskirchen DE, Keel-Jayakumar RA, Nicolau DP. Continuous and intermittent infusion beta-lactam antibiotics. *Casebook in Clinical Pharmacokinetics and Drug Dosing*. 1st ed. Ch. 3. New York, NY: McGraw-Hill Education/Medical; 2015.
24. Freitas RA Jr. Section 8.5.1 “Cytometrics”, *Nanomedicine, Volume I: Basic Capabilities*, Landes Bioscience, Georgetown, TX; 1999. Available from: <http://www.nanomedicine.com/NMIA/15.4.3.1.htm>. [Last cited on 2016 Jan 04]

CHAPTER 3
PREDICTING THE DURATION OF ANTIMALARIAL TREATMENT WITH
HEME DEGRADATION INHIBITORS OF BLOOD SCHIZONTICIDES
USING MATHEMATICAL MODELS

Panit Suavansri¹ and Nataphan Kitisin^{2*}

¹Department of Mathematics and Computer Science, Faculty of Science,
Chulalongkorn University, Phayathai Road, Patumwan, Bangkok, 10330, Thailand)

²Department of Mathematics and Computer Science, Faculty of Science,
Chulalongkorn University, Phayathai Road, Patumwan, Bangkok, 10330, Thailand)

*** Corresponding author, Email address: nataphan.k@gmail.com**

จุฬาลงกรณ์มหาวิทยาลัย

CHULALONGKORN UNIVERSITY

This article was accepted in Songklanakarin Journal of Science and
Technology (SJST).

Submitted 18 April 2017

Revised 05 June 2017

Accepted 03 July 2017

Abstract

The mathematical model of the death rate of malaria parasite due to the antimalarial drugs in this paper is established to predict the treatment duration and the drug dosage. This model bases on the probabilities, pharmacokinetics and pharmacodynamics (PK/PD), biology, medical sciences, theoretical physics and chemistry. The death rate of malaria parasite is derived from the flow rate of drug molecules with respect to malaria parasite by using the theory of blood convection and probabilities. Coupled with the malaria model, the numerical results are generated. In conclusion, the numerical result for the treatment duration from our model ranges between 1 to 10 days, conforming to the actual clinical data of the patient.

Keywords: Malaria, Death rate, Probability

1. Introduction

For several thousand years, humans have been suffered and killed by various lethal diseases. Infectious diseases caused by pathogens such as bacteria, virus, protozoa (especially malaria) and fungi have resulted in high fatality across the general population. In particular, Malarial disease is also one of the most lethal infectious diseases in human history (Li, Ruan, & Xiao, 2011). Severity of malarial disease is well documented in so many countries, especially in Africa and Asia (CDC, 2016). Malaria is the infectious, contagious disease caused by the specific protozoa called *Plasmodium*. There are 5 species of genus *Plasmodium* that can infect human which are: *P. vivax*, *P. ovale*, *P. malariae*, *P. falciparum* and *P. knowlesi*. All of them are transmitted by female *Anopheles* mosquitoes (Li, Ruan, & Xiao, 2011). Thus, in order to treat the patients with malarial infection, several physicians have tried to administer various antimalarial drugs and then use clinical trials to collect the data on the duration of treatments of the certain drugs. Furthermore, each patient blood must be sent to laboratory to evaluate the pathogen density and the treatment has to be monitored continuously before calling off the intravenous or oral drug administration. Therefore, the effective mathematical model to predict the termination time of the treatment is the main focus of this study.

The pathophysiology of malaria in human body consists of two cycles: sexual and asexual cycles. After a female *Anopheles* mosquito bites and releases sporozoites in her saliva into human bloodstream, sporozoites will travel via bloodstream and enter the liver. Once there, the germ will invade the hepatocytes or liver cells, replicate itself

and leave the liver cells to infect healthy red blood cells (RBCs). This intracellular malaria parasite in infected red blood cell (iRBC) then develops into various stages: early to late trophozoite and early to late schizont sequentially. During the late schizont stage, the intracellular parasites which are called merozoite will be released through the ruptured membrane of the iRBC (Li, Ruan, & Xiao, 2011). They will spread throughout the bloodstream and infect new healthy RBCs. This process is known as the asexual cycle. While the parasites are in the iRBCs, they need to extract heme from hemoglobin in cytoplasm of the RBCs and convert it into hemozoin or malarial pigment. The process is vital to the parasites since heme is water-soluble and toxic to them while water-insoluble hemozoin is not. Thus, one of the methods to get rid of the parasite is to inhibit this process. Our study will focus only on the anti-malarial drugs which target the hemozoin formulation or heme degradation inhibition (ter Kuile et al., 1993; Wilairatana & Looareesuwan, 1996).

There has been a mathematical model pertaining the population of the normal within-host malaria parasites according to Austin, White, Anderson (1998). However, their model did not take into account of the effect of the drug treatment. In this paper, we will incorporate the consequence of the drug to the population of the malaria parasites. The main idea is that blood flow will transfer the drug molecules to bind iRBCs, and therefore eliminate the iRBCs (see Figure 1). Nevertheless, to translate this real situation into mathematical models, there must be some assumptions and hypotheses with the fundamental of physics, chemistry, microbiology and pharmacology that we have to adapt. The following assumptions and hypotheses were made: (i) the collision or binding rate between drug molecule and iRBC depends on the relative velocity between both of them, (ii) probability of binding or capturing between

drug molecule and iRBC depends on five probability factors, derived from theoretical physics and chemistry, (iii) the drug is effective in the sense that for the right condition one drug molecule can annihilate one iRBC, and (iv) the level of the plasma drug is constant and time-independent. Hence, the formulation of this mathematical model bases on various scientific disciplines. For instance, the relative velocity and convective rate, which are used to construct the flow rate of drug for eliminating malaria parasite, base on physics. Conversion of plasma into drug molecules uses the knowledges from chemistry and pharmacology. Moreover, the mathematical model of within-host malaria is derived from pathology of malaria. Thus, the death rate of malaria parasite should be more accurate.

First, the shape of drug molecules is assumed to be spherical instead of the prolate spheroid as shown in Figure 1 and we will estimate an average radius of the drug molecule as in the followings. Define $r_w^{(drug)}$ and $r_l^{(drug)}$ to be the half width and half length of the prolate spheroidal shape of drug molecule. Next, we evaluate an average radius of this drug molecule (Pabst & Gregorová, 2007), by calculating the geometric mean of $r_w^{(drug)}$ and $r_l^{(drug)}$. Thus, the average radius of drug molecule in (Brinkman, 1949; Pabst & Gregorová, 2007), called Stokes radius and denoted by $r^{(stoke)}$, can be derived from its prolate volume $V^{(prolate)}$ in terms of $r_w^{(drug)}$ and $r_l^{(drug)}$ as follows:

$$V^{(sphere)} = V^{(prolate)},$$

$$\frac{4}{3}\pi\left(r^{(stoke)}\right)^3 = \frac{4}{3}\pi r_l^{(drug)}\left(r_w^{(drug)}\right)^2,$$

$$r^{(stoke)} = \left(r_l^{(drug)}\left(r_w^{(drug)}\right)^2\right)^{1/3}.$$

Similar to the case of a particle diffused in the certain fluid such as oil, we model the diffusion of drug molecule and iRBC in the bloodstream accordingly. Therefore, as illustrated in Figure 1, the average radius of drug molecule, defined as

$$r^{-(drug)} = \left(r_l^{(drug)} \left(r_w^{(drug)} \right)^2 \right)^{1/3}, \text{ can be written in the similar form as } r^{(stoke)}.$$

Before formulating the death rate of the malaria parasite due to drug, it is important to note the pathogenesis of the malaria and how the antimalarial drug mechanism works. The purpose of heme degradation in *Plasmodium sp.* is to eliminate heme by converting water-soluble and toxic heme into water-insoluble and nontoxic substances, called hemozoin or malarial pigment, enabling to excrete (de Villiers & Egan, 2009). This study focuses on chloroquine, mefloquine and halofantrine as antimalarial drugs with the mechanism of heme degradation inhibition by binding iron (Fe(II)) in Fe(II)-protoporphyrin IX (Fe(II)PPIX or heme). On the other hand, we also use artesunate of artemisinin group as antimalarial drugs with mechanism of heme degradation inhibition without binding Fe(II)PPIX. Mechanism of artesunate has not yet been clearly understood but there are strong evidents that either intraparasitic ferrous heme and free ferrous iron will convert artesunate into free radicals by cleaving the artesunate's peroxide bridge. Afterward, these intraparasitic free radicals would eliminate the parasite by destroying the lipid layer of the parasitic cell membrane, vacuole sac and other parasitic structures such as parasitic enzymes. As parasitic enzymes converting water-soluble toxic hemes (Fe(II)-protoporphyrin IX (Fe(II)PPIX)) into excretable hemozoin (heme crystals (Fe(III)PPIX)) which occurs in vacuole sac are destroyed, the heme degradation are inhibited. When vacuole sac

ruptures, free radicals are released and therefore destroy the parasites (ter Kuile et al., 1993; Wilairatana & Looareesuwan, 1996).

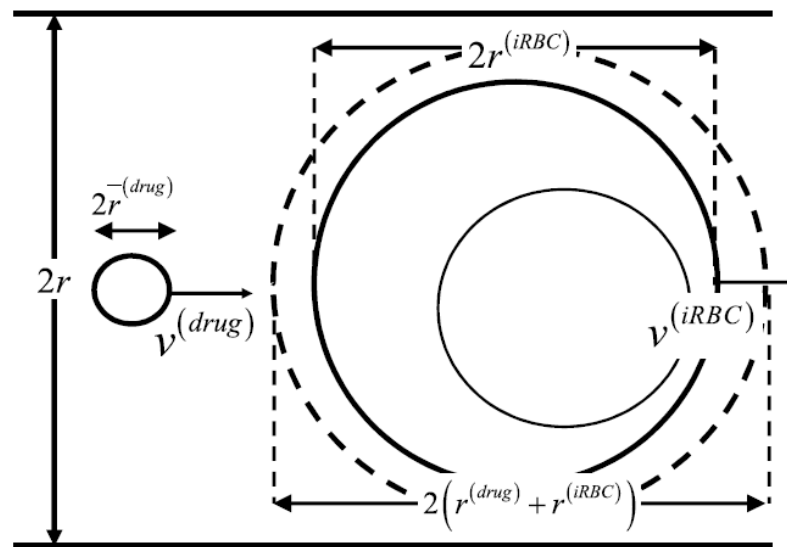


Figure 1. The transportation of the drug molecule to an intracellular parasite within infected red blood cell (iRBC) by convection of bloodstream (see parameters in Section 2).

จุฬาลงกรณ์มหาวิทยาลัย
CHULALONGKORN UNIVERSITY

2. Materials and Methods

This section reviews the contents in each subsection that will be used to formulate the death rate of the malaria parasites due to drug. First, we discuss the relative velocity between drug molecule and iRBC, based on theoretical physics, which we use to find the specific blood volume that contains particular drug mass used to kill the parasite. Second, five probabilistic binding factors between drug molecule and

iRBC that we will use to determine the effective drug molecules will be discussed. Five probability factors are as follows (i) position probability factor used to determining a binding chance by position alignment between drug and iRBC, (ii) binding probability factor of the drug molecule and intracellular parasite, but not the iRBC's cytoplasm, (iii) capture probability factor which is the ability of drug to transport and does not deviate from target, (iv) orientation probability factor which is the probability of local collision between the drug and iron molecules in heme, (v) population probability factor is the ability of the drug molecule to attach only to iRBC, but not the normal RBC. Since five probability factors are sequentially continuous and independent, they can be multiplied to give the total probability factor. In order to use the total probability factor to evaluate the effective of the drug molecules, we need to compute mass of the drug. To do so, we have to convert the specific blood volume derived from the relative velocity into drug mass by using the plasma drug concentration and taking into account of the parameters of chemistry, such as Avogadro's number and molecular mass as well. Consequently, we are able to calculate the total drug molecules within all capillaries and venules of human host. Note that this death rate of the malaria parasites due to the drug is the same as the death rate of the iRBC's since we consider only the blood schizonticides. Finally, by subtracting the dynamic population of iRBCs in normal malaria model with our death rate due to the drug, we then simulate numerical results for predicting the duration of treatment as shown in Figure 2.

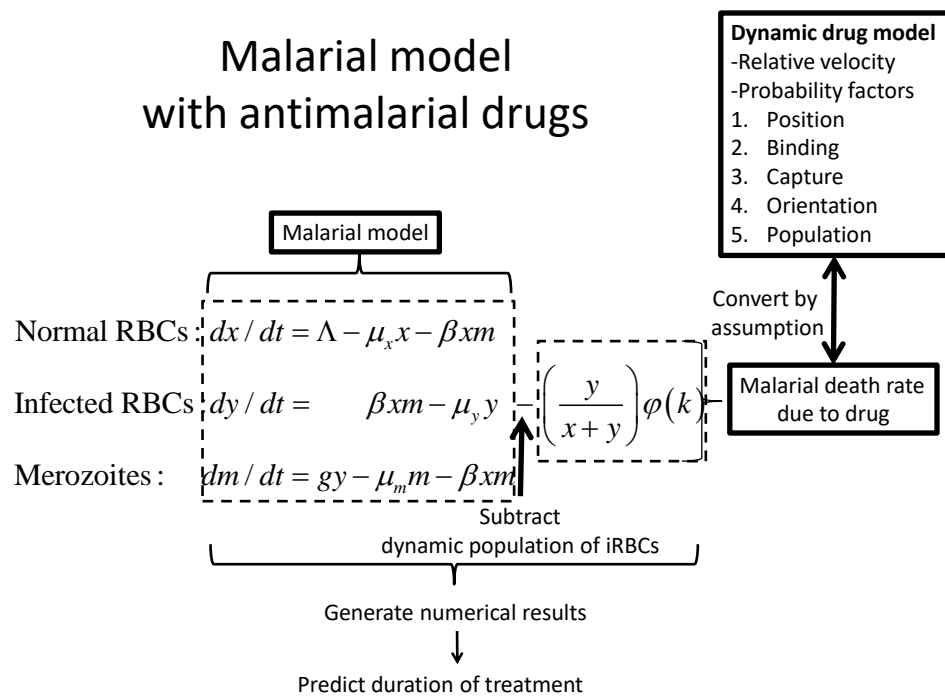


Figure 2. Algorithm for formulating the death rate of the malaria parasites due to drug by using five probability factors and the relative velocity between drug molecule and parasite, and predicting the duration of treatment.

2.1 Relative velocity between drug molecule and infected red blood cell

According to the principal of velocity in physics, since iRBC is larger than drug molecule, the velocity of iRBC is slower than drug molecule, i.e. $v^{(iRBC)} < v^{(drug)}$ (Agasanapura, Baltus, & Chellam, 2011), where $v^{(iRBC)}$ and $v^{(drug)}$ are the velocities of iRBC and drug molecule, respectively. Define $v^{(relative)} = v^{(drug)} - v^{(iRBC)}$ to be the relative velocity of drugs with respect to the velocity of iRBC. After t units time, the length vasculature containing drug molecule is $tv^{(relative)}$. Since $v^{(iRBC)}$ and $v^{(drug)}$ can be obtained from using a term called local lag coefficient (denoted by G) (Agasanapura,

Baltus, & Chellam, 2011), $v^{(iRBC)} = G^{(iRBC)}v^{(blood)}$ and $v^{(drug)} = G^{(drug)}v^{(blood)}$, where $G^{(drug)}$ and $G^{(iRBC)}$ are two local lag coefficients of drug and iRBC, respectively. Note that $G^{(drug)} > G^{(iRBC)}$. Hence, the relative velocity is

$$v^{(relative)} = v^{(drug)} - v^{(iRBC)} = \left(G^{(drug)} - G^{(iRBC)} \right) v^{(blood)}.$$

2.2 Position probability factor

The collision of drug molecules and iRBCs can be modeled by modifying the probabilistic model of ship grounding in (Mazaheri, 2009), traveling straight-forward through a waterway in straight-line. In this study, iRBCs, assumed to be stationary with respect to drug, act as obstacles or shoals and wait to bind with drug molecules. While the width of waterway represents the diameter of vasculature. We generalize this phenomenon from one-dimension (1D) to 2D. By our assumptions, iRBC's shape is spherical as shown in Figure 1. Since positions of both drug molecules and iRBC have been already aligned, position probability factor is defined as

$$p^{(position)} = \frac{\pi \left(r^{(iRBC)} + r^{(drug)} \right)^2}{\pi r^{(vessel)^2}} = \left(\frac{r^{(iRBC)} + r^{(drug)}}{r^{(vessel)}} \right)^2,$$

where $r^{(vessel)}$ is a radius of human blood vessel in cross-sectional view.

2.3 Binding probability factor

In 2007, Preetam Ghosh had done his doctoral dissertation concerning the Stochastic Models for In-silico Event-based Biological Network Simulation (Preetam, 2007). They used some probability theory to calculate the chance of binding between protein molecule and DNA. This suggests that the probability of collision between protein molecule and DNA during time Δt is $p^{(binding)} = \frac{\delta V}{V}$, where δV is a collision volume. In this work, after an antimalarial drug molecule enters iRBC with position probability factor, it must also enter an intracellular parasite to bind heme and inhibit heme degradation. Consequently, we define the total volume of iRBC and a volume of an intracellular parasite as $V^{(iRBC)}$ and $V^{(parasite)}$, respectively. Note that $V^{(parasite)}$ is the collision volume analogous to δV in (Preetam, 2007). Hence, for the antimalarial drug molecule to attach and eliminate the parasite, the binding probability factor should be defined as

$$p^{(binding)} = \frac{\delta V}{V} = \frac{V^{(parasite)}}{V^{(iRBC)}}.$$

Remark that the binding probability factor and the parasite volume fraction in (Ye et al., 2013), used in our numerical simulation, are the same.

2.4 Capture probability factor

Before determining the position and binding probability factors, the transportation of drug molecule can deviate from the target which is the iRBC. By the principal of physics, the longer distance between drug molecule and iRBC, the less

chance of them binding together. Hence, the capture probability in (Berg & Purcell, 1977) defined as

$$p^{(capture)} = \frac{r^{(iRBC)}}{r^{(iRBC)} + l},$$

is used and taken into account of this situation, where l is a length of human blood vessel.

2.5 Orientation probability factor

As the principal of chemistry, two substrates must bind together with correct orientation with the binding sites (Taroni, Jones, & Thornton, 2000). Thus, the orientation probability factor, defined as the probability of binding site of substrate attaching to an active site of enzyme, is the ratio of the binding area to the total surface area of drug molecule and denoted by

$$p^{(orientation)} = \frac{\pi z^2}{4} / \left\{ 2\pi \left(r_w^{(drug)} \right)^2 \left(1 + \frac{r_w^{(drug)}}{e r_l^{(drug)}} \sin^{-1} e \right) \right\},$$

is used and taken into account of this situation. The binding area ($\frac{\pi z^2}{4}$) is the circular area with diameter z , and the total surface area of drug molecule which is of the prolate spheroid shape, is $2\pi \left(r_w^{(drug)} \right)^2 \left(1 + \frac{r_w^{(drug)}}{e r_l^{(drug)}} \sin^{-1} e \right)$, where e is the eccentricity of the ellipse.

2.6 Population probability factor

Since both normal RBCs and iRBCs can be attached by drug molecule, the population probability factor, denoted by

$$p^{(population)} = \frac{y(t)}{x(t) + y(t)},$$

is used to evaluate the probability related to iRBCs only, where $x(t)$ and $y(t)$ are the populations of normal RBCs and iRBCs at time t , respectively.

2.7 Total probability

We have five probability factors involved in calculating the binding chance between drug molecule and iRBC. Again, they are position, binding, capture, orientation and population probability factors. As all of them are independent, the total probability factor can be defined as

$$p^{(total)} = p^{(position)} \times p^{(binding)} \times p^{(capture)} \times p^{(orientation)} \times p^{(population)}.$$

2.8 Mathematical model of malaria

Our study uses the mathematical model of malaria in (Austin, White, & Anderson, 1998). This model contains three dynamic populations: infected red blood cells (iRBCs), populations normal or uninfected red blood cells and extracellular parasites or merozoites, denoted by $y = y(t)$, $x = x(t)$ and $m = m(t)$, respectively. The model is given by

$$\begin{aligned} dx/dt &= \Lambda - \mu_x x - \beta xm, \\ dy/dt &= \beta xm - \mu_y y, \\ dm/dt &= gy - \mu_m m - \beta xm, \end{aligned}$$

where μ_x , μ_y and μ_m are the natural death rate of uninfected RBCs, infected RBCs and merozoites, Λ is the production rate of normal RBCs, β is the infectivity of merozoites and g is the number of merozoites released per infected RBCs (see their values of all parameters in Table 2).

2.9 Dynamic drug model

Our model to formulate the death rate of the malaria parasite in this paper has taken into account of both capillaries and venules. The death rate can be modeled in the following steps: (i) evaluate the number of drug molecules attaching parasites per unit time (ii) use the assumption that the drug is effective in the sense that for the right condition one drug molecule can annihilate one iRBC's cell. First, we compute the amount of drug from the knowledge of the plasma drug concentration in the specific blood volume. This specific blood volume is similar to the collision volume which is explained in the binding probability factor of the previous section. The blood volume must be considered in all the number of vessels, denoted by $N^{(vessel)}$. Thus, if the cross-sectional area of a vessel is $\pi \left(r^{(vessel)} \right)^2$ and the length that blood volume sweeps with time t is $v^{(relative)} t$, then the total blood volume is $\pi \left(r^{(vessel)} \right)^2 N^{(vessel)} v^{(relative)} t$. Therefore, drug mass in this particular volume at time t is can be calculated by multiplying plasma drug concentration at time t , denoted by $C(t)$. We can convert this drug mass into the

number of drug molecules by divided by molecular mass of the drug M , and multiplying with Avogadro's number A . Since parasite elimination process occurs in all vessels, the total number of drug molecules at time t , denoted by $N^{(drug)}$, is $N^{(drug)} = \pi \left(r^{(vessel)} \right)^2 C(t) A v^{(relative)} t / M$. Now will take into account of the probabilistic chance of the binding will result in the effectiveness of the elimination process of the parasites as follows: (a) Obtain the interval of time that drug molecules can follow parasites by using the proportion of time in vessels, called transit time and denoted by τ , and the circulatory time, denoted by ρ . (b) Obtain the drug molecules that have not bounded to any target by using the free fraction of drug, denoted by α . (c) multiply with the total probability factor as before. (d) divide by the total blood volume of patient, denoted by $V^{(blood)}$. Finally, convert $N^{(drug)}$ into the rate by dividing by t .

The death rate of the malaria parasites in this paper can be formulated as shown in Figure 3 with parameters in Table 2. Note that the death rate is also considered in both capillaries and venules.

Hence, the death rate of the malaria parasites will be defined as:

$$\Psi(t) = \frac{\pi \alpha N^{(vessel)} \tau \left(r^{(vessel)} \right)^2 C(t) A p^{(total)} v^{(relative)}}{\rho M V^{(blood)}} .$$

Moreover, since antimalarial drug molecules can follow infected red blood cells in both capillaries and venules, the total death rate of the malaria parasites is defined as:

$$\Psi^{(total)}(t) = \Psi^{(capillary)}(t) + \Psi^{(venule)}(t).$$

Note that by one of our assumptions, the anti-malarial drug intravenous route administration maintains the constant plasma drug concentration. Consequently, it makes the flow rate of drug molecule depend only on the constant drug concentration k . Therefore, the flow rate of drug molecule $\Psi(k)$, which is time-independent, is used instead of $\Psi(t)$. Before generating numerical results, dynamic variables x and y in the population probability factor are extracted from $\Psi^{(total)}(k)$. If we define

$$\varphi(k) = \Psi^{(total)}(k) / p^{(population)} = \left(\frac{x+y}{y} \right) \Psi^{(total)}(k),$$

then, the death rate of malaria parasite is $\Psi^{(total)}(k) = \left(\frac{y}{x+y} \right) \varphi(k)$. This shows us that there is no the death rate of malaria parasite when there is no parasitaemia, i.e. $\Psi^{(total)}(k) \rightarrow 0$ as $y \rightarrow 0$. This conforms the real situation.

Finally, the mathematical model of within-host malaria parasite after antimalarial drug administration becomes

$$\begin{aligned} dx/dt &= \Lambda - \mu_x x - \beta xm, \\ dy/dt &= \beta xm - \mu_y y - \left(\frac{y}{x+y} \right) \varphi(k), \\ dm/dt &= gy - \mu_m m - \beta xm. \end{aligned}$$

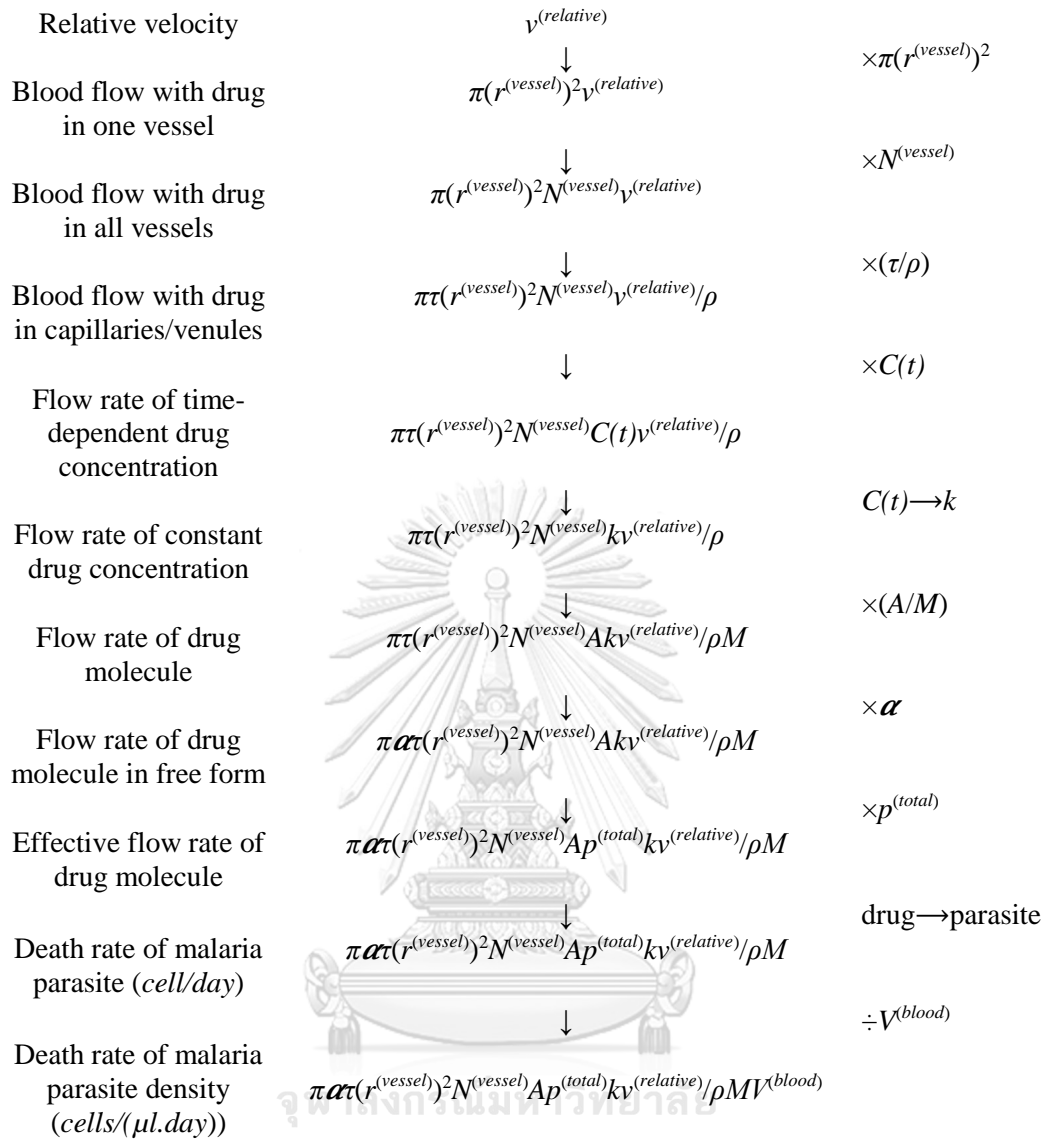


Figure 3. This diagram shows formulation of the death rate of malaria parasite.

3. Results and Discussion

This section illustrates the numerical results for the antimalarial drugs: artesunate, chloroquine, mefloquine and halofantrine in the cases of monotherapy, drug resistance and combination therapy. These numerical results use parameters given in Table 1 and 2. The first subsection of monotherapy shows the numerical results of artesunate, chloroquine, mefloquine and halofantrine. Furthermore, we are using the patient's clinical data from White (2011) to compare with our numerical results, shown in Figure 4. The second subsection of drug resistance illustrates the numerical results of the four drugs, stated in the previous subsection with resistance shown in Figure 5. The third subsection of combination therapy illustrates the numerical results of chloroquine, mefloquine and halofantrine with their resistance and artemisinin-based combination therapy or ACT shown in Figure 5.

Table 1. Parameters of chloroquine, mefloquine, halofantrine and artesunate.

| Notations | r_l (nm) | r_w (nm) | M | α | k (ng/ml) | References |
|--------------|------------|------------|----------|----------|-------------|--|
| Chloroquine | 0.7856 | 0.35525 | 319.8721 | 0.45 | 120 | (Karbwang et al., 1992; White, 1992) |
| Mefloquine | 0.6333 | 0.33765 | 378.3122 | 0.02 | 500-638 | (White, 1992) |
| Halofantrine | 0.86655 | 0.427 | 500.4237 | 0.02 | 1000 | (Veenendaal et al., 1991; White, 1992) |
| Artesunate | 0.7619 | 0.37065 | 384.4208 | 0.38 | 110-310 | (Ashton et al., 1998; Morris et al., 2011) |

Table 2. Parameters for numerical simulations in case of malarial infection.

| Symbols | Value | Variables | References |
|-------------------|-----------------------|--|---|
| $G^{(drug)}$ | 1 | lag coefficient of drug in capillary and venule | (Agasanapura, Baltus, & Chellam, 2011) |
| $G^{(iRBC)}$ | 0.6,0.9 | lag coefficient of iRBC in capillary and venule, respectively. | (Agasanapura, Baltus, & Chellam, 2011) |
| $x(0)$ | 5×10^6 | initial normal density of normal RBCs (<i>cells/μl</i>) | (Li, Ruan, & Xiao, 2011) |
| Λ | 4.15×10^4 | production rate of RBCs (<i>cells/μl/day</i>) | (Li, Ruan, & Xiao, 2011) |
| $r^{(RBC)}$ | 3.9 | radius of RBC (μ m) | (Ye et al., 2013) |
| $r^{(iRBC)}$ | 3.9 | radius of iRBC (μ m) | (Ye et al., 2013) |
| $V^{(iRBC)}$ | 86-116 | volume of iRBC (μ m ³) | (Ye et al., 2013) |
| $\delta^{(iRBC)}$ | 0.03-0.8 | parasite volume fraction | (Ye et al., 2013) |
| g | 12 | product rate of merozoites (<i>/day</i>) | (Li, Ruan, & Xiao, 2011) |
| β | 2×10^{-9} | infective rate (<i>μl/cell.day</i>) | (Li, Ruan, & Xiao, 2011) |
| μ_x | 8.3×10^{-3} | decay rate of RBCs (<i>/day</i>) | (Li, Ruan, & Xiao, 2011) |
| μ_y | 1 | decay rate of iRBCs (<i>/day</i>) | (Li, Ruan, & Xiao, 2011) |
| μ_m | 48 | decay rate of merozoites (<i>/day</i>) | (Li, Ruan, & Xiao, 2011) |
| $m(0)$ | 10^4 | initial density of merozoites (<i>cells/μl</i>) | (Austin, White, & Anderson, 1998; Li, Ruan, & Xiao, 2011) |
| ρ | 60 | blood circulatory time (<i>s</i>) | (Dilsizian, & Pohost, 2010) |
| $r^{(capillary)}$ | 3 | radius of capillary (μ m) | (Khurana, 2006) |
| $r^{(venule)}$ | 10 | radius of venule (μ m) | (Khurana, 2006) |
| τ | 1 | transit time (<i>s</i>) of capillary and venule | (Khurana, 2006) |
| l | 200,50-500 | Length (μ m) of capillary and venule, respectively. | (Radivoj, & Krstic, 1997) |
| $v^{(blood)}$ | 0.3,4 | blood velocity (<i>mm/s</i>) in capillary and venule, respectively. | (Khurana, 2006; Vosse van de, & van Dongen, 1998) |
| N | $10^9, 10^7$ | number of capillaries and venule, respectively. | (Pollak, 2005) |
| $V^{(blood)}$ | 5 | whole blood volume (liters) | (Higgins et al., 2009) |
| $X(t_0)$ | 10^5 | parasite density in blood at t_0 | (Ali et al., 2008; White, 2011) |
| A | 6.02×10^{23} | Avogadro's number | (Staver, & Lumpe, 1993) |
| ε | 40-50 | Ratio of drug efflux in case of resistant parasite to susceptible parasite | (Krogstad et al., 1988) |

3.1 Monotherapy

Since most parameters of *Plasmodium sp.* such as physical structures (length, width, etc.) and biological data (growth, death, infective and merozoite-releasing rate) are quite similar, this study will treat all *Plasmodium sp.* as the same. To conform our numerical results with the real situation, we use the parasite clearance curves from White (2011), which represent as the real world. Figure 1 in White (2011) shows two parasite clearance curves of *P. falciparum* with the same treatment consisting of time on pre-treatment and parasite density. Figure 4 in White (2011) shows normalized parasite clearance curves of *P. falciparum* consisting of parasitemia versus time in patients with artesunate therapy in Western Cambodia and Western Thailand.

Figure 4(a), 4(b), 4(c) and 4(d) are numerical results of artesunate, chloroquine, mefloquine and halofantrine, respectively. These four Figures consist of parasite density versus time post-admission or days of treatment. After numerical simulating, the duration of treatment and the clearance of parasite time of chloroquine, mefloquine, halofantrine and artesunate are quite the same. First, although each the therapeutic level of plasma drug concentration of four drugs are different, treatment durations from our results are within range 1 to 10 days as shown in Figure 4(a)-4(d) which are near the real world by comparing with Figure 1 and 4 in White (2011). Second, all descending graphs of four drugs are linear and similar to the real information of Figure 1 in White (2011). Observe that although their average plasma drug concentrations in Figure 4(a)-4(d) are widely different, the duration of the treatment from numerical results are within range 1 to 10 days. The reason is that most physicians intend to finish the treatment for the malarial infection within a week to prevent patients from turning into severe or complicated malaria. Observe that clearance of parasite time of mefloquine and

halofantrine shown in Figure 4(c) and 4(d) are longer than chloroquine shown in Figure 4(b) despite the fact that mefloquine and halofantrine are more recent drugs than chloroquine. In fact, there is evident of chloroquine-resistance in *Plasmodium*. Thus, this study also includes numerical results in the case of drug resistance in the next subsection.



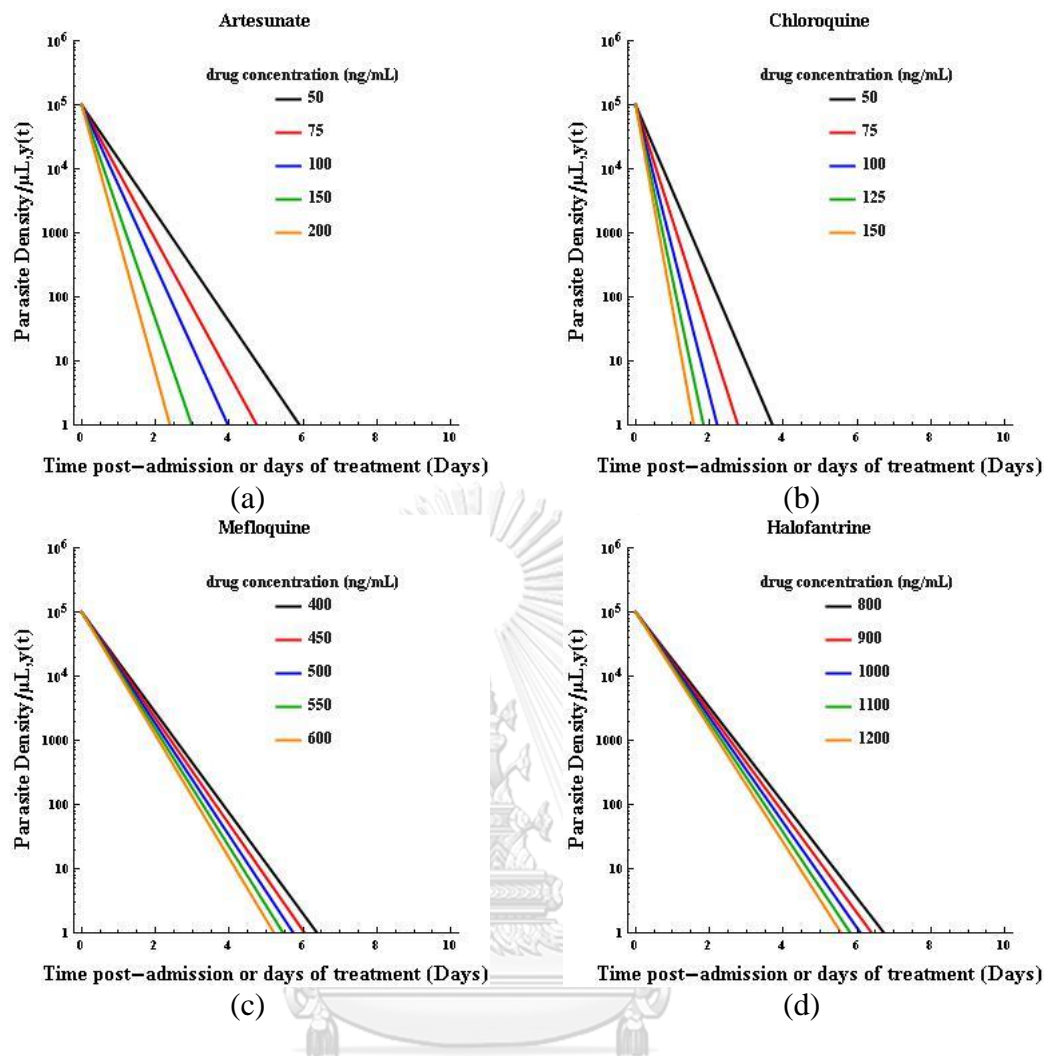


Figure 4. Our numerical results from artesunate, chloroquine, mefloquine and halofantrine, shown in Figure 4(a), 4(b), 4(c) and 4(d), respectively.

3.2 Drug resistance

There are many ways that the malaria parasites can develop the drug resistance. There are strong evidences that the malaria parasite can increase the drug efflux from their cells (Sinha, Medhi, & Sehgal, 2014). However, resistance of *Plasmodium sp.* occurs only for some certain drugs. For instance, chloroquine-resistant *P. vivax* are found to exist only in a few countries such as Papua New Guinea, Indonesia, Burma

(Myanmar), India, and Central and South America (CDC, 2016). At present, there has been no evidence of chloroquine resistance in *P. ovale*, *P. malariae* and *P. knowlesi* (CDC, 2016). Furthermore, *P. falciparum* also resists other non-quinoline groups, such as mefloquine and halofantrine (de Villiers & Egan, 2009). This study uses the drug efflux mechanism to generate numerical result. Thus, an additional assumption that all *Plasmodium species* resist all drugs in this study except artemisinin is needed. Thus, we consider the case of drug resistance by taking into account of the ratio of drug efflux in case of resistant parasite to susceptible parasite, denoted by ε (see this value in Table 2). This parameter ε can be applied by dividing with the death rate of malaria parasite, then the death rate of malaria parasite with drug resistance is $\left(\frac{y}{x+y}\right)\frac{\varphi(k)}{\varepsilon}$. Note that after incorporating the death rate of malaria parasite with the parameter of drug resistance ε , treatment durations of all Figure 5(a), 5(c) and 5(e) are elongated more than normal cases. This shows us that the parameter of resistance conforms with the real situation. This implies that drug resistance can affect the duration of treatment.

3.3 Combination therapy

This study also considers the combination therapy of chloroquine, mefloquine and halofantrine with artesunate, called the artemisinin-based combination therapy or ACT. Before generating the numerical results, the death rate of the malaria parasites due to the combination therapy is formulated by the partial summation of the death rates in each drug in the combination. Then, the death rate of the malaria parasites in case of

ACT is $\left(\frac{y}{x+y}\right)\left(\frac{\varphi^{(drug)}(k)}{\varepsilon} + \varphi^{(artesunate)}(k)\right)$, where $\varphi^{(drug)}(k)$ is the death rate of the

malaria parasites used chloroquine, mefloquine or halofantrine, and $\varphi^{(artemunate)}(k)$ is the death rate of the malaria parasites used artesunate. Hence, after numerical simulation, the duration of treatment or clearance of the parasite time in Figure 5(b), 5(d) and 5(f) are shortened when compare with Figure 5(a), 5(c) and 5(e) in case of chloroquine, mefloquine or halofantrine, respectively.



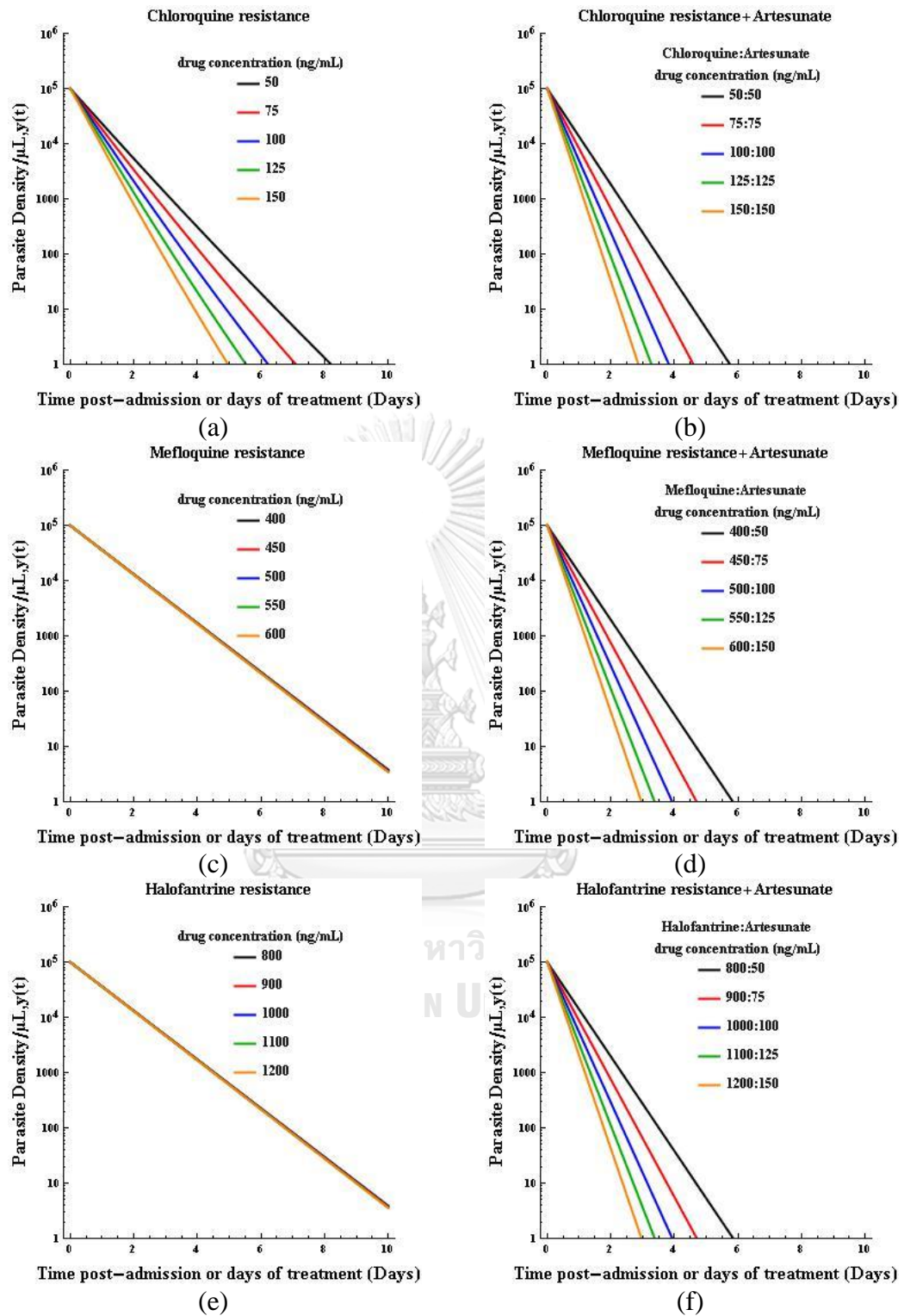


Figure 5. Numerical results of chloroquine, mefloquine and halofantrine with their resistance and artesunate-based combination therapy (ACT).

4. Conclusions

The numerical results from our model illustrate that the duration of treatment or the period time needed to eliminate the infected red blood cells is 1-10 days, which conform to the patients' clinical data. Thus, the assumptions in this study which incorporate the pathophysiology of malaria within the host to construct five probability factors under theories of physics and chemistry for estimating the effective drugs, pharmacokinetics and pharmacodynamics for converting plasma drug concentration to the population of malaria parasite, are compatible with the real-world situation. Furthermore, this method is quite simple and effective to predict the duration of treatment by using only parasite density from patient's blood at one certain time without continuous monitoring of patient's blood since other parameters are already available. Finally, we hope that our model could be used to estimate the antimalarial drug dosage for the patient's treatment.



Acknowledgments

This research was supported by scholarship 60/40 of Chulalongkorn University.

References

1. Agasanapura, B. N., Baltus, R. E., & Chellam, S. (2011). Effect of Convective Hindrance On Microfiltration of Rod Shaped Particles. *AIChE Journal, Proceedings of Conference for Annual Meeting*, 5-29.
2. Ali, H., Ahsan, T., Mahmood, T., Bakht, S. F., Farooq, M. U., & Ahmed, N. (2008). Parasite density and the spectrum of clinical illness in falciparum malaria. *Journal of the College of Physicians and Surgeons--Pakistan*, 18(6), 362-368. doi: 06.2008/JCPSP.362368
3. Ashton, M., Hai, T. N., Sy, N. D., Huong, D. X., Van Huong, N., Niêu, N. T., & Cống, L. D. (1998). Artemisinin pharmacokinetics is time-dependent during repeated oral administration in healthy male adults. *Drug Metabolism and Disposition Journal*, 26(1), 25-27.
4. Austin, D. J., White, N. J., & Anderson, R. M. (1998). The Dynamics of Drug Action on the Within-host Population Growth of Infectious Agents: Melding Pharmacokinetics with Pathogen Population Dynamics. *Journal of Theoretical Biology*, 194(3), 313-339.
5. Brinkman, H. C. (1949). A calculation of the viscous force exerted by a flowing fluid on a dense swarm of particles. *Applied Scientific Research*, 27-34.
6. Centers for Disease Control and Prevention, Treatment of Malaria. (2016, November 04). Guidelines For Clinicians (United States). Retrieved from https://www.cdc.gov/malaria/diagnosis_treatment/clinicians2.html

7. de Villiers, K. A., & Egan, T.J. (2009). Recent advances in the discovery of haem-targeting drugs for malaria and schistosomiasis. *Molecules*,14(8), 2868-2887. doi: 10.3390/molecules14082868
8. Dilsizian, V., & Pohost, G. M. (2010). *Cardiac CT, PET and MR, Multislice Cardiac Tomography: Myocardial Function, Perfusion, and Viability*. Hoboken, New Jersey, United States: Wiley-Blackwell
9. Higgins, J. M., Eddington, D. T., Bhatia, S. N., & Mahadevan, L. (2009). Statistical Dynamics of Flowing Red Blood Cells by Morphological Image Processing. *Computational Biology*, doi: 10.1371/journal.pcbi.1000288D. J.
10. Karbwang, J., Bunnag, D., Harinasuta, T., Chittamas, S., Berth, J. & Druilhe, P. (1992) Pharmacokinetics of quinine, quinidine and Cinchonine when given as combination. *Southeast Asian Journal of Tropical Medicine and Public Health*, 23(4), 773-776.
11. Khurana, I. (2006). *Textbook Of Medical Physiology; Dynamics of Circulation: Pressure and Flow of Blood and Lymph*: Elsevier
12. Li, Y., Ruan, S., & Xiao, D. (2011). The Within-Host dynamics of malaria infection with immune response. *Mathematical Biosciences and Engineering*, 8(4), 999-1018.
13. Mazaheri, A. (2009). Probabilistic Modeling of Ship Grounding, Retrieved from <http://www.merikotka.fi/safgof/ProbabilisticModelingofShipGrounding.pdf>
14. Morris, C. A., Duparc, S., Borghini-Fuhrer, I., Jung, D., Shin, C. S., & Fleckenstein, L. (2011). Review of the clinical pharmacokinetics of artesunate and its active metabolite dihydroartemisinin following intravenous,

- intramuscular, oral or rectal administration. *Malaria Journal*, 10, 263. doi: 10.1186/1475-2875-10-263
15. Pabst, W., & Gregorová, E. (2007). Characterization of particles and particle systems. ICT Prague. Retrieved from http://old.vscht.cz/sil/keramika/Characterization_of_particles/CPPS%20_English%20version_.pdf
16. Pollak, A. N. (2005). Emergency Care and Transportation of the Sick and Injured. United States of America: Library of Congress Cataloging-in-Publication Data
17. Preetam, G. (2007). Stochastic Models for In-silico Event-based Biological Network Simulation (Doctoral dissertation). University of Texas, Arlington.
18. Berg, H. C., & Purcell, E.M. (1977). Physics of chemoreception. *Biophysical Journal*, 20(2),193-219.
19. Radivoj, V., & Krstic, (1997). Human Microscopic Anatomy: An Atlas for Students of Medicine and Biology. Berlin Heidelberg, Germany: Springer-Verlag
20. Krogstad, D. J., Schlesinger, P. H., & Herwaldt, B. L. (1988). Antimalarial agents: mechanism of chloroquine resistance. *Antimicrobial Agents and Chemotherapy*, 32(6), 799-801.
21. Sinha, S., Medhi, B., & Sehgal, R. (2014). Challenges of drug-resistant malaria. *Parasite*. 21(61). doi: 10.1051/parasite/2014059
22. Staver, J. R., & Lumpe, A. T. (1993). A content analysis of the presentation of the mole concept in chemistry textbooks. *Journal of Research in Science Teaching*, (30)4. doi: 10.1002/tea.3660300402

23. Taroni, C., Jones, S., & Thornton, J. M. (2000). Analysis and prediction of carbohydrate binding sites. *Protein Engineering*, 13(2), 89-98. doi: 10.1093/protein/13.2.89
24. ter Kuile, F., White, N. J., Holloway, P., Pasvol, G., & Krishna, S. (1993). *Plasmodium falciparum*: in vitro studies of the pharmacodynamic properties of drugs used for the treatment of severe malaria. *Experimental Parasitology*, 76(1), 85-95.
25. Veenendaal, J. R., Parkinson, A. D., Kere, N., Rieckmann, K. H., & Edstein, M. D. (1991). Pharmacokinetics of halofantrine and n-desbutylhalofantrine in patients with *falciparum* malaria following a multiple dose regimen of halofantrine. *European Journal of Clinical Pharmacology*, 41(2), 161-164.
26. Vosse van de, F. N., & van Dongen, M. E. H. (1998). Cardiovascular Fluid Mechanics - lecture notes - Materials Technology. Retrieved from <http://www.mate.tue.nl/people/vosse/docs/cardio.pdf>
27. White, N. J. (1992). Antimalarial pharmacokinetics and treatment regimens. *British Journal of Clinical Pharmacology*, 34(1), 1-10.
28. White, N. J. (2011). The parasite clearance curve. *Malaria Journal*. 10(278), 1-8. doi: 10.1186/1475-2875-10-278
29. Wilairatana, P., & Looareesuwan, S. (1996). Artesunate : A Potent Antimalarial Drug for *Falciparum* Malaria. *Journal of Infectious Diseases and Antimicrobial Agents*, 3(13), 119-121.
30. Ye, T., Phan-Thien, N., Khoo, B. C., & Lim, C. T. (2013). Stretching and relaxation of malaria-infected red blood cells. *Biophysical Journal*, 105(5), 1103-1109. doi: 10.1016/j.bpj.2013.07.008

CHAPTER 4
PREDICTING THE DURATION OF CHLOROQUINE, MEFLOROQUINE,
HALOFANTRINE AND ARTESUNATE FOR BLOOD SCHIZONTICIDAL
EFFECT USING MATHEMATICAL MODELS OF MALARIA WITH
IMMUNE RESPONSE

Panit Suavansri¹ and Nataphan Kitisin^{2*}

¹Department of Mathematics and Computer Science, Faculty of Science,
Chulalongkorn University, Phayathai Road, Patumwan, Bangkok, 10330, Thailand)

²Department of Mathematics and Computer Science, Faculty of Science,
Chulalongkorn University, Phayathai Road, Patumwan, Bangkok, 10330, Thailand)

*** Corresponding author, Email address: nataphan.k@gmail.com**

จุฬาลงกรณ์มหาวิทยาลัย
CHULALONGKORN UNIVERSITY

This article appears in Thai Journal of Pharmacology (TJP), Volume 39,
Number 2 (2017) p23-48.

Submitted 25 August 2017

Revised 27 November 2017

Accepted 26 December 2017

Published 31 December 2017

Abstract

This paper focuses on the mathematical model of the death rate of malaria parasite due to chloroquine, mefloquine, halofantrine and artesunate together with the immune response in order to determine the treatment period. The basic knowledge of probabilities, pharmacology, microbiology, medicines, physics and chemistry are used to support this model and hypotheses. One of the hypotheses is the convective theory used for calculating and converting the flow rate of drug molecules with respect to malaria parasite into the death rate of malaria parasite. Other instruments are five probability factors, which the authors use to determine the efficiency of the drugs parasites. Applied this model of death rate with normal malaria model and take into account of the immune response, the treatment durations result in the ranges between 1 to 15 days and are compatible with the real clinical data.

Keywords: Malaria, death rate, probability

1. Introduction

Malaria is a dangerous infectious disease due to transmission of *Plasmodium* parasites by biting of female *Anopheles* mosquitoes.¹ In 2015, there were malaria dissemination in 91 countries and WHO estimated that there were 212 million cases of malaria worldwide (within a range of 148 to 304 million). There are 429,000 people, who are died from malaria (within a range of 235,000 to 639,000).² Since the treatment of patients with malarial infection needs the advance methods for laboratory investigation that rarely exists in those developing countries, mathematical models can help to solve some of this problem. For example, the laboratory investigation needs to record the parasite density every day during the treatment period in order to determine when the treatment should be terminated, while the mathematical model in this study predicts the day that the parasite density will be cleared from bloodstream with just one blood sampling. Hence, the objective of this paper is to predict the treatment duration for the patient infected by malaria with immune response by constructing the mathematical model of the death rate of malaria. The numerical results are shown to be comparable to the actual treatment duration.

Before establishing the mathematical model, the pathogenesis of malaria and the mechanism of action of antimalarial drug are taken into account. The pathogenesis of malaria consists of two main cycles: sexual and asexual cycles. First, the sexual cycle needs to be reviewed. After a female *Anopheles* mosquito bites the patient infected malaria, a malarial agent called gametocyte is released from this patient and enters to the mosquito's stomach. When both male and female gametocytes (or

microgametocytes and macrogametocytes, respectively) meet together, a zygote occurs by their reproductive process. Afterward, a zygote gradually develops into oocyst containing sporozoites. At the end of this sexual cycle, sporozoites are released from oocyst and enter into a human host bloodstream soon after this mosquito bites the human host. Second, the asexual cycle begins when the parasites are already in the human. After sporozoites come into a human host blood, they travel along blood circulation to invade liver cells. When sporozoites mature and convert into schizonts, liver cells are ruptured and release schizonts. Then, these schizonts will spread into blood system to infect healthy red blood cells (RBCs). They grow and develop into various stages within the infected red blood cells (iRBCs): early and late trophozoites, early and late schizonts, respectively. Finally, malaria parasites in the late schizonts, called merozoites, are mature, they are released into host blood and re-infect normal RBCs or normal liver cells again and again.³

The pathogenesis of malaria is different in each species. *P. falciparum* has two main phases in stage of intracellular parasites while *P. malariae*, *P. ovale*, *P. vivax* and *P. knowlesi* have only one phase. After extracellular parasites of *P. falciparum* infect normal RBCs, they can circulate in blood system freely. This situation and iRBCs in this phase are called circulating process and circulating iRBCs, respectively. If they survive from drugs or other factors, then they will fully grow and attach an intraluminal wall of capillaries and post-capillary venules of specific vital organs: brain, lungs, heart, kidneys and liver.^{4,5} This situation and iRBCs in this phase are called sequestration process and sequestered iRBCs (Figure 1(a)). Thus, antimalarial drug has to spend time following the circulating iRBCs, but not the sequestered iRBCs which takes less time for the drug to kill.

During the entire lifetime of malaria parasites in the phase of iRBCs, they consume hemoglobin in the RBC's cytoplasm. However, they have to protect themselves from toxic and water-soluble hemes from digested hemoglobin by changing them into malarial pigment, known as non-toxic and water-insoluble hemozoin. Hence, the mechanism of antimalarial drugs killing parasites is to inhibit this conversion.^{6,7} There are many antimalarial drugs involved with this inhibition such as chloroquine, artesunate, halofantrine and mefloquine. Remark that the route of mefloquine is oral. However, the authors will treat mefloquine via the intravenous route, which is also the same as chloroquine so that both of them can be correspondingly compared their results. Although the mechanism of artesunate is still unclear, the authors will treat artesunate as quinolines to generate numerical simulation.

The following assumptions and hypotheses were made: (i) the rate of collision between an iRBC and a drug molecule is determined by the relative velocity between both of them, based on the convective velocity in physics (see the subsection 1 in Material and Methods), (ii) probability of binding and capturing between both of them are calculated by five probability factors, based on the effective collision with the proper orientation of the collision theory in molecular chemistry, (iii) the drug is effective in the sense that for the right condition one drug molecule can annihilate or kill one iRBC, and (iv) the drug concentration in plasma is steady and time-independent since the rate of drug administration with normal saline solution via intravenous route is almost constant. This situation illustrates in Figure 1(b).

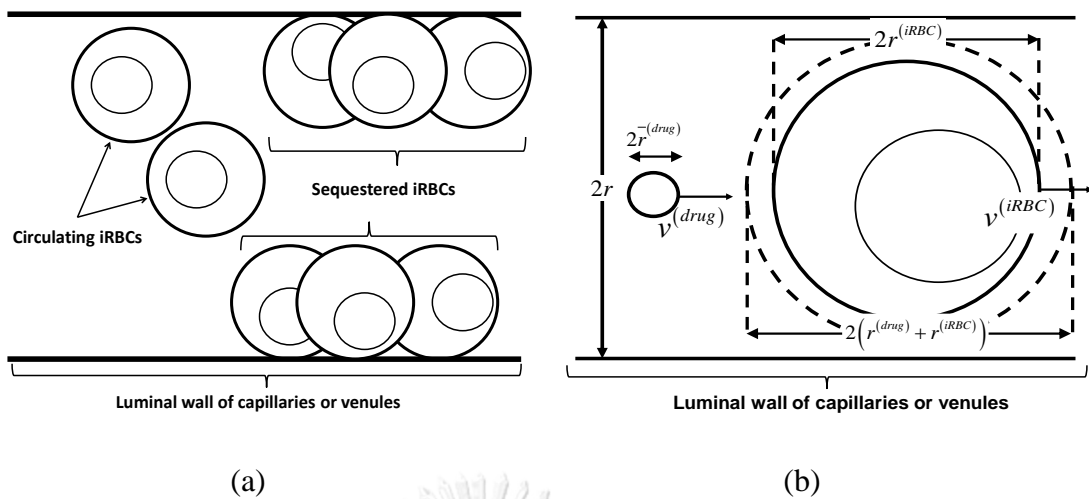


Figure 1. (a) Circulating and sequestered iRBCs in *P. falciparum*. (b) The transportation of the drug molecule to an intracellular parasite within an iRBC by convection of bloodstream (see parameters and values in Table 1 and 2).

The assumption of equality between two volumes of prolate spheroid and sphere, represented as the structure of drug molecules, has to be concerned for calculating probability conveniently. To use spherical shape as drug structure, there is the principal conversion from prolate spheroid to sphere by calculating the geometric mean of the width and length of prolate spheroid, based on the equality of two volumes of prolate spheroid and sphere.⁸

First, define $r_w^{(drug)}$ and $r_l^{(drug)}$ to be the half width and half length of the structure of drug molecule, considered as prolate spheroid. Then, the volume of prolate spheroid, defined as $V^{(prolate)}$, is $V^{(prolate)} = \frac{4}{3} \pi (r_w^{(drug)})^2 r_l^{(drug)}$. Similarly, the volume of sphere,

defined as $V^{(sphere)}$, is $V^{(sphere)} = \frac{4}{3}\pi(r^{(drug)})^3$. Thus, from the assumption of equality

$V^{(prolate)} = V^{(sphere)}$, the average radius of drug molecule is called Stokes radius^{8,9} and

denoted by $r^{(stoke)} = r^{-(drug)} = \left(\left(r_w^{(drug)} \right)^2 r_l^{(drug)} \right)^{1/3}$.

2. Materials and Methods

In this section, the authors try to calculate the relative velocity when the drug molecules follow malaria parasites along blood circulation. The scope of this study is to process the values of various parameters under proper assumptions. For example, the authors treat the mechanism of drug action as the collision rate between a drug molecule and a parasite, which is derived from the relative velocity of the convection of bloodstream without involving the Brownian movement. Furthermore, the death rate of malaria parasite is derived from five probability factors and the flow rate of drug molecules by using this relative velocity. Remark that only the active drug molecules using with the relative velocity will be used to formulate the death rate of malarial parasite, which will be subtracted from the mathematical models of malaria. The reason is that after binding parasites, the active drug molecules are ready to kill parasites and afterward will be converted into an inactive form, which will be excreted out of host body. Therefore, pharmacokinetics and pharmacodynamics, which occur after binding between drug molecules and parasites, are not relevant to the mathematical models. However, if some drugs have complex mechanism of pharmacokinetics such as

inhibiting of protein synthesis by binding at DNA or RNA of parasite, the probability of collision would be affected. First, the relative velocity between a drug molecule and an iRBC is used to determine the specific blood volume that contains the amount of particular drug. Second, the amount of this particular drug that can effectively kill a parasite has to be calculated by taking into account of the five probability factors of binding between a drug molecule and an iRBC. Five probability factors are formulated as follows (i) position probability factor determined by binding chance in the sense of position alignment between a drug molecule and an iRBC, (ii) binding probability factor of binding between a drug molecule and an intracellular parasite, but not the cytoplasmic iRBC, (iii) capture probability factor or chance of drug traveling that does not deviate from an iRBC, (iv) orientation probability factor or the probability of attachment between an active site of drug and iron molecules in heme, (v) population probability factor is the ratio of the drug molecule to only one iRBC, but not the normal RBC or immune effectors. Then, the total probability factor can be approximately estimated by the multiplying all of them and will result in the effective of the drug molecules. Before using the total probability, drug mass is needed to be computed. First, the specific blood volume, derived from the relative velocity, has to be changed into drug mass by multiplying drug concentration in plasma and the parameters of chemistry, such as Avogadro's number and molecular mass, which are used to convert the amount drug mass into the number of drug molecule. Furthermore, the total of drug molecules in human host occurs in all capillaries and venules of human host. Remark that this paper will focus only on schizonticides with chloroquine, mefloquine, halofantrine and artesunate. Finally, after converting the flow rate of drug molecules into the death rate of malaria parasite, this death rate is subtracted from the dynamic

population of iRBCs of malaria model in normal state and then simulates numerical results to predict treatment duration in cases of *P. non-falciparum* and *P. falciparum*, shown in Figure 2 and 3, respectively. Thus, all processes in these subsections are explained as follows.

2.1 Relative velocity between a drug molecule and an infected red blood cell

According to the fundamental of the relative velocity in physics, since a drug molecule is smaller than an iRBC, the velocity of drug molecule is faster than an iRBC, i.e. $v^{(drug)} > v^{(iRBC)}$, where $v^{(drug)}$ and $v^{(iRBC)}$ are two velocities of a drug molecule and an iRBC, respectively. Denote $v^{(relative)} = v^{(drug)} - v^{(iRBC)}$ as the relative velocity of drug with respect to the velocity of iRBC. Since $v^{(iRBC)}$ and $v^{(drug)}$ can be determined by multiplying between each local lag coefficient of them (denoted by $G^{(drug)}$ and $G^{(iRBC)}$ as two local lag coefficients of a drug and an iRBC, respectively) and the flow rate of blood (denoted by $v^{(blood)}$). Then, $v^{(iRBC)} = G^{(iRBC)}v^{(blood)}$ and $v^{(drug)} = G^{(drug)}v^{(blood)}$, where $G^{(drug)}$ and $G^{(iRBC)}$ are two local lag coefficients of a drug and an iRBC, respectively (see also Figure 1(b)).¹⁰

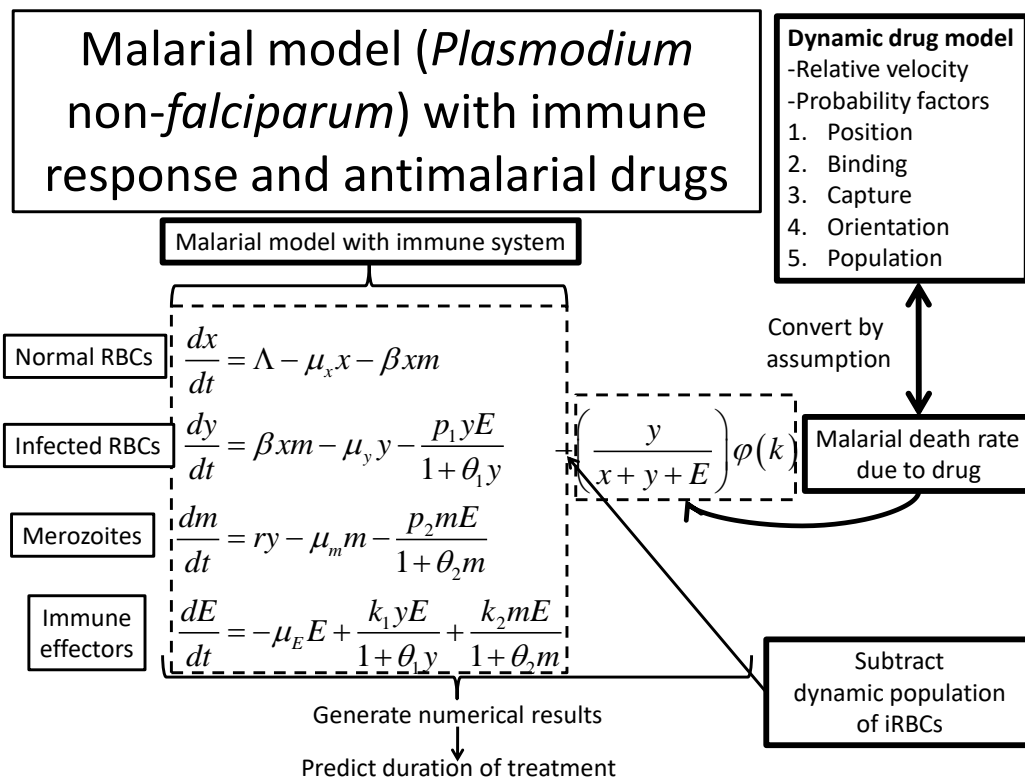


Figure 2. Algorithm for modeling the death rate of the malaria parasites in case of *P. non-falciparum* due to chloroquine, mefloquine, halofantrine and artesunate with immune response. Five probability factors and the relative velocity between a drug molecule and a parasite are used in order to predict the treatment duration.

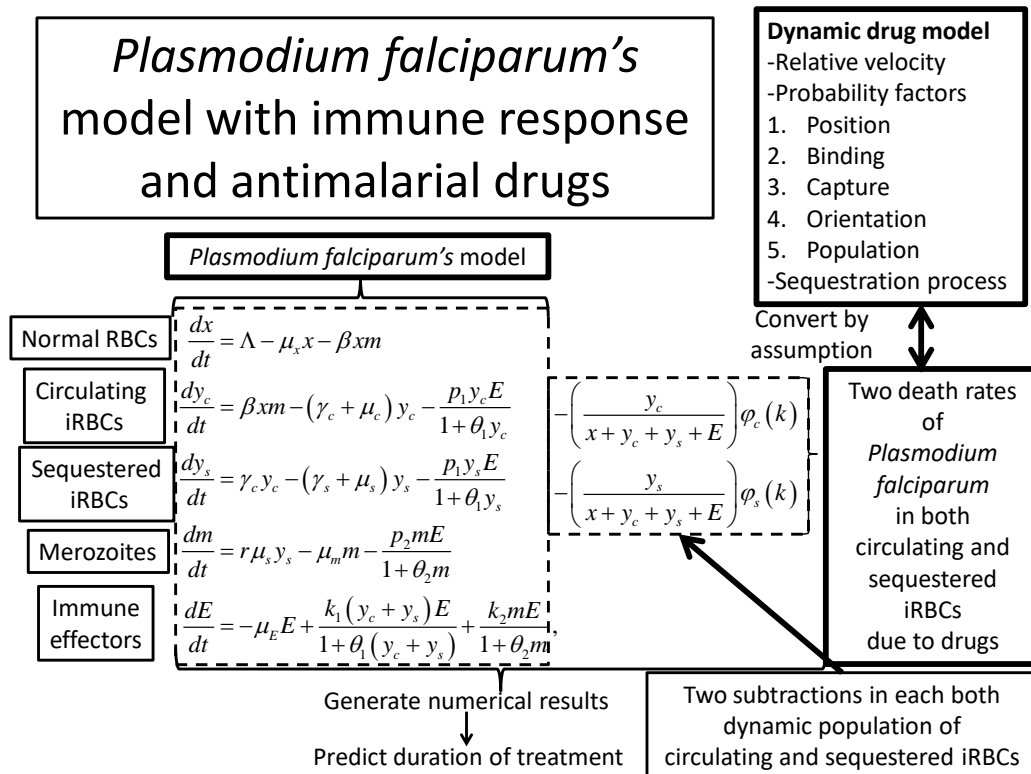


Figure 3. Algorithm for modeling the death rate of the malaria parasites in case of *P. falciparum* due to chloroquine, mefloquine, halofantrine and artesunate with the immune response. Five probability factors and the relative velocity between a drug molecule and a parasite are used in order to predict the treatment duration

2.2 Position probability factor

Our situation in this paper that drug molecules move along blood vessels to bind with iRBCs is comparable to the straight-forward traveling of ships to collide with shoals or obstacles in water channels. The collision between drug molecules and iRBCs will occur if both of them are aligned in appropriate or correct position. Hence, the probabilistic model of ship grounding¹¹ is used to find the effective drug molecules

which are potential to kill iRBCs. Nevertheless, since our situation is concerned in two-dimension (2D), the probabilistic model¹¹ is needed to be generalized from 1D to 2D before using in our model. Thus, the modified probability is defined to be the position probability factor in this paper by

$$p^{(position)} = \frac{\pi \left(r^{(iRBC)} + r^{-(drug)} \right)^2}{\pi r^2} = \left(\frac{r^{(iRBC)} + r^{-(drug)}}{r^{(vessel)}} \right)^2,$$

where $r^{(iRBC)}$ and $r^{(vessel)}$ are two radii of an iRBC and a human blood vessel in cross-sectional view, respectively.

2.3 Binding probability factor

The total volume of iRBCs, denoted by $V^{(iRBC)}$, contains two volumes. One of them is the volume of an intracellular parasite, denoted by $V^{(parasite)}$. The drug molecules must bind the volume $V^{(parasite)}$ to kill this parasite. The chance of binding between drug molecules and a parasite within iRBCs by using the modified probability,¹² called the binding probability factor and defined as

$$p^{(binding)} = \frac{V^{(parasite)}}{V^{(iRBC)}}.$$

Note that our binding probability factor is the parasite volume fraction.¹³

2.4 Capture probability factor

Before the events of position and binding between a drug molecule and an iRBC, a drug molecule can deviate from the iRBC during traveling. Based on physics, the longer distance between them, the less probability of binding together between them. Therefore, the capture probability¹⁴ will be used to determine this probability in this situation, which is defined as

$$p^{(capture)} = \frac{r^{(iRBC)}}{r^{(iRBC)} + l},$$

where l is the length of blood vessel of human host.

2.5 Orientation probability factor

In view of chemistry, a product of chemical reaction occurs when each binding site of the substrates bind together with correct orientation. Thus, this probability is defined as the orientation probability factor,¹⁵ which is the ratio of the binding area to the total surface area of a drug molecule and denoted by

$$p^{(orientation)} = \frac{\pi z^2}{4} / \left\{ 2\pi \left(r_w^{(drug)} \right)^2 \left(1 + \frac{r_w^{(drug)}}{e r_l^{(drug)}} \sin^{-1} e \right) \right\}.$$

Remark that the binding area of a drug molecule ($\frac{\pi z^2}{4}$) is circular with the diameter z . Since our hypothesis is that the structure of drug molecule is a prolate spheroid, the total surface area of a drug molecule is

$$2\pi \left(r_w^{(drug)} \right)^2 \left(1 + \frac{r_w^{(drug)}}{e r_l^{(drug)}} \sin^{-1} e \right)$$

where e is the eccentricity of the ellipse.

2.6 Population probability factor

Since a drug molecule can attach RBCs, iRBCs and immune effectors, drug molecules have to avoid normal RBCs and immune effectors. Thus, in case of *P. falciparum*, the probability in this situation, defined as the population probability factor, is

$$p^{(population)} = \frac{y(t)}{x(t) + y(t) + E(t)}.$$

In both cases of circulating and sequestration processes, there are two population probability factors of *P. falciparum*, which are

$$p_c^{(population)} = \frac{y_c(t)}{x(t) + y_c(t) + y_s(t) + E(t)}, \text{ and}$$

$$p_s^{(population)} = \frac{y_s(t)}{x(t) + y_c(t) + y_s(t) + E(t)}, \text{ respectively.}$$

2.7 Total probability

To find the total probability of five probability factors, the authors will assume that they are independent in each other. Then, the total probability can be derived by multiplying them together, which is

$$p^{(total)} = p^{(position)} \times p^{(binding)} \times p^{(capture)} \times p^{(orientation)} \times p^{(population)}.$$

2.8 Mathematical model of malaria

In 2011, Yilong *et al.*¹ had constructed the mathematical model of the within-host dynamics of malaria infection with immune response as shown in Figure 4(a). Since this paper studies both *P. falciparum* and *P. non-falciparum*, the authors modify the following two models, which are derived from Yilong *et al.*¹ with Bichara *et al.*¹⁶ and then adapt to the *P. falciparum*'s model with immune response as shown in Figure 4(a) and 4(b). Remark that the immune effectors, defined as E , represent the immune effect, which concerns only the white blood cells and does not include the RBCs (see Yilong *et al.*¹ in details). Thus, these two models are used together with our death rates to generate numerical results to predict treatment duration.

$$\begin{aligned}
 \frac{dx}{dt} &= \Lambda - \mu_x x - \beta xm, & \frac{dx}{dt} &= \Lambda - \mu_x x - \beta xm, \\
 \frac{dy}{dt} &= \beta xm - \mu_y y - \frac{p_1 y E}{1 + \theta_1 y}, & \frac{dy_c}{dt} &= \beta xm - (\gamma_c + \mu_c) y_c - \frac{p_1 y_c E}{1 + \theta_1 y_c}, \\
 \frac{dm}{dt} &= ry - \mu_m m - \frac{p_2 m E}{1 + \theta_2 m}, & \frac{dy_s}{dt} &= \gamma_c y_c - (\gamma_s + \mu_s) y_s - \frac{p_1 y_s E}{1 + \theta_1 y_s}, \\
 \frac{dE}{dt} &= -\mu_E E + \frac{k_1 y E}{1 + \theta_1 y} + \frac{k_2 m E}{1 + \theta_2 m}. & \frac{dm}{dt} &= r \gamma_s y_s - \mu_m m - \frac{p_2 m E}{1 + \theta_2 m}, \\
 & & \frac{dE}{dt} &= -\mu_E E + \frac{k_1 (y_c + y_s) E}{1 + \theta_1 (y_c + y_s)} + \frac{k_2 m E}{1 + \theta_2 m}.
 \end{aligned}$$

(a) (b)

Figure 4. The mathematical model of within-host malaria parasite with immune response¹ in cases of (a) *P. non-falciparum* and (b) *P. falciparum* from Yilong *et al.*¹ with Bichara *et al.*¹⁶ with our modification, respectively. All variables, parameters

and values can be seen in Table 1 and 2.

2.9 Dynamic drug model

The steps for constructing the death rate of malaria parasite are the following (i) find the number of drug molecules binding parasites per unit time (ii) assume that the effective drug killing parasites satisfied the correct condition in the sense that one iRBC can be annihilated per one drug molecule. First, in the scope of one blood vessel, if the length that blood volume sweeps with time t is $v^{(relative)}t$ with its the cross-sectional area of a vessel is $\pi(r^{(vessel)})^2$, then the specific blood volume in one vessel is $\pi(r^{(vessel)})^2 v^{(relative)}t$. Second, change this specific blood volume into drug mass by multiplying plasma drug concentration $C(t)$ and convert the amount of this drug mass into the number of drug molecules again by multiplying Avocado's number A and dividing by the molecular mass of this drug M . Afterward, the authors interpolate this flow rate of drug molecules into all blood vessels of the whole human body. Thus, the flow rate of drug molecules, denoted by $N^{(drug)}$, is
$$N^{(drug)} = \pi(r^{(vessel)})^2 C(t)Av^{(relative)}t / M .$$
 Since there are a few effects with hemodynamics of human host, two probabilistic chances of the binding of drug molecules and parasites in view of blood circulation have to be taken into account as follows: (a) find the period of time that drug molecules can follow parasites by determining the ratio of time in blood vessels, called transit time and denoted by τ , and the circulatory time, denoted by ρ . (b) use the ratio of only unbounded drug molecules

to all drug molecules, i.e. the free fraction of drug, denoted by α . (c) multiply both of them with the total probability factor as before. (d) divide by the total blood volume of patient, denoted by $V^{(blood)}$. Finally, change $N^{(drug)}$ into the rate by dividing by t . Then, the death rate of the malaria parasites is defined as

$$\Psi(t) = \frac{\pi\alpha N^{(vessel)}\tau\left(r^{(vessel)}\right)^2 C(t)Ap^{(total)}v^{(relative)}}{\rho MV^{(blood)}}$$

(see also Figure 5).

Since this death rate is considered in both capillaries and venules, the two death rates in cases of both capillaries and venules are needed to be constructed separately. Therefore, the total death rate of the malaria parasites is defined as

$$\Psi^{(total)}(t) = \Psi^{(capillary)}(t) + \Psi^{(venule)}(t).$$

By one of the assumptions satisfied in our situation, the antimalarial treatment by intravenous route of drug administration maintains the constant level of drug concentration in plasma. First, if drug concentration does not depend on time, then the drug concentration constant k will be used instead of $C(t)$. Second, the variables of the population of $x(t)$, $y(t)$ and $E(t)$ in population probability factor have to be extracted from the death rate before simulating the results in order to determine the dynamic of malaria parasites conveniently. Hence, define

$$\varphi(k) = \Psi^{(total)}(k) / p^{(population)} = \left(\frac{x + y + E}{y} \right) \Psi^{(total)}(k),$$

where the death rate of malaria parasite in other form is given by

$$\Psi^{(total)}(k) = \left(\frac{y}{x + y + E} \right) \varphi(k).$$

Thus, when iRBCs are totally killed, i.e. $y \rightarrow 0$, the death rate tends to zero, i.e. $\Psi^{(total)}(k) \rightarrow 0$. This statement conforms the real situation. Hence, *P. non-falciparum*'s model with antimalarial drug and immune response is

$$\begin{aligned}\frac{dx}{dt} &= \Lambda - \mu_x x - \beta xm, \\ \frac{dy}{dt} &= \beta xm - \mu_y y - \frac{p_1 y E}{1 + \theta_1 y} - \left(\frac{y}{x + y + E} \right) \varphi(k), \\ \frac{dm}{dt} &= ry - \mu_m m - \frac{p_2 m E}{1 + \theta_2 m}, \\ \frac{dE}{dt} &= -\mu_E E + \frac{k_1 y E}{1 + \theta_1 y} + \frac{k_2 m E}{1 + \theta_2 m}.\end{aligned}$$

In case of *P. falciparum*, there are two phases of iRBCs in *P. falciparum*. The authors will illustrate the formulation of death rate of malaria parasite in case of *P. falciparum* in circulating process and *P. non-falciparum* at once because both of them have almost the same pathophysiology. The algorithm of modeling this death rate in both cases can be concluded as follows: (i) find the quantity of drug molecules attaching circulating iRBCs in case of *P. falciparum* or total iRBCs in case of *P. non-falciparum* per unit time, (ii) assume that drug molecules in the sense for the correct condition that one iRBC can be annihilated by only one drug molecule (see also Figure 6).

For the population probability factor in case of *P. falciparum*, since the circulating and sequestered processes in the phase of intracellular parasites of *P. falciparum* are different in the sense of pathophysiology, the formulation of death rate of malaria parasite is separated into two parts. One death rate in the circulating process is almost the same as the case of *P. non-falciparum*, i.e. two population probability factors of them are different as follows:

$$p_c^{(population)} = \frac{y_c}{x + y_c + y_s + E},$$

$$p_s^{(population)} = \frac{y_s}{x + y_c + y_s + E}, \text{ and}$$

$$p^{(population)} = \frac{y}{x + y + E},$$

are three population probability factors in case of circulating and sequestered processes in *P. falciparum*, and *P. non-falciparum*, respectively.



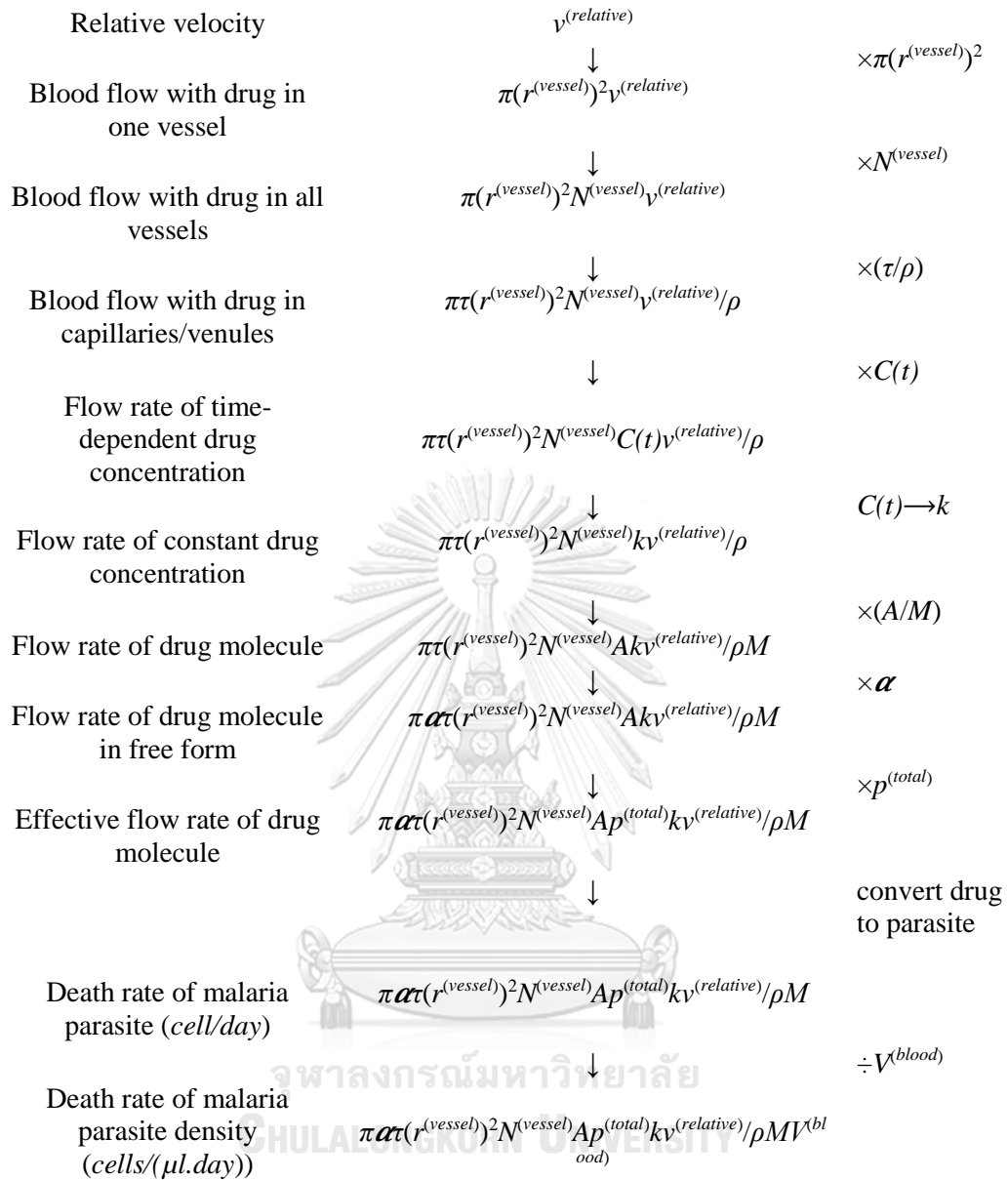


Figure 5. This diagram shows formulation of the death rate of malaria parasite

density, where $p^{(population)} = \frac{y}{x + y + E}$ in $p^{(total)}$.

The first difference between the circulating and sequestered processes is that sequestered iRBCs attach with the luminal wall of blood vessels, i.e. $v_s^{(iRBC)} = 0$. Thus, the relative velocity between drug molecules and sequestered iRBCs is

$$v_s^{(relative)} = v_s^{(drug)}.$$

The second difference is that sequestration process occurs only in specific vital organs of human host, which are brain, heart, left and right lungs, liver and left and right kidneys.^{4,5} Therefore, the death rate of malaria parasite in sequestration process is determined only in blood vessels of specific vital organs.

Define $N_{(vital)}^{(capillary)}$ and $N_{(vital)}^{(venule)}$ as the number of total capillaries and total venules of all specific vital organs, respectively. To determine both $N_{(vital)}^{(capillary)}$ and $N_{(vital)}^{(venule)}$, the authors assume that the number of blood vessels of an organ is directly proportional to this organ's weight. Thus, if $W^{(vital)}$ and $W^{(body)}$ are defined as the two weights of all specific vital organs and whole body, respectively, then $W^{(vital)}/W^{(body)}$, $N_{(vital)}^{(capillary)}/N^{(capillary)}$ and $N_{(vital)}^{(venule)}/N^{(venule)}$ are equal, i.e.

$$\frac{W^{(vital)}}{W^{(body)}} = \frac{N_{(vital)}^{(capillary)}}{N^{(capillary)}} = \frac{N_{(vital)}^{(venule)}}{N^{(venule)}}.$$

Since the percentage of kidneys, lungs, liver, heart and brain to whole body weight 0.49%, 1.72%, 2.09%, 0.51% and 1.98%, respectively¹⁷, the total percentage of all specific vital organs, defined as λ , is

$$\lambda = \frac{W^{(vital)}}{W^{(body)}} = 1.98 + 0.51 + 2.09 + 1.72 + 0.49\% = 6.79\%.$$

Incorporating λ with $\Psi_s^{(total)}(t)$, then two death rates of *P. falciparum* in circulating and sequestration process are

$$\Psi_c(t) = \frac{\pi\alpha N^{(vessel)}\tau r^2 C(t) Ap^{(total)}}{\rho M} (G^{(drug)} - G^{(iRBC)}) v^{(blood)},$$

$$\Psi_s(t) = \frac{\pi\alpha N^{(vessel)}\tau r^2 C(t) Ap^{(total)}}{\rho M} \lambda G^{(drug)} v^{(blood)}.$$



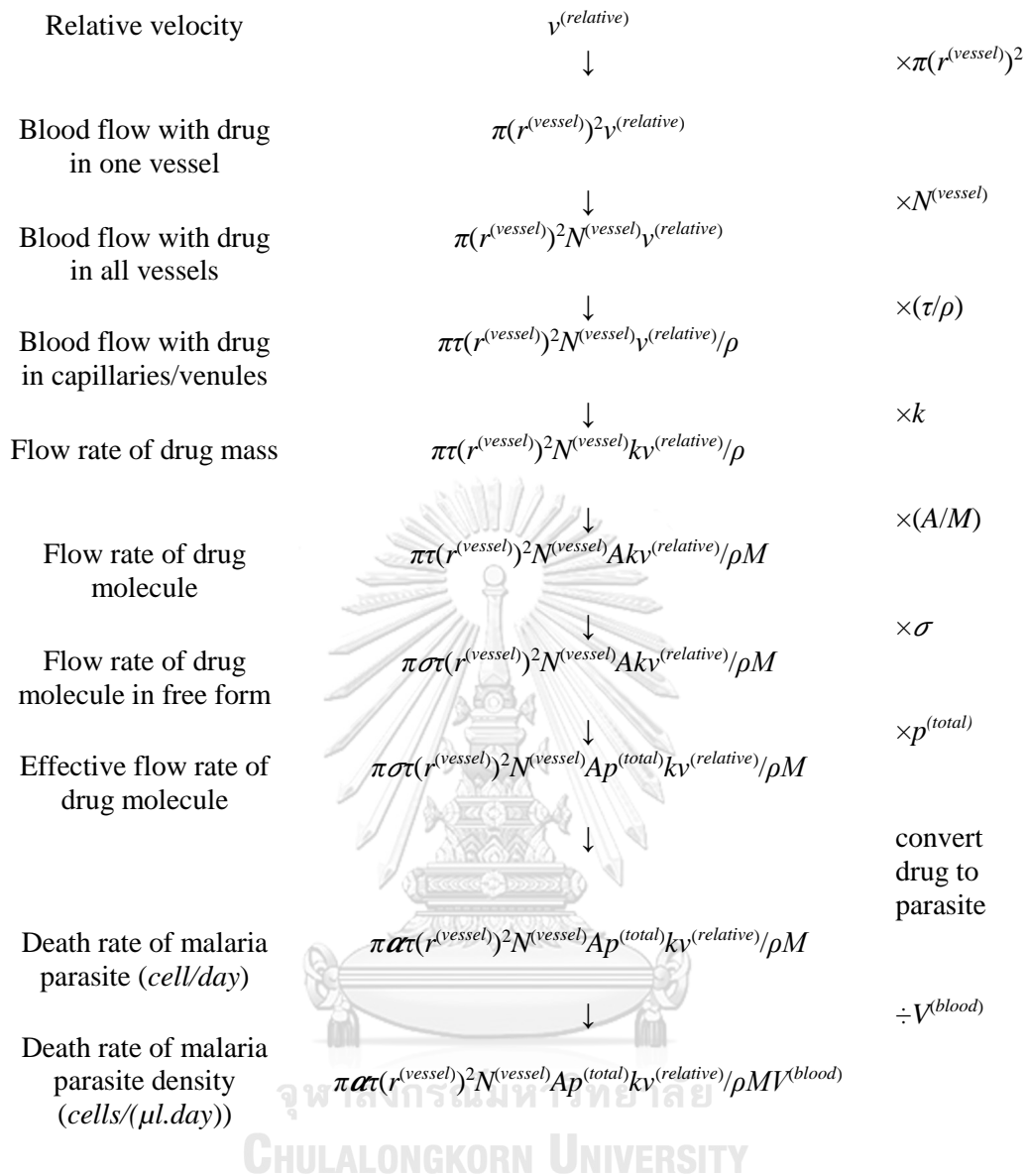


Figure 6. This diagram shows the first step formulation of the death rate of

circulating iRBCs, where $p_c^{(population)} = \frac{y_c}{x + y_c + y_s + E}$ in $p_c^{(total)}$.

Both death rates are considered in only capillaries and venules, then

$$\begin{aligned}\Psi_c^{(total)}(k) &= \Psi_c^{(capillary)}(k) + \Psi_c^{(venule)}(k), \\ \Psi_s^{(total)}(k) &= \Psi_s^{(capillary)}(k) + \Psi_s^{(venule)}(k).\end{aligned}$$

Before coupling these two death rates in the mathematical model of *P. falciparum*, both of them have to be formulated in terms of the standard variables such that x , y_c , y_s and E in the dynamic system as the following steps: (i) since both two population probability factors in cases of circulating and sequestered iRBCs are

$$p_c^{(population)} = \frac{y_c}{x + y_c + y_s + E} \text{ and } p_s^{(population)} = \frac{y_s}{x + y_c + y_s + E},$$

(ii) define

$$\begin{aligned}\varphi_c(k) &= \Psi_c^{(total)}(k) / p_c^{(population)} = \left(\frac{x + y_c + y_s + E}{y_c} \right) \Psi_c^{(total)}(k), \\ \varphi_s(k) &= \Psi_s^{(total)}(k) / p_s^{(population)} = \left(\frac{x + y_c + y_s + E}{y_s} \right) \Psi_s^{(total)}(k),\end{aligned}$$

(iii) subtract both $\Psi_c^{(total)}(k) = \left(\frac{y_c}{x + y_c + y_s + E} \right) \varphi_c(k)$ and $\Psi_s^{(total)}(k) = \left(\frac{y_s}{x + y_c + y_s + E} \right) \varphi_s(k)$ from the dynamic variables y_c and y_s in the mathematical model of *P. falciparum*. Thus, the mathematical model of *P. falciparum* with antimalarial drugs and immune response is

$$\begin{aligned} \frac{dx}{dt} &= \Lambda - \mu_x x - \beta xm, \\ \frac{dy_c}{dt} &= \beta xm - (\gamma_c + \mu_c) y_c - \frac{p_1 y_c E}{1 + \theta_1 y_c} - \left(\frac{y_c}{x + y_c + y_s + E} \right) \varphi_c(k), \\ \frac{dy_s}{dt} &= \gamma_c y_c - (\gamma_s + \mu_s) y_s - \frac{p_1 y_s E}{1 + \theta_1 y_s} - \left(\frac{y_s}{x + y_c + y_s + E} \right) \varphi_s(k), \\ \frac{dm}{dt} &= r \mu_s y_s - \mu_m m - \frac{p_2 m E}{1 + \theta_2 m}, \\ \frac{dE}{dt} &= -\mu_E E + \frac{k_1 (y_c + y_s) E}{1 + \theta_1 (y_c + y_s)} + \frac{k_2 m E}{1 + \theta_2 m}, \end{aligned}$$

where all parameters and values are in Table 1 and 2.

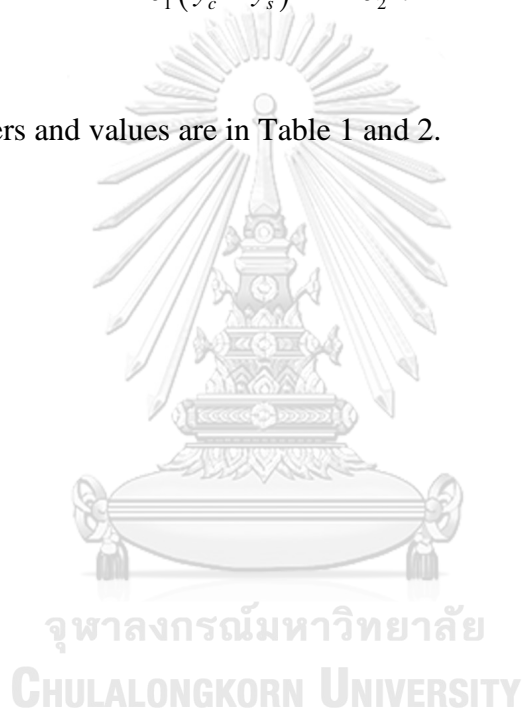


Table 1. Parameters for numerical simulations in case of malarial infection.

| Symbols | Value | Variables | Ref. |
|-------------------|-----------------------|--|-------|
| $G^{(drug)}$ | 1 | lag coefficient of a drug in capillary and venule | 10 |
| $G^{(iRBC)}$ | 0.6,0.9 | lag coefficient of an iRBC in capillary and venule, respectively. | 10 |
| $x(0)$ | 5×10^6 | initial normal density of normal RBCs (<i>cells/μl</i>) | 1 |
| A | 4.15×10^4 | production rate of RBCs (<i>cells/μl/day</i>) | 1 |
| $r^{(RBC)}$ | 3.9 | radius of RBC (μ m) | 13 |
| $r^{(iRBC)}$ | 3.9 | radius of iRBC (μ m) | 13 |
| $V^{(iRBC)}$ | 86-116 | volume of iRBC (μ m ³) | 13 |
| $\delta^{(iRBC)}$ | 0.03-0.8 | parasite volume fraction | 13 |
| g | 12 | product rate of merozoites (<i>/day</i>) | 1 |
| β | 2×10^{-9} | infective rate (<i>μl/cell.day</i>) | 1 |
| μ_x | 8.3×10^{-3} | decay rate of RBCs (<i>/day</i>) | 1 |
| μ_y | 1 | decay rate of iRBCs (<i>/day</i>) | 1 |
| μ_c | 0.42 | decay rate of circulating iRBCs (<i>/day</i>) | 16 |
| μ_s | 0.08 | decay rate of sequestered iRBCs (<i>/day</i>) | 16 |
| γ_c | 1.03 | transition rate from circulating to sequestered iRBCs (<i>/day</i>) | 16 |
| γ_s | 0.74 | transition rate from sequestered iRBCs to merozoites (<i>/day</i>) | 16 |
| p_1 | 10^{-8} | removal rate of all iRBCs by immune system | 1 |
| p_2 | 10^{-8} | removal rate of merozoites by immune system | 1 |
| k_1 | 2.5×10^{-5} | proliferation rate of immune effectors by all iRBCs | 1 |
| k_2 | 4.69×10^{-5} | proliferation rate of immune effectors by merozoites | 1 |
| θ_1 | 5×10^{-4} | $1/\theta_1$ half saturation constant for $y_c(t)$ and $y_s(t)$ | 1 |
| θ_2 | 6.67×10^{-4} | $1/\theta_2$ half saturation constant for $m(t)$ | 1 |
| μ_m | 48 | decay rate of merozoites (<i>/day</i>) | 1 |
| $m(0)$ | 10^4 | initial density of merozoites (<i>cells/μl</i>) | 1 |
| $E(0)$ | 10^4 | initial density of immune effectors (<i>cells/μl</i>) | 1 |
| ρ | 60 | blood circulatory time (s) | 18 |
| $r^{(capillary)}$ | 3 | radius of capillary (μ m) | 19 |
| $r^{(venule)}$ | 10 | radius of venule (μ m) | 19 |
| τ | 1 | transit time (s) of capillary and venule | 19 |
| l | 200,50-500 | Length (μ m) of capillary and venule, respectively. | 20 |
| $v^{(blood)}$ | 0.3,4 | blood velocity (<i>mm/s</i>) in capillary and venule, respectively. | 19,21 |
| N | $10^9, 10^7$ | number of capillaries and venule, respectively. | 22 |
| $V^{(blood)}$ | 5 | whole blood volume (liters) | 23 |
| $X(t_0)$ | 10^5 | parasite density in blood at t_0 | 24,25 |
| A | 6.02×10^{23} | Avogadro's number | 26 |
| ε | 40-50 | Ratio of drug efflux in case of resistant parasite to susceptible parasite | 27 |

Table 2. Parameters of chloroquine, mefloquine, halofantrine and artesunate
(see all parameters in Table 1).

| Notations | $r_l(nm)$ | $r_w(nm)$ | M | α | $k (ng/ml)$ | Ref. |
|--------------|-----------|-----------|----------|----------|-------------|-------|
| Chloroquine | 0.7856 | 0.35525 | 319.8721 | 0.45 | 120 | 28 |
| Mefloquine | 0.6333 | 0.33765 | 378.3122 | 0.02 | 500-638 | 29 |
| Halofantrine | 0.86655 | 0.427 | 500.4237 | 0.02 | 1000 | 29,30 |
| Artesunate | 0.7619 | 0.37065 | 384.4208 | 0.38 | 110-310 | 31,32 |

3. Results and Discussion

This section describes the results of the numerical simulation from using artesunate, chloroquine, mefloquine and halofantrine. They represent the antimalarial drugs for three cases: single drug treatment or monotherapy, drug resistance and artemisinin-based combination therapy or ACT.

In case of single drug treatment, the treatment durations for clearing parasite of all chloroquine, mefloquine, halofantrine and artesunate in case of *P. non-falciparum* are the same pattern (straight line in log-linear axis). These patterns and treatment durations in Figure 7(a), 7(b), 7(c) and 7(d) are also similar to Figure 1 and 4 in White²⁵. Furthermore, in case of *P. falciparum*, the numerical results from artesunate, chloroquine, mefloquine and halofantrine in Figure 8(a), 8(b), 8(c) and 8(d), respectively, also show that their patterns are also straight line in log-linear axis as well.

In case of drug resistance, *Plasmodium sp.* occurs only for some certain drugs. Chloroquine-resistant *P. vivax* are found in Papua New Guinea, Indonesia, Burma

(Myanmar), India, and Central and South America but not *P. ovale*, *P. malariae* and *P. knowlesi*.³ *P. falciparum* also resists other non-quinoline groups, such as mefloquine and halofantrine.³³ Consequently, in order to obtain our numerical results, the only drug efflux will be considered for our mechanism of drug resistance (see Sinha *et al.*³⁴ in details), which can be formulated in mathematical formula. Thus, an assumption that all *Plasmodium sp.* resist all drugs except artemisinin is added in this study for numerical analysis. In the process of calculation, the efficacy of drug resistance is defined as the ratio of drug efflux in case of resistant parasite to susceptible parasite, denoted by ε (see this value in Table 1), and applied by dividing with the death rate of malaria parasite. Thus, the death rates of malaria parasite with drug resistance are $\left(\frac{y_c}{x + y_c + y_s + E}\right) \frac{\varphi_c(k)}{\varepsilon}$, $\left(\frac{y_s}{x + y_c + y_s + E}\right) \frac{\varphi_s(k)}{\varepsilon}$, and $\left(\frac{y}{x + y + E}\right) \frac{\varphi(k)}{\varepsilon}$ in cases of *P. falciparum* with circulating and sequestration process, and other *Plasmodium sp.*, respectively (see also Table 3). According to the simulation, those patterns of results from chloroquine, mefloquine and halofantrine are unchanged but their durations are longer than the results without drug resistance, as shown in Figure 9(a), 9(c) and 9(e) in case of *P. non-falciparum*, and Figure 10(a), 10(c) and 10(e) in case of *P. falciparum*, respectively. Thus, this parameter of resistance conforms with the real patient's data that it can affect treatment duration.

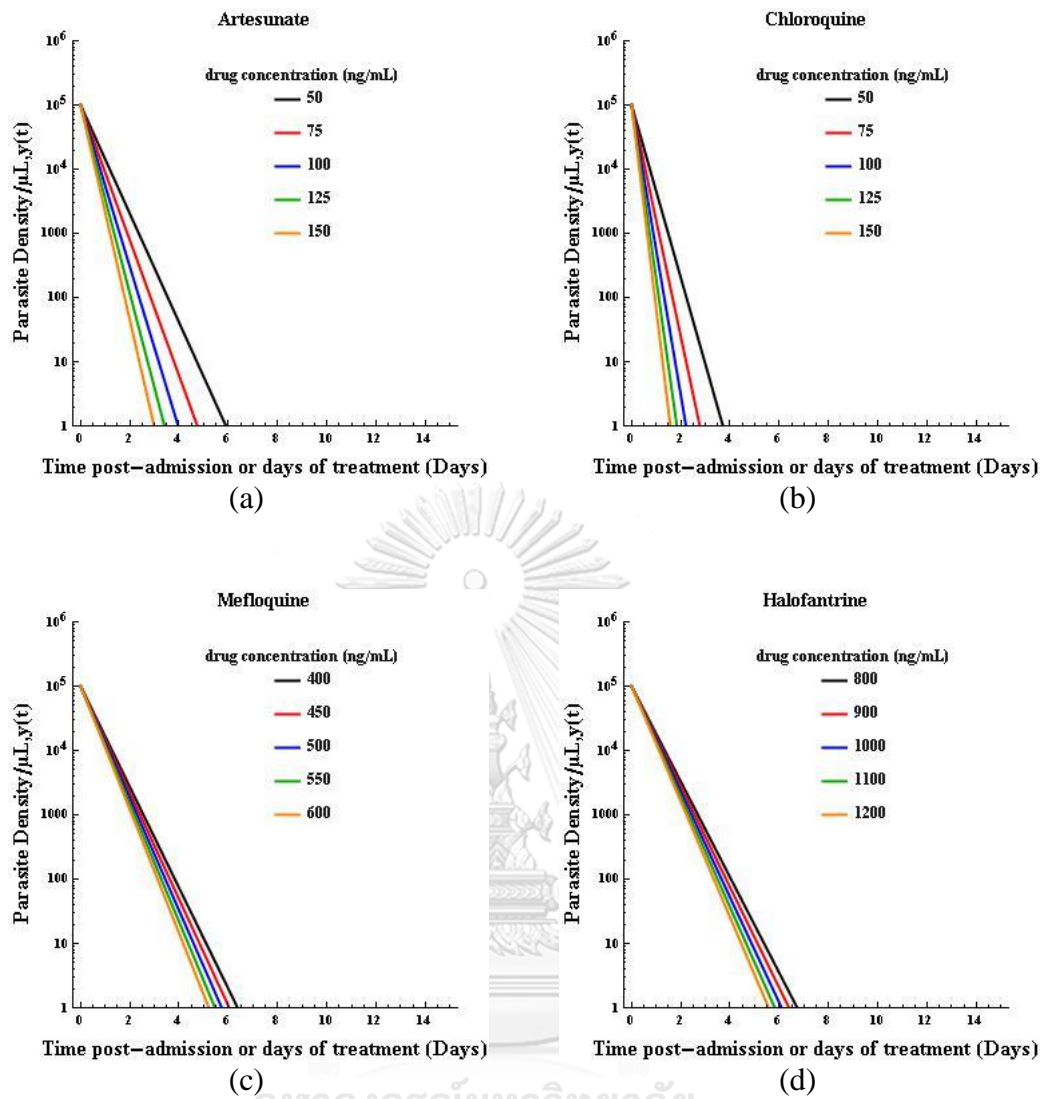


Figure 7. Comparison between real patient's data of Figure 1 and 4 in White²⁵ and our numerical results from (a) artesunate, (b) chloroquine, (c) mefloquine and (d) halofantrine in case of *P. non-falciparum*.

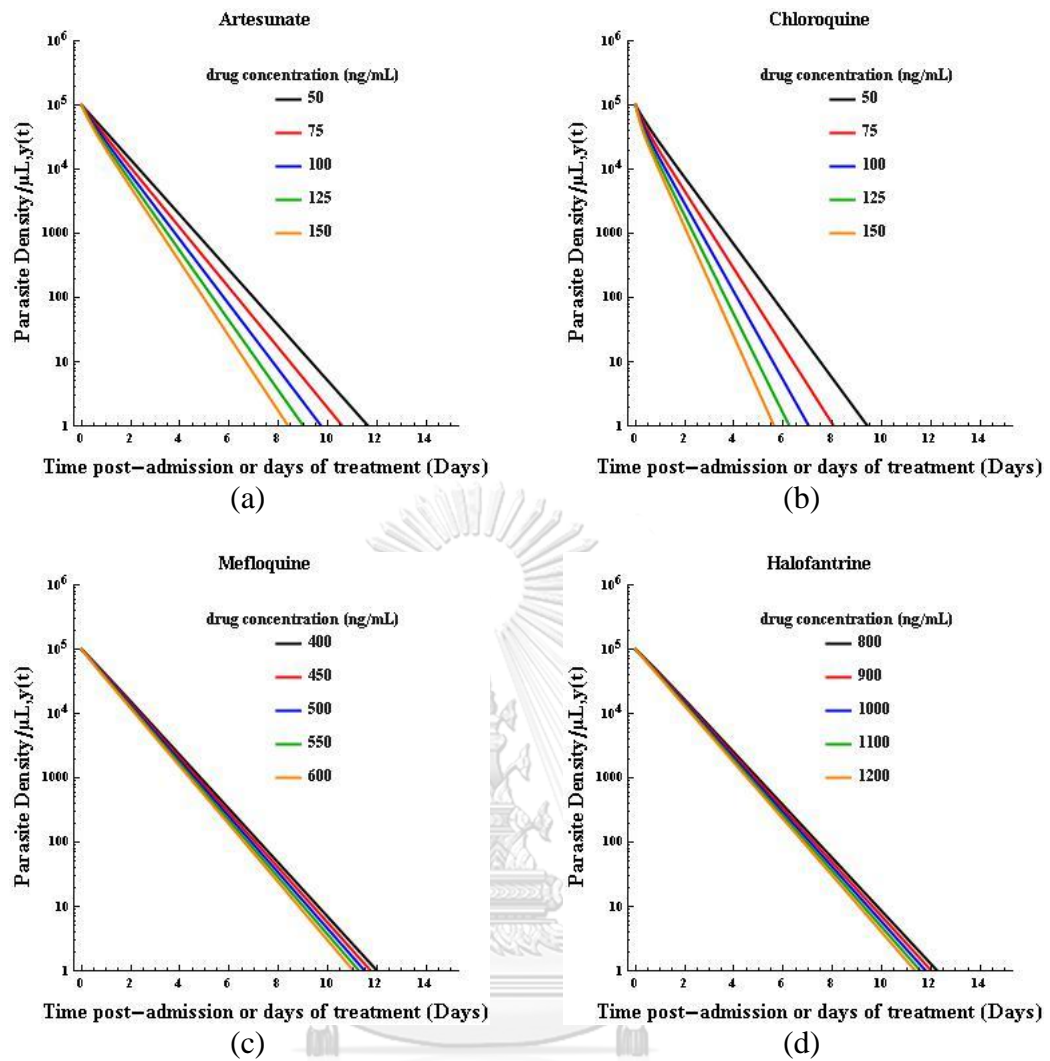


Figure 8. Our numerical results from artesunate, chloroquine, mefloquine and halofantrine in case of *P. falciparum*, shown in Figure 8(a), 8(b), 8(c) and 8(d), respectively.

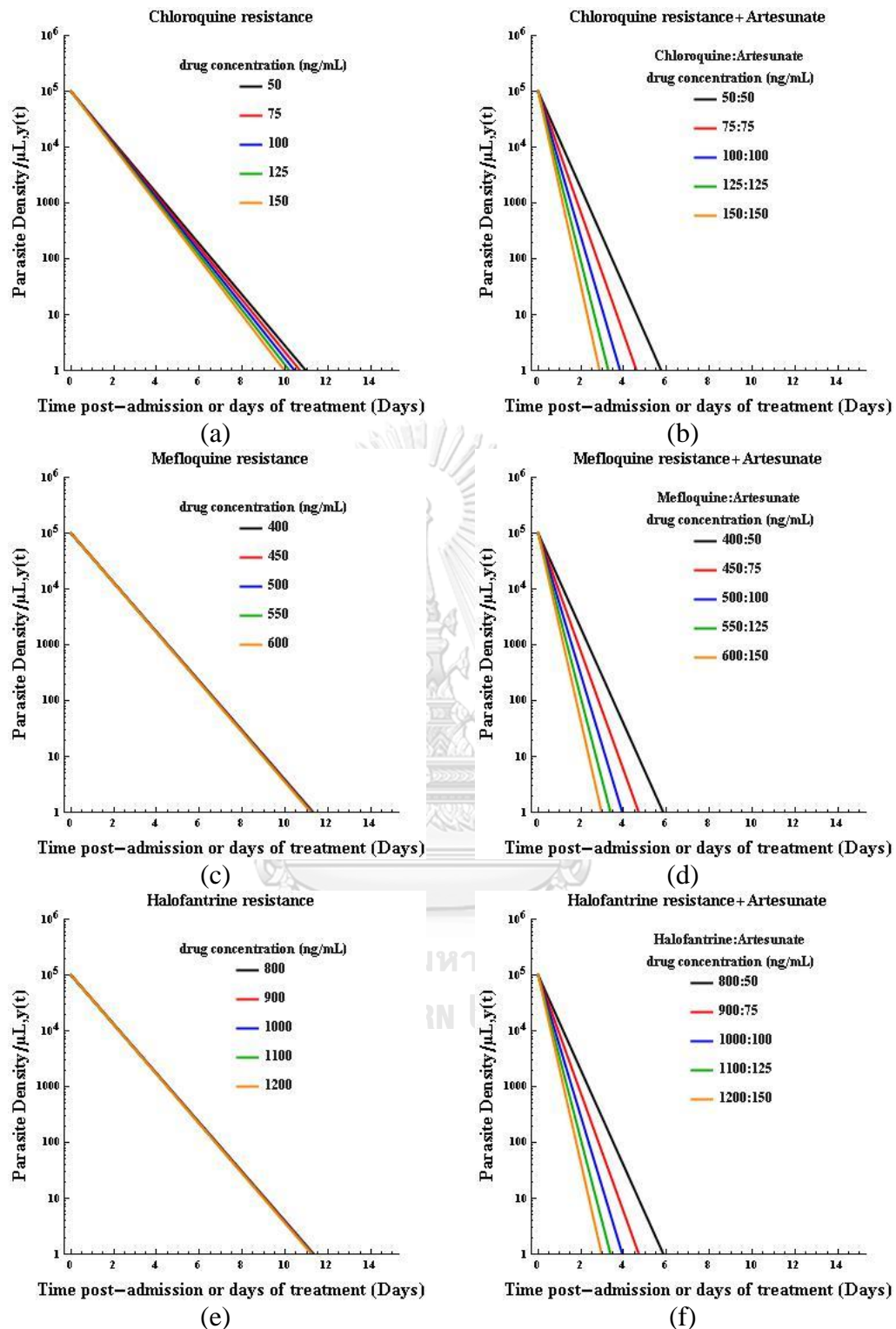


Figure 9. Numerical results of chloroquine, mefloquine and halofantrine with drug resistance and artesunate-based combination therapy (ACT) in case of *P. non-falciparum*.

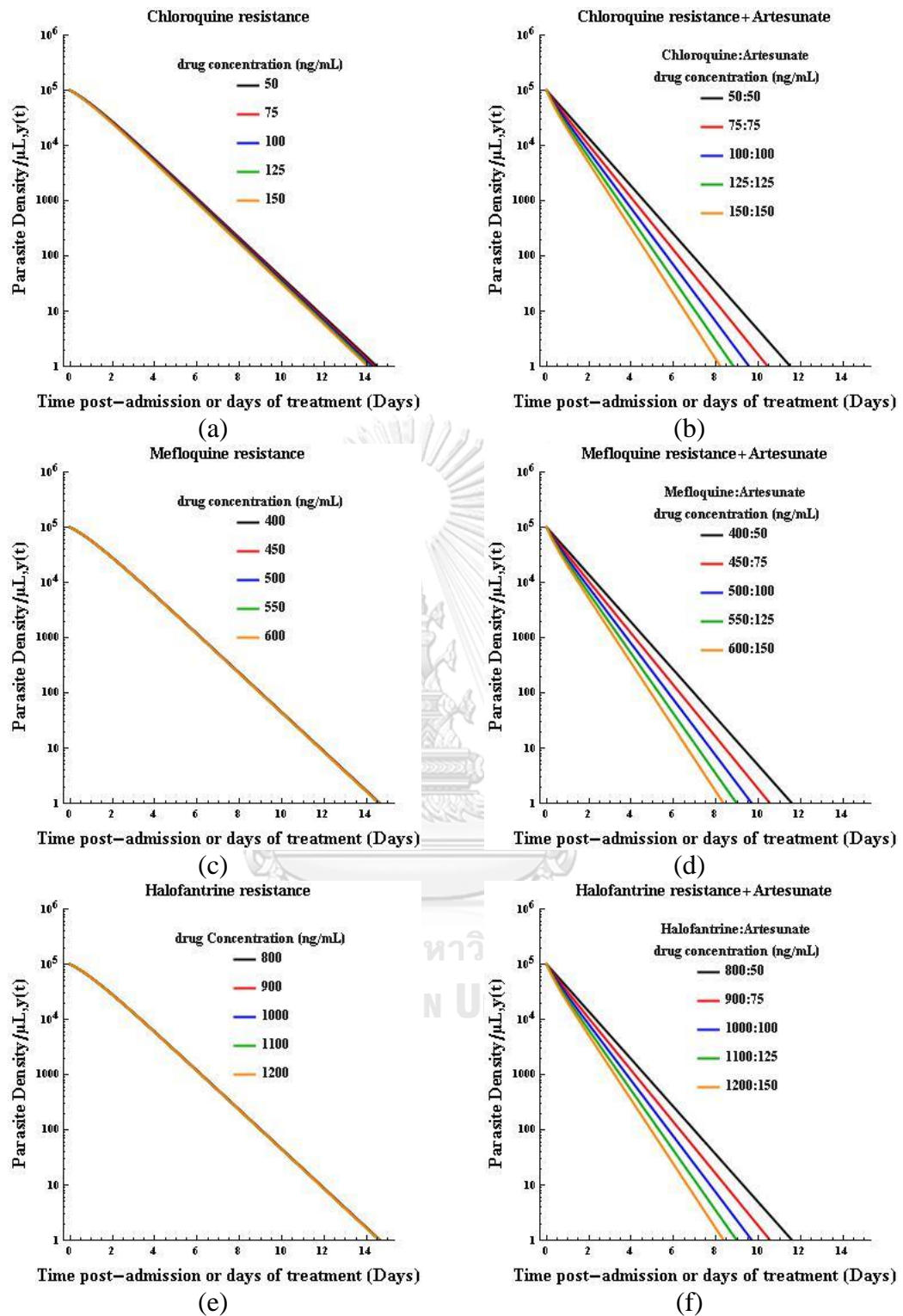


Figure 10. Numerical results of chloroquine, mefloquine and halofantrine with drug resistance and artesunate-based combination therapy (ACT) in case of *P. falciparum*.

In case of monotherapy with resistance and combination with artemisinin (or ACT), the death rate of the malaria parasites in this case is modeled by the partial summation of the death rates in each drug and artesunate with its resistance. In view of calculation, the death rates of the malaria parasite are

$$\begin{aligned} & \left(\frac{y_c}{x + y_c + y_s + E} \right) \left(\frac{\varphi_c^{(drug)}(k)}{\varepsilon} + \varphi_c^{(artesunate)}(k) \right), \\ & \left(\frac{y_s}{x + y_c + y_s + E} \right) \left(\frac{\varphi_s^{(drug)}(k)}{\varepsilon} + \varphi_s^{(artesunate)}(k) \right), \quad \text{and} \\ & \left(\frac{y}{x + y + E} \right) \left(\frac{\varphi^{(drug)}(k)}{\varepsilon} + \varphi^{(artesunate)}(k) \right), \end{aligned}$$

in cases of *P. falciparum* with circulating and sequestration process, and *P. non-falciparum*, respectively (see also Table 3). After generating the results, all treatment durations in case of *P. non-falciparum* in Figure 9(b), 9(d) and 9(f), and *P. falciparum* in Figure 10(b), 10(d) and 10(f), are shortened with respect to monotherapy. This confirms that ACT is more effective than monotherapy. Thus, the suggestion is that artesunate should be used in case of drug resistance.

Table 3. The death rates of malaria parasite in cases of general drug, drug with resistance, artesunate and artemisinin-based combination therapy, and population probability factors.

| Species | <i>Plasmodium falciparum</i> | | Other <i>P. species</i> |
|---|---|---|--|
| Process | Circulating | Sequestration | - |
| Population probability factor | $\frac{p_c^{(population)} \text{ or } y_c}{x + y_c + y_s + E}$ | $\frac{p_s^{(population)} \text{ or } y_s}{x + y_c + y_s + E}$ | $\frac{p^{(population)} \text{ or } y}{x + y + E}$ |
| Death rates of the malaria parasites | | | |
| Drug | $p_c^{(population)} \varphi_c^{(drug)}(k)$ | $p_s^{(population)} \varphi_s^{(drug)}(k)$ | $p^{(population)} \varphi^{(drug)}(k)$ |
| Drug with resistance | $\frac{p_c^{(population)} \varphi_c^{(drug)}(k)}{\varepsilon}$ | $\frac{p_s^{(population)} \varphi_s^{(drug)}(k)}{\varepsilon}$ | $\frac{p^{(population)} \varphi^{(drug)}(k)}{\varepsilon}$ |
| Artesunate | $p_c^{(population)} \varphi_c^{(artesunate)}$ | $p_s^{(population)} \varphi_s^{(artesunate)}$ | $p^{(population)} \varphi^{(artesunate)}(k)$ |
| Artemisinin-based combination therapy (ACT) | $p_c^{(population)} \times \left(\frac{\varphi_c^{(drug)}(k)}{\varepsilon} + \varphi_c^{(artesunate)} \right)$ | $p_s^{(population)} \times \left(\frac{\varphi_s^{(drug)}(k)}{\varepsilon} + \varphi_s^{(artesunate)} \right)$ | $p^{(population)} \times \left(\frac{\varphi^{(drug)}(k)}{\varepsilon} + \varphi^{(artesunate)}(k) \right)$ |

4. Conclusion

The numerical results from the mathematical model of the within-host malaria parasite with antimalarial drugs taking with the immune response of both *Plasmodium falciparum* and other *Plasmodium species* illustrate that all treatment durations are within 1-15 days in cases of all artesunate, chloroquine, mefloquine and halofantrine. Furthermore, treatment duration or the period time to kill both circulating and sequestered iRBCs in these results are 2-12 days, which conform to the patients' clinical data. However, in order to use this research, all of above conditions in this study must be met. The weak points in this study are concerning too many assumptions are needed. Therefore, the improvement for this research is to reduce these conditions or assumptions to make the model conforming to the actual results. Finally, our mathematical models of malaria parasite with antimalarial drugs together with the immune response under hypotheses used with pharmacology, theoretical physics and chemistry are reasonably comparable to the real clinical data from laboratory results and therefore meet our objective to mathematically predict the duration of treatment.

Acknowledgements

This study was funded by Scholarship 60/40 of Chulalongkorn University.

References

1. Li Y, Ruan S, Xiao D. The Within-Host dynamics of malaria infection with immune response. *Math Biosci Eng.* 2011 Oct 1;8(4):999-18.
2. World health organization [Internet]. Malaria: Information for travellers. [updated 2017 Jan 27; cited 2017 Aug 3]. Available from: <http://www.who.int/malaria/travellers/en/>
3. Centers for Disease Control and Prevention (CDC) [Internet]. CDC - Malaria - About Malaria - Biology. [updated 2016 Mar 16; cited 2017 Aug 3]. Available from: <https://www.cdc.gov/malaria/about/biology/>
4. Ockenhouse CF, Ho M, Tandon NN, Van Seventer GA, Shaw S, White NJ, et al. Molecular basis of sequestration in severe and uncomplicated *Plasmodium falciparum* malaria: differential adhesion of infected erythrocytes to CD36 and ICAM-1, *J Infect Dis.* 1991 Jul;164(1):163-9.
5. Franke-Fayard B, Fonager J, Braks A, Khan SM, Janse CJ. Sequestration and tissue accumulation of human malaria parasites: can we learn anything from rodent models of malaria? *PLoS Pathog.* 2010 Sep 30;6(9): e1001032.
6. Terkuile F, White NJ, Holloway P, Pasvol G, Krishna S. *Plasmodium falciparum*: *in vitro* studies of the pharmacodynamic properties of drugs used for the treatment of severe malaria. *Exp Parasitol.* 1993 Feb;76(1):85-95.
7. Wilairatana P, Looareesuwan S. Artesunate: A potent antimalarial drug for *Falciparum* malaria. *J Infect Dis Antimicrob Agents.* 1996 Sep;3(13):119-121.
8. Pabst W, Gregorová E [Internet]. ICT Prague: Characterization of particles and particle systems [cited 2017 Aug 3]. Available from:

[http://old.vscht.cz/sil/keramika/Characterization_of_particles/CPPS_English
version_.pdf](http://old.vscht.cz/sil/keramika/Characterization_of_particles/CPPS_English_version_.pdf)

9. Brinkman HC. A calculation of the viscous force exerted by a flowing fluid on a dense swarm of particles. *Appl. Sci. Res.* 1949;1:27-34.
10. Agasanapura BN, Baltus RE, Chellam S. Effect of convective hindrance on microfiltration of rod shaped particles. *Proceedings of the 2011 AIChE Annual Meeting*; 2011 Oct 16-21; Minneapolis, USA. New York: NY American Institute of Chemical Engineers; 2011.
11. Mazaheri A. Probabilistic modeling of ship grounding – A review of the literature: Espoo: Helsinki University of Technology; 2009.
12. Ghosh P. Stochastic models for in-silico event-based biological network simulation [dissertation]. Arlington, TX: University of Texas at Arlington; 2007.
13. Ye T, Phan-Thien N, Khoo BC, Lim CT. Stretching and relaxation of malaria-infected red blood cells. *Biophys J.* 2013 Sep 3;105(5):1103-9.
14. Berg HC, Purcell EM. Physics of chemoreception. *Biophys J.* 1977 Nov;20(2):193-219.
15. Taroni C, Jones S, Thornton JM. Analysis and prediction of carbohydrate binding sites. *Protein Eng.* 2000;13(2):89-98.
16. Bichara D, Cozic N, Iggidr A. On the estimation of sequestered infected erythrocytes in Plasmodium falciparum malaria patients. *Math Biosci Eng.* 2014;11(4):741-59.

17. Tanna JA, Patel PN, Kalele SD. Relation between organ weights and body weight in adult population of Bhavnagar Region-a post-mortem study. *J Indian Acad Forensic Med.* 2011 Jan-Mar;33(1):57-9.
18. Yan RT, George RT, Lima JAC. Multislice cardiac tomography: myocardial function, perfusion, and viability. In: Dilsizian V, Pohost GM, editors. *Cardiac CT, PET and MR.* 2nd ed. Hoboken: Wiley-Blackwell; 2010. p. 259-277.
19. Khurana I. *Textbook of medical physiology.* Kundli: Elsevier; 2006.
20. Krstic RV. *Human microscopic anatomy: an atlas for students of medicine and biology.* Ochsenfurt-Hohestadt: Springer-Verlag, Berlin Heidelberg; 1997.
21. van de Vosse FN, van Dongen MEH. Cardiovascular fluid mechanics - lecture notes - Materials Technology Chapter 8 "Flow patterns in the microcirculation" [Internet]. Eindhoven University of Technology, Faculty of Mechanical Engineering (MaTe), Faculty of Applied Physics (NT); 1998 [cited 2016 Nov 4]. Available from: <http://www.mate.tue.nl/people/vosse/docs/cardio.pdf>
22. Pollak AN, editor. *Emergency Care and Transportation of the Sick and Injured.* 10th ed. Sudbury: Jones & Bartlett Publishers; 2005.
23. Higgins JM, Eddington DT, Bhatia SN, Mahadevan L. Statistical dynamics of flowing red blood cells by morphological image processing. *PLoS Comput Biol.* 2009 Feb;5(2):1-10.
24. Ali H, Ahsan T, Mahmood T, Bakht SF, Farooq MU, Ahmed N. Parasite density and the spectrum of clinical illness in falciparum malaria. *J Coll Physicians Surg Pak.* 2008 Jun;18(6):362-8.
25. White NJ. The parasite clearance curve. *Malaria J.* 2011;10:278.1-8.

26. Staver JR, Lumpe AT. A content analysis of the presentation of the mole concept in chemistry textbooks. *JRST* 1993 April;30(4):321-37.
27. Krogstad DJ, Schlesinger PH, Herwaldt BL. Antimalarial agents: mechanism of chloroquine resistance. *Antimicrob Agents Chemother.* 1988 Jun; 32(6): 799-801.
28. Karbwang J, Bunnag D, Harinasuta T, Chittamas S, Berth J, Druilhe P. Pharmacokinetics of quinine, quinidine and Cinchonine when given as combination. *Southeast Asian J Trop Med Public Health.* 1992 Dec;23(4): 773-6.
29. White NJ. Antimalarial pharmacokinetics and treatment regimens. *Br J Clin Pharmacol.* 1992 Jul;34(1):1-10.
30. Veenendaal JR, Parkinson AD, Kere N, Rieckmann KH, Edstein MD. Pharmacokinetics of halofantrine and n-desbutylhalofantrine in patients with falciparum malaria following a multiple dose regimen of halofantrine. *Eur J Clin Pharmacol.* 1991;41(2):161-4.
31. Ashton M, Hai TN, Sy ND, Huong DX, Van Huong N, Niêu NT, Cống LD. Artemisinin pharmacokinetics is time-dependent during repeated oral administration in healthy male adults. *Drug Metab Dispos.* 1998 Jan;26(1):25-7.
32. Morris CA, Duparc S, Borghini-Fuhrer I, Jung D, Shin CS, Fleckenstein L. Review of the clinical pharmacokinetics of artesunate and its active metabolite dihydroartemisinin following intravenous, intramuscular, oral or rectal administration. *Malar J.* 2011 Sep 13;10:263,1-17.
33. de Villiers KA, Egan TJ. Recent advances in the discovery of haem-targeting drugs for malaria and schistosomiasis. *Molecules.* 2009;14(8): 2868-87.

34. Sinha S, Medhi B, Sehgal R. Challenges of drug-resistant malaria. *Parasite*. 2014;21(61):1-15.



CHAPTER 5

CONCLUSION AND DISCUSSION

5.1 Main Concepts and Analysis of the Dissertation

In general, there are several existing methods used to predict the treatment duration for a patient with infection. For example, physicians can use the statistical data from the laboratory to predict the treatment duration. Usually, the time to stop the drug administration is the day that patient recovers from the symptoms such as fever, etc. Moreover, statistic prediction is easier to apply than the mathematical models since there is no need to use the complex methods such as solving the system of differential equations, coding the mathematical computation program, etc. However, the disadvantage of prediction by using statistics method is that there must be enough data. Thus, if there is the new pathogen, which has never been dealt with before, then statistic method cannot be applied. In contrast, although the new pathogen is unknown, the prediction of treatment duration from the mathematical models can always be determined by the measurement of some certain parameters such as the width and length of pathogen, the natural growth and death rate, which are theoretically enough to calculate the duration of treatment.

In this dissertation, the death rate in the form of the mathematical model can be applied with not only to bacteria or malaria, but also other pathogens in patient's blood such as protozoa, virus (in case of viremia), fungi, etc. The reason is that our model uses the relative velocity from the convection of blood, which is always available.

The results from our model about the treatment durations and patterns from the numerical results of bacteria and malaria with and without immune response in this

research are compatible to the real-world situation. Nevertheless, there are some comments and suggestions of using the mathematical model to formulate the death rate of pathogen in this dissertation, detailed in the next sections.

We prepared the mathematical model to predict the duration of treatment. Our models are determined by the measurement of some certain parameters such as the width and length of pathogen, the natural growth and death rate of pathogens. Furthermore, our method should be flexible enough if we need to apply it to unknown pathogen by adjusting the appropriate parameters.

5.2 The Differences of Results between Bacteria and Malaria

Before discussing the numerical results, note that the horizontal and vertical axes in the graph respectively represent the log-linear scale and the time of treatment. This implies that the straight line decreases in the graph near the exponential decay. Our numerical simulation shows that the graphs of numerical results in case of bacteria decrease exponentially while the two cases of *P. non-falciparum* and malaria with immune response are log-linear straight. This situation can be explained by noting that there is the population probability factor in cases of *P. non-falciparum* and malaria with immune response but not in the case of bacteria. The purpose of population probability factor is to modify the death rate of pathogens in order to make the model compatible the actual results. Consequently, if the density of pathogens is almost zero, then the death rate of pathogens should be very small. Thus, the population probability factor will make the difference in the model between bacteria and malaria.

5.3 Numerical Results in Case of Malaria

5.3.1 Monotherapy with or without Immune Response

The numerical results in case of malaria with immune response are quite similar to the case of malaria without immune response until the population of the immune effectors increase substantially. Figure 1(a)-1(f) show the treatment durations of patients treated by antimalarial drug halofantrine and the numerical results of the malarial case with immune response. First, the treatment durations in Figure 1(a) with the initial density of immune effectors of $E(0)=10^4/\mu L$ blood. Then, as the density of immune effectors are increased to $E(0)=10^4, 10^6, 10^7, 10^8, 10^9$ and $10^{10}/\mu L$ blood in Figure 1(a), 1(b), 1(c), 1(d), 1(e) and 1(f), respectively, the parasite densities decrease dramatically and the treatment durations shorten. Observe that after the immune effectors increase, the parasite densities (or iRBCs, denoted as $y(t)$) decrease faster and the treatment durations are shorter. This phenomenon indicates the effect of the immune response and the drug to the malarial parasites. Thus, this conforms to the real-world situation that the immune effect can help the drug to get rid of the malarial parasites. Note that the other drugs in this work, artesunate, chloroquine and mefloquine, have also the same characteristic. Hence, this concludes that the antimalarial drug administration with the help immune effect can better treat the patients with malaria infection.

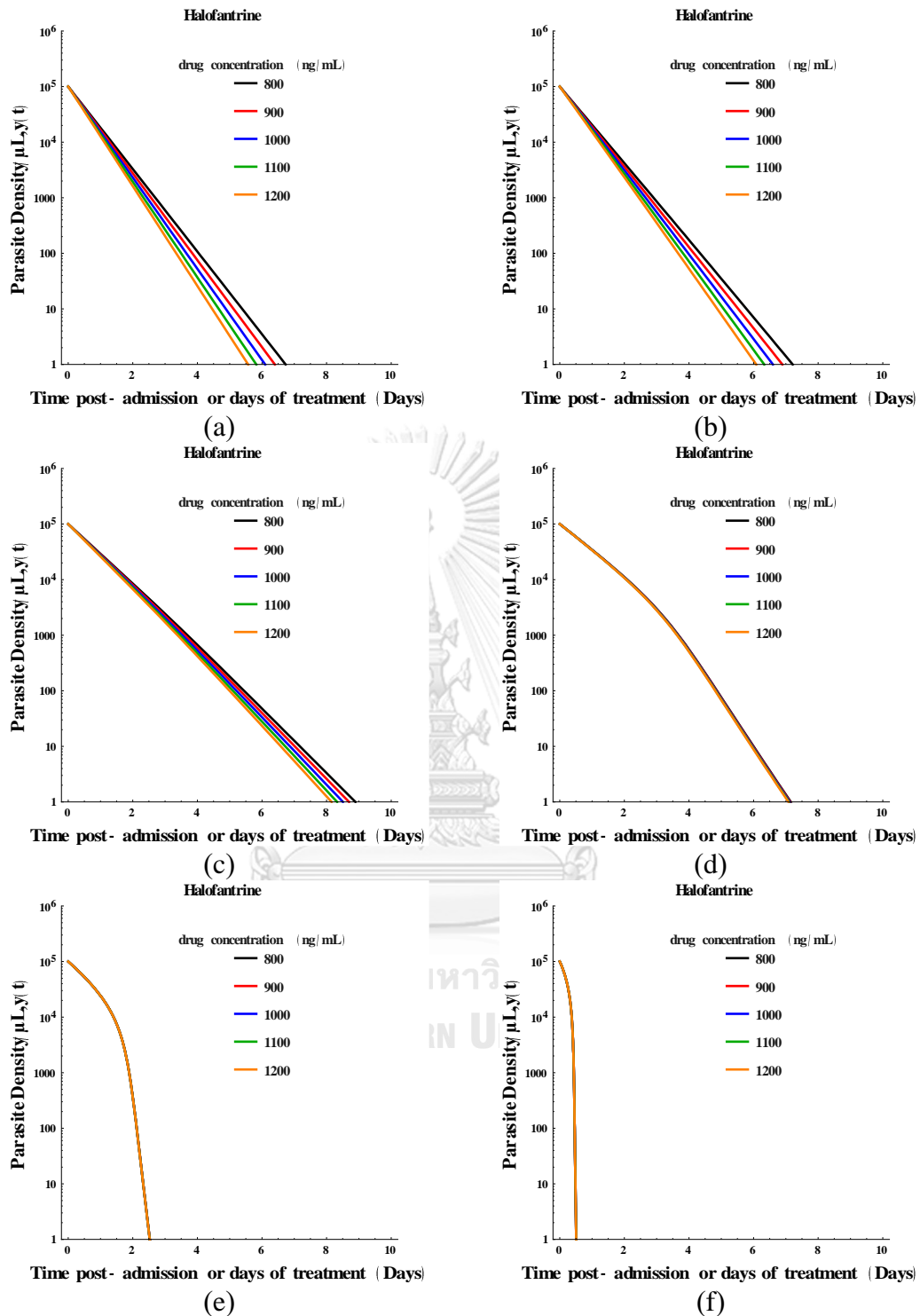
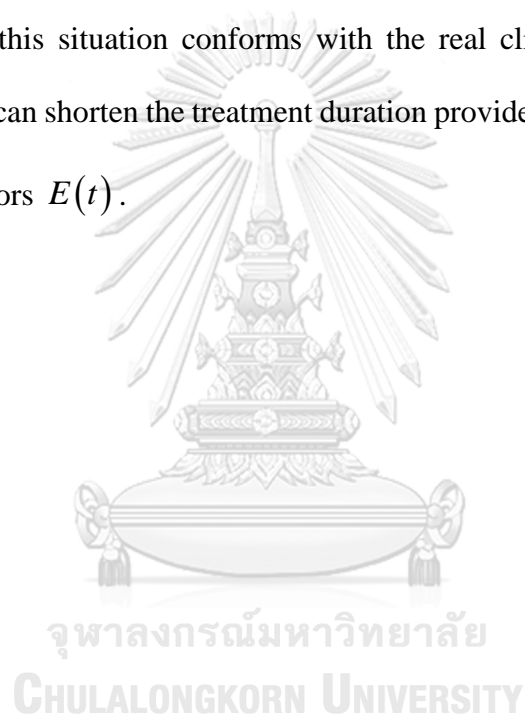


Figure 1. Figure 1(a)-1(f) show the numerical results between the parasite density and days of treatment with the initial density of immune effectors $E(0) = 10^4, 10^6, 10^7, 10^8, 10^9$ and $10^{10}/\mu\text{L}$ blood in Figure 1(a), 1(b), 1(c), 1(d), 1(e) and 1(f), respectively.

5.3.2 Differences between Monotherapy and Drug Resistance with Immune Response in both of them

Figure 2(a)-2(d) illustrate the relation between the parasite density $y(t)$ and t with various density of initial immune effectors $E(0)$. When the density of initial immune effectors $E(0)$ increase, the parasite density $y(t)$ decrease faster. This situation can be explained pathologically by the effects of the immune effectors on the parasites. Hence, this situation conforms with the real clinical data. Therefore, the immune response can shorten the treatment duration provided the patients have enough the immune effectors $E(t)$.



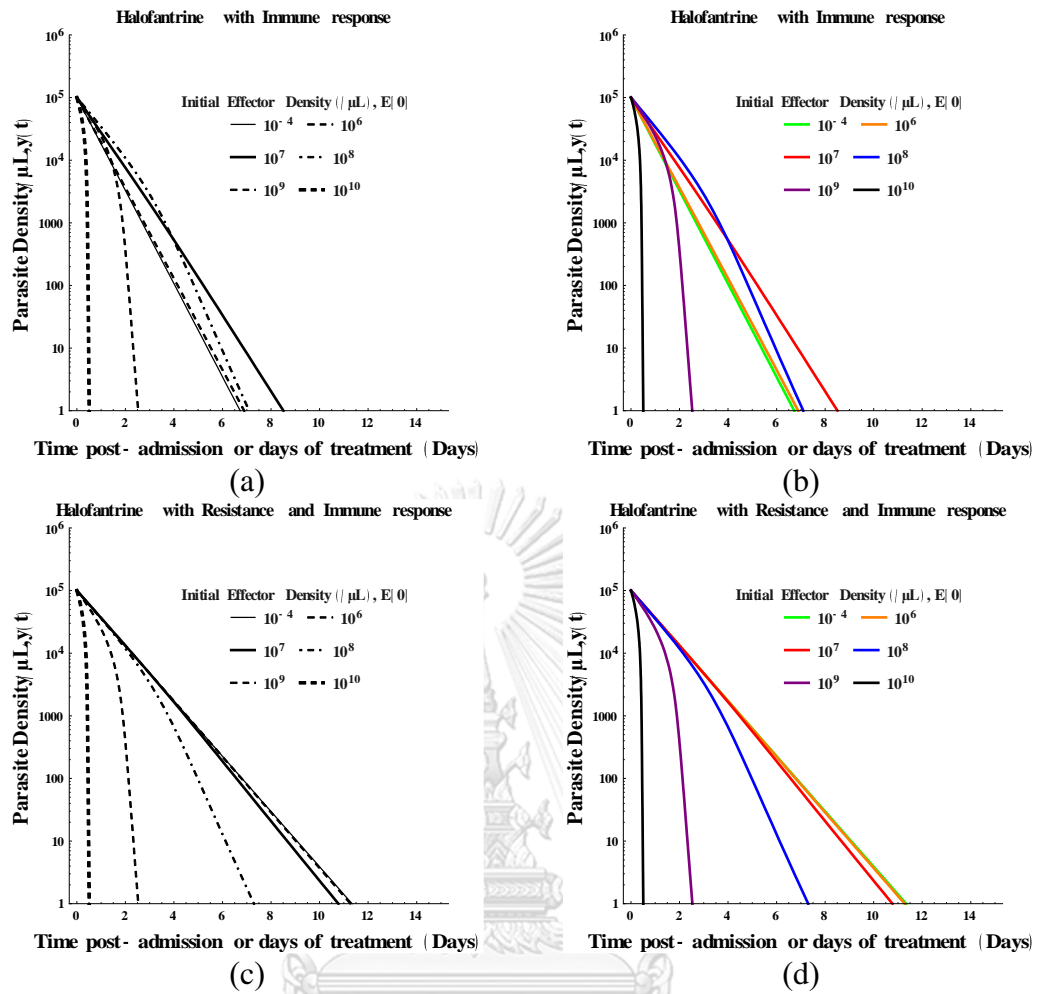


Figure 2. Figure 2(a) and 2(b) show the numerical results between the parasite density and days of treatment with the initial density of immune effectors $E(0)=10^4$, 10^6 , 10^7 , 10^8 , 10^9 and $10^{10}/\mu\text{L}$ blood in black-white and color version, respectively. Figure 2(c) and 2(d) represent the same situations as in Figure 2(a) and 2(b) with drug resistance added on.

5.4 Connection of the Results from Researches between Three Articles

Our first article is concerning the case of bacteria. Since the mathematical model of bacteria requires only one differential equation, which involves the natural growth and death rates, this case represents the simplest type of death rate of pathogens [2]. The principle of the relative velocity is based on the physics principles. Furthermore, the numerical results in this case show that the treatment durations are conforming to the treatment durations from the actual patient's data [11]. However, the graph patterns from numerical simulations are quite different from the real patient's data. The reason is that the simplicity of one differential equation of bacteria might not be enough to give the specific characteristics of the graph pattern of the real patient's data. Moreover, the death rate of pathogens in this study should also be applicable to other type of pathogens as well. This leads us to the results of other two articles, which deal with malaria instead of bacteria.

Our second article deals with the malaria parasites except *Plasmodium falciparum*. This case is more complex than the case of bacteria since it consists of three main types of populations as follows: 1) normal red blood cells (RBCs), 2) infected red blood cells (iRBCs), and 3) extracellular parasites or merozoites [3]. In this case, we use three differential equations in order to formulate the death rate of the malaria parasite. As a result from the numerical simulations, we find that the numerical results are more compatible to the actual patient's data than the case of bacteria model. The correlation can be described as follows: 1) the duration of treatment is 2-12 days, and 2) the pattern of graph is the log-linear type. The reason can be explained from the consequences of more differential equations that we use. Remark that the mechanisms of drug action in the cases of bacteria and malaria parasite are also different. In

particular, the binding probability factor in the death rate of bacteria is the chance of binding between a drug molecule and enzyme, while the binding probability factor in the death rate of malaria parasite is the chance of binding between a drug molecule and the numerous ferric ion from hemoglobin. Although the binding probability factors in the cases of bacteria and malaria are different, the durations of treatment are still comparable to the actual treatment durations in both cases. Hence, the difference of the mechanism of drug has been taken care of by using the different models.

Before we introduce the third article, we recall the pathogen of *Plasmodium falciparum*. In case of *Plasmodium falciparum*, iRBCs are divided into two main types: circulating and sequestered iRBCs. Note that the behavior of circulating iRBCs is the same as the iRBCs from other *Plasmodium species* while the behavior of sequestered iRBCs is quite different. The first characteristic of the sequestered iRBCs is that they are fixed at the luminal walls of capillaries and venules. In particular, they do not float around in the bloodstream. Thus, their relative velocity does not need to be included in the equations, and the drug molecules can move quickly to bind the sequestered iRBCs [6]. The second characteristic of sequestered iRBCs is that the sequestration process occurs specially only in vital organs: brain, heart, lungs, liver and kidneys [7, 8]. Although the binding between drug molecules and iRBCs in the case of *Plasmodium falciparum* is probably faster than the case of *P. malariae*, *P. vivax*, *P. ovale* and *P. knowlesi*, the durations of treatment in case of *Plasmodium falciparum* are longer than the case of *P. malariae*, *P. vivax*, *P. ovale* and *P. knowlesi*. Our results still conform to the real-world situation that *Plasmodium falciparum* is more violent than other *Plasmodium species*, i.e. the lifespan of *Plasmodium falciparum* is longer and it is harder to get rid of the *P. malariae*, *P. vivax*, *P. ovale* and *P. knowlesi*.

In our third article, we consider the case of all *Plasmodium species* with immune response. There are some additional modifications in this case as follows: 1) we add some more mathematical terms to the differential equations of iRBCs and merozoites, and 2) there is one more additional differential equation to describe the immune effectors. The numerical results show that the immune system does have some effects in the population of the malaria parasite. Mathematically, the immune system will shorten the treatment durations which is also compatible to the real-world situation.

5.5 Limitation of the Research

There are few limitations of the applications of our results as follows:

1) The pathogens must mainly reside in patient's blood circulation. If pathogens are mainly in other places such as certain organs (brain, lungs, heart, stomach, liver, kidneys, colons, skin, etc.), gastrointestinal tract, respiratory tract or reproductive tract, then our method of using the relative velocity cannot be applied. However, there have been other several methods that can be applied in this situation such as Brownian motion, the rate of mass action, etc. These methods, including the relative velocity, are used to model the mechanism of binding between drug molecules and pathogens into the mathematical framework (see the explanations below). Remark that the calculation of binding probability factor between a drug molecule and a pathogen by using the Brownian motion and the rate of mass action have to take into account for the movement in all directions while our method of the relative velocity involves the movement in single direction along the bloodstream. Thus, the method of the relative

velocity is simpler to compute when the calculation involves other factors such as probability factors.

2) The mechanism of binding between a drug molecule and a pathogen must occur mainly through the physical collision. If the mechanism of drug action is too complex, then the probability factors in our model may not be accurate enough, and therefore make it more difficult to incorporate with the relative velocity. For instance, the structure of drug molecules can change in several steps during the chemical reaction before the binding can take place. Consequently, the parameters of the drug molecules such as the structure, the shape, the area of active of the binding site need to be continuously adjusted as well.

3) All parameters of pathogens and drug molecules must be available. This is necessary otherwise the results cannot be simulated in order to make a prediction. Note that the parameters of human blood circulation system in this dissertation can be applied to other pathogens as well since the model will use the same human related parameters.



5.6 Suggestion and Future Research

The pathogens, used in our model, must satisfy our hypotheses as follows:

- 1) Pathogens must reside mainly in patient's blood circulation.
- 2) The binding mechanism between a drug molecule and a pathogen is not too complex to translate it into the mathematical forms.
- 3) The numerical data for each parameter must be available in order to generate the numerical results.

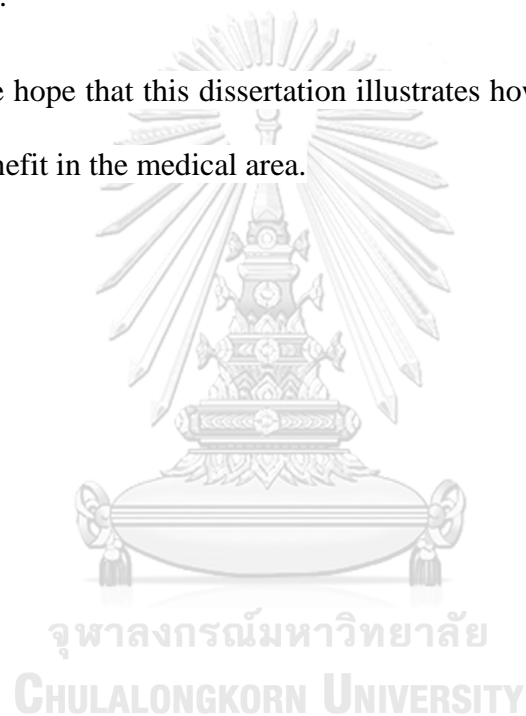
In order to apply our method to predict the treatment duration for other pathogens, we must take into account of the different mechanism. For instance, in case of HIV virus, there must be some certain parameters which have to be modified before formulating its death rate. For example, the binding action between drug molecule and HIV is different since HIV's shape is not spheroid. Currently, some antiviral drugs need to bind the HIV's DNA of a helical shape. Thus, the binding probability factor in the case of HIV is different from the one in our model.

In present, for the case of malaria, there are evidences that there are actually more than two main stages of iRBCs (circulating and sequestered iRBCs). In particular, there are 4 stages, consisting of early trophozoite, late trophozoite, early schizont and late schizont. Therefore, the mechanism of drug action in each stage of iRBCs must be separated into each stage of iRBCs and take into account in each of differential equation related to the population of iRBCs. For instance, most antimalarial drugs such as chloroquine can attack only iRBCs in the stage of schizont, while artemisinin and artesunate can attack every stage of iRBCs. Therefore, further modification of our model should lead to more accurate prediction of the treatment duration.

5.7 Conclusion and Discussion

Nowadays, there are a lot of patients suffering from pathogen infection in many developing countries. Some developing countries do not have the technological advances or resources to detect the density of pathogens in patient's blood. Consequently, the mathematical model in this dissertation may help physicians detect the density of pathogens and therefore determine the drug dosage for the patient with relatively low cost.

Finally, we hope that this dissertation illustrates how mathematical model can work and have benefit in the medical area.



REFERENCES

1. Organization, W.H. *About WHO: What we do*. 2018 [cited 2018 24/04]; Available from: <http://www.who.int/about/what-we-do/en/>.
2. Austin, D., N. White, and R. Anderson, *The dynamics of drug action on the within-host population growth of infectious agents: melding pharmacokinetics with pathogen population dynamics*. *Journal of theoretical biology*, 1998. **194**(3): p. 313-339.
3. Li, Y., S. Ruan, and D. Xiao, *The within-host dynamics of malaria infection with immune response*. *Math. Biosci. Eng*, 2011. **8**(4): p. 999-1018.
4. Brooks, G., et al., *Jawetz Melnick&Adelbergs Medical Microbiology 26/E*. 2012: McGraw Hill Professional.
5. Suavansri, P. and N. Kitisin, *Predicting the Duration of Chloroquine, Mefloquine, Halfantrine and Artesunate for Blood Schizonticidal Effect using Mathematical Models of Malaria with Immune Response*. *Thai J Pharmacol*; Vol, 2017. **39**(2): p. 23.
6. Bichara, D., N. Cozic, and A. Iggidr, *On the estimation of sequestered infected erythrocytes in Plasmodium falciparum malaria patients*. *Mathematical Biosciences and Engineering (MBE)*, 2014. **11**(4): p. 741-759.
7. Franke-Fayard, B., et al., *Sequestration and tissue accumulation of human malaria parasites: can we learn anything from rodent models of malaria?* *PLoS pathogens*, 2010. **6**(9): p. e1001032.
8. Ockenhouse, C.F., et al., *Molecular basis of sequestration in severe and uncomplicated Plasmodium falciparum malaria: differential adhesion of infected erythrocytes to CD36 and ICAM-1*. *Journal of Infectious Diseases*, 1991. **164**(1): p. 163-169.
9. Berg, H.C. and E.M. Purcell, *Physics of chemoreception*. *Biophysical journal*, 1977. **20**(2): p. 193-219.
10. Ghosh, P., *Stochastic models for in-silico event-based biological network simulation*. 2007: The University of Texas at Arlington.
11. Hackett, S., et al., *Meningococcal bacterial DNA load at presentation correlates with disease severity*. *Archives of disease in childhood*, 2002. **86**(1): p. 44-46.
12. Bosede, O.R., F.S. Emmanuel, and O.J. Temitayo, *On some numerical methods for solving initial value problems in Ordinary Differential Equations*. *IOSR Journal of Mathematics*, 2012. **1**(3): p. 25-31.
13. Logan, J.D., *A first course in differential equations*. 2015: Springer.
14. Atkinson, K., W. Han, and D.E. Stewart, *Numerical solution of ordinary differential equations*. Vol. 108. 2011: John Wiley & Sons.

APPENDIX

APPENDIX A

NUMERICAL METHOD

A.1 Background Information

There are various numerical methods for solving the differential equations such as Euler method, Runge-Kutta method, etc. In 1768, Leonhard Euler established the oldest and simplest method, called Euler method, to numerically approximate the solutions with certain initial conditions [12]. The Euler method is originated from the finite difference method [13]. The finite difference method is the basic concept of solving the differential equations with initial conditions, also called an initial value problem, on the interval $t_0 \leq t \leq t_N$, which are

$$x'(t) = F(x(t), t), x(t_0) = x_0.$$

To approximate a continuous solution by using a discrete solution. In particular, both sequences of x and t , which are X_0, X_1, X_2, \dots and t_0, t_1, t_2, \dots , are constructed from the discrete model of differential equation. Afterward, we divide the sequence t_0, t_1, t_2, \dots with an equal interval h , called the step size. That is, $t_{n+1} = t_n + h$. Next, we use the iterative process to evaluate X_1, X_2, X_3, \dots from X_0, X_1, X_2, \dots , respectively. Consequently, the numerical solutions are obtained. Note that the iterative process can be terminated by defining $N = \frac{t_N - t_0}{h}$ [13].

To apply this numerical method to our research, we have the system of differential equations which is the initial value problems. Since each mathematical model of malaria is multi-variables system, we need to modify each variable in order to apply the numerical method [13] (see the section of system of equations in details).

In this dissertation, we use the computational program to numerically solve the system of differential equations. Furthermore, this program can provide the best appropriate step size to optimize the numerical results.

A.2 Numerical Methods for Solving Initial Value Problems in the System of Differential Equations

There are various numerical methods to approximate the solutions of differential equations such as Euler method or Runge-Kutta method [13]. However, both methods require an initial condition in order to numerically solve the problem [13]. Hence, this section will describe how, we will apply two methods of Euler and Runge-Kutta in this work.

A.2.1 The initial value problem

The initial value problem is the problem of solving a differential equation, defined as

$$X'(t) = F(X(t), t),$$

with unknown $X = X(t)$ subject to a condition $X(t_0) = X_0$ [12]. Note that an initial condition is defined as $X(t_0) = X_0$, where t_0 and $X(t_0)$ are given. This initial condition is necessary in order to use the Euler method and Runge-Kutta method since both methods start from this initial condition before continuing the iteration process with certain step size.

Table 1. Table 1 shows the initial density or conditions of six variables, $x(0)$, $y(0)$, $y_c(0)$, $y_s(0)$, $m(0)$, and $E(0)$ in cases of *P. non-falciparum*, *P. falciparum*, *P. non-falciparum* with immune response, and *P. falciparum* with immune response, where x , y , y_c , y_s , m , and E are the density of normal RBCs, infected RBCs (iRBCs), circulating iRBCs, sequestered iRBCs, and immune effectors, respectively [5].

| Case | The Initial Density (cells/ μ L) | | | | | |
|---|--------------------------------------|--------|-----------------|----------|--------|-----------|
| | $x(0)$ | $y(0)$ | $y_c(0)$ | $y_s(0)$ | $m(0)$ | $E(0)$ |
| <i>P. non-falciparum</i> | | 10^5 | - | - | | |
| <i>P. falciparum</i> | 4.9×10^6 | - | 5×10^4 | | 10^4 | 10^{-4} |
| <i>P. non-falciparum</i> with immune response | | 10^5 | - | - | | |
| <i>P. falciparum</i> with immune response | | - | 5×10^4 | | | |

This research uses these initial densities in Table 1 in order to generate the numerical results in each of the two articles (see Chapter 3 and 4). These initial conditions of all six variables can be adjusted in order to analyze the numerical results in various cases. We can also whether these results are compatible with the actual results. For instance, if $y(0)$ are very large, then antimalarial drug will not have the effect on the density. Similarly, if $E(0)$ are very low, then the immune response becomes useless (see details in Chapter 5).

A.2.2 Euler method

Euler method is the simplest numerical method for the initial value problems [12]. The key of Euler method is the iteration process. First, we note that

$$X'(t) \approx \frac{1}{h} [X(t+h) - X(t)],$$

which is called a forwarding difference approximation and h is called the step size [13].

Hence, if we define $X'(t) = F(X_n(t), t)$, then by using the Euler method, we will get

$$X_{n+1} = X_n + hF(X_n(t_n), t_n), n = 0, 1, \dots, N-1.$$

The process of applying the Euler method to find the numerical solution is therefore as follows:

1. Define the system $\frac{dX}{dt} = F(X, t)$ with the initial values $X(t_0) = X_0$.
2. Define two sequences X_0, X_1, X_2, \dots at discrete times $t_0 < t_1 < t_2 < \dots < t_n < \dots$
3. Create the step size by dividing the interval $[t_0, t_N]$ with N segments, denoted by $h = \frac{t_N - t_0}{N}$
4. Compute $X_0, X_1, X_2, \dots, X_N$

In particular, we have $X_n = \begin{bmatrix} x_n \\ y_n \\ m_n \end{bmatrix}$, $\begin{bmatrix} x_n \\ y_{c,n} \\ y_{s,n} \\ m_n \\ E_n \end{bmatrix}$, $\begin{bmatrix} x_n \\ y_n \\ m_n \\ E_n \end{bmatrix}$ or $\begin{bmatrix} x_n \\ y_{c,n} \\ y_{s,n} \\ m_n \\ E_n \end{bmatrix}$ in cases of *P. non-*

falciparum, *P. falciparum*, *P. non-falciparum* with immune response, and *P. falciparum* with immune response, respectively. After we obtain the numerical solution, we can plot graph to determine the treatment durations by locating the intersection point between the graphs.

A.2.3 Systems of equations

Since our mathematical models for each type of malarial parasites are the systems of equations, these models need to be adjusted in order to satisfying the Euler method.

In case of *P. non-falciparum*, we apply the Euler method to the system of equation given in [2] as follows:

$$\begin{aligned} x_{n+1} &= x_n + h(\Lambda - \mu_x x_n - \beta x_n m_n), \\ y_{n+1} &= y_n + h\left(\beta x_n m_n - \mu_y y_n - \left(\frac{y_n}{x_n + y_n}\right)\phi(k)\right), \\ m_{n+1} &= m_n + h(g y_n - \mu_m m_n - \beta x_n m_n). \end{aligned}$$

In case of *P. non-falciparum* with immune response, we apply the Euler method to the system of equations given in [3] as follows:

$$\begin{aligned}
x_{n+1} &= x_n + h(\Lambda - \mu_x x_n - \beta x_n m_n), \\
y_{n+1} &= y_n + h\left(\beta x_n m_n - \mu_y y_n - \frac{p_1 y_n E_n}{1 + \theta_1 y_n}\right), \\
m_{n+1} &= m_n + h\left(r y_n - \mu_m m_n - \frac{p_2 m_n E_n}{1 + \theta_2 m_n}\right), \\
E_{n+1} &= E_n + h\left(-\mu_E E_n + \frac{k_1 y_n E_n}{1 + \theta_1 y_n} + \frac{k_2 m_n E_n}{1 + \theta_2 m_n}\right).
\end{aligned}$$

In case *P. falciparum* with immune response, we apply the Euler method to the modified system of equation given in [3, 6] as follows:

$$\begin{aligned}
x_{n+1} &= x_n + h(\Lambda - \mu_x x_n - \beta x_n m_n), \\
y_{c,n+1} &= y_{c,n} + h\left(\beta x_n m_n - (\gamma_c + \mu_c) y_{c,n} - \frac{p_1 y_{c,n} E_n}{1 + \theta_1 y_{c,n}}\right), \\
y_{s,n+1} &= y_{s,n} + h\left(\gamma_c y_{c,n} - (\gamma_s + \mu_s) y_{s,n} - \frac{p_1 y_{s,n} E_n}{1 + \theta_1 y_{s,n}}\right), \\
m_{n+1} &= m_n + h\left(r \gamma_s y_{s,n} - \mu_m m_n - \frac{p_2 m_n E_n}{1 + \theta_2 m_n}\right), \\
E_{n+1} &= E_n + h\left(-\mu_E E_n + \frac{k_1 (y_{c,n} + y_{s,n}) E_n}{1 + \theta_1 (y_{c,n} + y_{s,n})} + \frac{k_2 m_n E_n}{1 + \theta_2 m_n}\right).
\end{aligned}$$

However, the drawback of using the Euler method is that it is more prone to truncation error.

A.2.4 Runge-Kutta method

In 1900, Carl Runge and Wilhelm Kutta developed a method to numerically approximate the solutions of differential equations, called Runge-Kutta method. The key idea to this method is to bypass the computation of the higher-order derivatives in

the Taylor method [14]. Thus, Runge-Kutta method is supposed to have less errors. The general recursion form of Runge-Kutta method is

$$X_{n+1} = X_n + hF(X_n, t_n, h).$$

There are two types of Runge-Kutta method, which are 2nd and 4th order. The 2nd order Runge-Kutta method (or the modified Euler method) is given by

$$X_{n+1} = X_n + \frac{h}{2} \left[F(X_n, t_n) + F(\tilde{X}_{n+1}, t_{n+1}) \right],$$

where $\tilde{X}_{n+1} = X_n + hf(X_n, t_n)$. However, the 4th order Runge-Kutta method is more popular and more accurate than the 2nd order Runge-Kutta method since the 4th order Runge-Kutta method involves more parameters than the 2nd type. In particular, the 4th order method is given by

$$X_{n+1} = X_n + \frac{h}{6} (k_1 + 2k_2 + 2k_3 + k_4),$$

where

$$k_1 = F(X_n(t_n), t_n),$$

$$k_2 = F\left(X_n(t_n) + \frac{h}{2}k_1, t_n + \frac{h}{2}\right),$$

$$k_3 = F\left(X_n(t_n) + \frac{h}{2}k_2, t_n + \frac{h}{2}\right),$$

$$k_4 = F(X_n(t_n) + hk_3, t_n + h).$$

Note that the Euler method is the special case of the 1st order Runge-Kutta method is [12].

In the case of malaria with and without immune response, there are at least three variables in the system of differential equations. Thus, in order to apply the Runge-Kutta method to the mathematical model of malarial parasites, the recursion process need to be modified as in the case of Euler method. First, in case of *P. non-falciparum* without immune response as in the 2nd article, there are three variables of dynamic populations, which represent normal RBCs, iRBCs, and merozoites, denoted by x , y and m . Therefore, the Runge-Kutta equations in this case are given by

$$\begin{aligned}
 k_1 &= F(t_n, x_n, y_n, m_n), \\
 l_1 &= G(t_n, x_n, y_n, m_n), \\
 j_1 &= H(t_n, x_n, y_n, m_n), \\
 k_2 &= F\left(t_n + \frac{1}{2}h, x_n + \frac{1}{2}hk_1, y_n + \frac{1}{2}hl_1, m_n + \frac{1}{2}hj_1\right), \\
 l_2 &= G\left(t_n + \frac{1}{2}h, x_n + \frac{1}{2}hk_1, y_n + \frac{1}{2}hl_1, m_n + \frac{1}{2}hj_1\right), \\
 j_2 &= H\left(t_n + \frac{1}{2}h, x_n + \frac{1}{2}hk_1, y_n + \frac{1}{2}hl_1, m_n + \frac{1}{2}hj_1\right), \\
 k_3 &= F\left(t_n + \frac{1}{2}h, x_n + \frac{1}{2}hk_2, y_n + \frac{1}{2}hl_2, m_n + \frac{1}{2}hj_2\right), \\
 l_3 &= G\left(t_n + \frac{1}{2}h, x_n + \frac{1}{2}hk_2, y_n + \frac{1}{2}hl_2, m_n + \frac{1}{2}hj_2\right), \\
 j_3 &= H\left(t_n + \frac{1}{2}h, x_n + \frac{1}{2}hk_2, y_n + \frac{1}{2}hl_2, m_n + \frac{1}{2}hj_2\right), \\
 k_4 &= F(t_n + h, x_n + hk_3, y_n + hl_3, m_n + hj_3), \\
 l_4 &= G(t_n + h, x_n + hk_3, y_n + hl_3, m_n + hj_3), \\
 j_4 &= H(t_n + h, x_n + hk_3, y_n + hl_3, m_n + hj_3),
 \end{aligned}$$

$$k = \frac{1}{6}(k_1 + 2k_2 + 2k_3 + k_4),$$

$$l = \frac{1}{6}(l_1 + 2l_2 + 2l_3 + l_4),$$

$$j = \frac{1}{6}(j_1 + 2j_2 + 2j_3 + j_4),$$

$$\begin{aligned}
x_{n+1} &= x_n + hk, \\
y_{n+1} &= y_n + hl, \\
m_{n+1} &= m_n + hj, \\
t_{n+1} &= t_n + h, \\
F(x, y, m) &= \Lambda - \mu_x x - \beta xm, \\
G(x, y, m) &= \beta xm - \mu_y y - \left(\frac{y}{x+y} \right) \phi(k), \\
H(x, y, m) &= gy - \mu_m m - \beta xm.
\end{aligned}$$

The other malarial cases as in the 3rd article, which are *P. non-falciparum* with immune response and *P. falciparum* with immune response, can also benefit from the Runge-Kutta method by extending to four and five-dimensional system of differential equations, respectively. Therefore, the Runge-Kutta method should be the better choice for numerically approximating the solutions rather than the Euler method.

A.2.5 Determination of Treatment Duration

We note that the treatment duration can be determined by applying the numerical method such as the Euler method or Runge-Kutta method to our model consisting of the system of differential equations. However, there are still other ways to determine the treatment durations. The first one is to locate the intersection point between the graphs of parasite density and the time of treatment. For instance, if the parasite density is considered clear at $10^0=1$ cells/ μ L blood and the point of intersection is $(t_n, 1)$, then t_n will represent the treatment duration in this case. The second method is to plot the linear graph between the parasite density in logarithmic scale and time. Afterward, we can solve the time such that the parasite density is considered clear. For

instance, if (t_1, y_1) and (t_2, y_2) are the results from the numerical solution, and the graphs of results are assumed to be log-linear straight, then the treatment solution can be computed as $t_n = \left(\frac{\log y_n - \log y_0}{\log y_2 - \log y_0} \right) t_2$ or $\left(\frac{\log y_n - \log y_0}{\log y_1 - \log y_0} \right) t_1$. The third method is to generate the sequences between t_n and X_n . If it happens that $y_{n-1} > 0$ and $y_n < 0$ are between the time t_{n-1} and t_n , then the treatment duration is therefore between t_{n-1} and t_n .

A.3 Conclusion

In conclusion, we can apply the numerical methods, such as Euler method or Runge-Kutta method, to the mathematical models of malarial parasite in cases of *P. non-falciparum*, and both *P. non-falciparum* with immune response and *P. falciparum* with immune response in this research. However, the Euler method and the Runge-Kutta method may not be the best method for this research. For instance, the computation may take too much time and in danger of having runtime error. Furthermore, the Euler method may be outdated to evaluate such numerical solution since the accuracy of the Euler method is quite low.

VITA

Mr. Panit Suavansri was born in Bangkok, Thailand on May 11, 1983. He graduated with the degree in Bachelor of Science in Medical Science from Thammasat University in 2009. In 2011, he also completed his Bachelor of Science in Mathematics from Ramkhamhaeng University and Master of Science in Mathematics at Chulalongkorn University. Afterward, he started his Doctoral degree in Applied Mathematics and Computational Science at Chulalongkorn University in 2012. Panit got a special support for his Ph.D. study from the scholarship 60/40 of Chulalongkorn University. His publications are as follows: 1) Suavansri, P. (2016). Predicting the Duration of Antibacterial Treatment with Cell Wall Synthesis Inhibitors by using Mathematical Models, which appears in Thai Journal of Pharmaceutical Sciences (TJPS), 40(3)., and 2) Suavansri, P., & Kitisin, N. (2017). Predicting the Duration of Chloroquine, Mefloquine, Halofantrine and Artesunate for Blood Schizonticidal Effect using Mathematical Models of Malaria with Immune Response, which appears in Thai Journal of Pharmacology. Lastly, his article, Suavansri, P., & Kitisin, N. (2017) with title “Predicting the duration of antimalarial treatment with heme degradation inhibitors of blood schizonticides using mathematical models”, which had been accepted, will soon appear in the Songklanakarin Journal of Science & Technology.